EPS/Metop-SG

Scatterometer Mission Science Plan

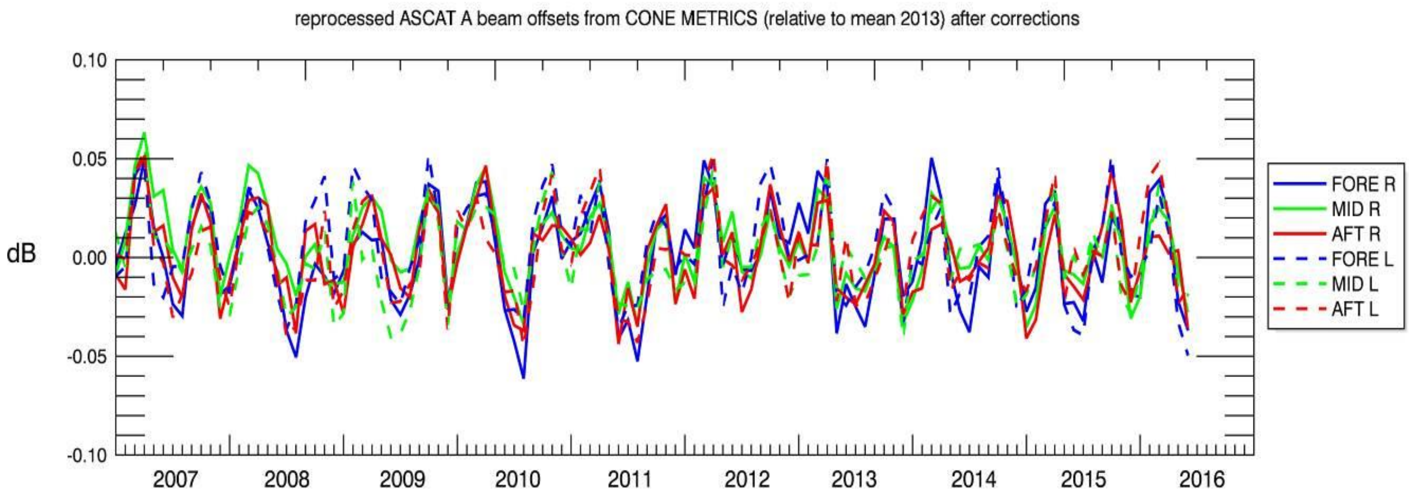

A report from the ESA/EUMETSAT

Scatterometer Science Advisory Group

Issue : 1.0

Date : 25 April 2019

Cover Figure:

Relative changes in the ASCAT-A antenna calibrations in dB computed using cone metrics over the oceans (Belmonte et al., 2017), showing the excellent calibration stability of ASCAT-A. Note that 0.01 dB calibration uncertainty in all 6 beams corresponds to approximately 0.01 m s^{-1} wind retrieval uncertainty in the wind components. The notable seasonal variation in all beams is due to the global ocean wind variability cycle. The excellent calibration stability of ASCAT makes this instrument a reference for intercalibration with Ku-band scatterometers and radiometers alike. Moreover, ERS- and ASCAT-based thematic climate data records (CDR) over land, ocean and cryosphere will be an excellent basis for the validation of climate data records based on model reanalyses, such as from ECMWF (ERA).

Cone metrics has made it possible to precisely intercalibrate the ERS and ASCAT scatterometers, although the two instruments had not any significant mission overlap. Cone metrics will further allow a significant improvement in the C-band geophysical model function (GMF) over the oceans and potentially lead to enhanced satellite attitude knowledge along the orbit phase, which may benefit ASCAT and SCA products, but also those from other Metop instruments. Concerning the relation with other scatterometers, ASCAT is used as a reference and ASCAT collocations benefit the development of Ku-band GMFs (Wang et al., 2017), scatterometer rain products (Brocca et al., 2017), quality control of Ku-band scatterometers in rain and, generally, improved understanding of error modelling and processing of scatterometers in terms of spatial representation, wind variability, etc.. Great prospects remain to expand our practical assets obtained with ASCAT and later on SCA to Ku-band and other scatterometers and radiometers, which will be much advanced with developments based on the stability of the ERS, ASCAT and SCA scatterometers and the control of it obtained with cone metrics.

Document Change Record

Issue / Revision	Date	Changed Pages / Paragraphs
V1.0	April 2019	First version after discussion at the first six Scatterometer SAG meetings.

Contributors

Name	Affiliation
Ad Stoffelen (editor)	KNMI, de Bilt, the Netherlands
Patricia De Rosnay	ECMWF, Reading, UK
Jean-Christophe Calvet	Meteo France, Toulouse, France
Lars Anders Breivik	Met Norway, Oslo, Norway
Signe Aaboe, Frode Dinessen	Met Norway, Tromsø, Norway
Christoph Reimer, Wolfgang Wagner	Vienna University of Technology, Austria
Alexis Mouche	IFREMER, Brest, France
Marcos Portabella	ICM, Barcelona, Spain
Giovanna De Chiara	ECMWF, Reading, UK
James Cotton	Met Office, Exeter, UK

Table of Contents

Executive Summary ... **6**

1 Introduction ... **12**

1.1 Purpose ... 12

1.2 Scope ... 12

1.3 Document Overview ... 12

2 Objectives ... **14**

2.1 The EPS/MetOp-SG Programme ... 15

2.2 The Scatterometer Mission ... 15

2.3 Innovative Objectives ... 17

3 Heritage ... **19**

3.1 The first C-band fan-beam Scatterometer Instrument: ESCAT ... 19

3.1.1 Measurement Space ... 22

3.1.2 Wind Quality ... 25

3.1.3 ESCAT over land ... 28

3.1.4 ESCAT and sea ice ... 29

3.2 The Advanced Scatterometer (ASCAT) ... 31

3.2.1 Calibration and ASCAT Performance ... 31

3.2.2 Spatial Resolution ... 31

3.2.3 Wind Processing ... 32

3.2.4 Land ... 34

3.2.5 Accumulated rain ... 34

3.2.6 Cryosphere ... 34

4 The SCA Instrument ... **36**

4.1 Technical summary ... 36

4.2 Scientific Challenges ... 36

4.2.1 Cross polarization and HH co-polarization ... 37

4.2.2 Spatial Resolution ... 39

4.2.3 Coverage ... 40

4.2.4 Potential Doppler Capability ... 42

5 **SCIENTIFIC PROSPECTS FOR SCA APPLICATIONS** **44**
5.1 Using SCA Wind Variability 44
5.2 Improving Land Applications 44
5.3 Sea Ice Application Evolution 46
5.4 Backscatter Assimilation over Land. 46
5.5 Wind Assimilation 47
5.6 Convection 48
5.7 Coupled Atmosphere-Ocean-Land Assimilation 49
5.8 Extreme Wind Speeds 49
5.9 Doppler Scatterometer 49
6 **Data processing and products** **51**
6.1 Near-Real Time and Quasi-Real Time 51
6.1.1 Level 1b 51
6.1.2 Level 2 Wind 51
6.1.3 Level 2 Soil Moisture 58
6.1.4 Level 3 and Level 4 60
6.2 Climate data records 62
6.3 Future developments 64
7 **Performance monitoring** **65**
7.1 Near-Real Time 65
7.1.1 NWP collocation 65
7.1.2 Calibration 66
7.1.3 Quality Control and Monitoring 67
7.2 Climate data records 68
8 **Outreach needs** **69**
9 **Research and development needs** **70**
9.1 SCA and the constellation 70
9.2 SCA advances 71
9.3 Nowcasting, NWP and reanalyses needs 72
10 **References** **74**
10.1 Literature 74
10.2 Acronym List 88

EXECUTIVE SUMMARY

This Science Plan describes the heritage, background, processing and control of C-band scatterometer data and its remaining exploitation challenges in view of SCA on EPS/MetOp-SG.

SCA

The EPS/MetOp-SG C-band-wavelength Scatterometer instrument (called SCA here) has a direct heritage from instruments such as the Advanced Scatterometer (ASCAT) flown on the Metop satellites. Variables to be derived from SCA measurements include (EURD, 2013):

- Ocean surface wind vector and wind variability
- Land surface soil moisture, vegetation and accumulated rain
- Sea-ice type and extent
- Freeze/thaw state

The EPS-SG Mission Requirements Document (MRD) provides a description of the scatterometer mission objectives. As a baseline, the expected performance of SCA is that of ASCAT. However, the SCA design represents three major innovations w.r.t. ASCAT and in this report science and application benefits for these items are discussed in particular:

- The addition of a cross-polarisation (VH) channel;
- Enhanced spatial resolution;
- Enhanced spatial coverage.

Moreover, the potential implementation of an ocean Doppler capability to retrieve the ocean motion vector has been investigated in some detail and is presented.

Applications

Scatterometry measurements provide ocean surface wind vectors, which are an important input to global and regional NWP. They are also used as a forcing agent in ocean models to improve the modelling of waves, storm surges and ocean currents. Moreover, observations supporting the coupled atmosphere-ocean system are fundamental for seasonal and longer term forecasting, e.g., allowing an adequate representation of phenomena such as El Niño and the atmospheric and ocean circulation more in general. The NRT demand for ocean wind observations is further emphasized by the increased need for accurate storm and hurricane forecasting in the nowcasting application. More recently, economic interest in coastal wind forecasts and climatologies is increasing, due to developments in, e.g., off-shore energy applications and transport.

Over land surface, scatterometer measurements are exploited to retrieve surface soil moisture estimates used for NWP assimilation. Surface soil moisture is of major importance in global and regional NWP, because of the direct impact on many physical, chemical and biological processes and feedback loops taking place at the land surface and within the atmosphere. Moreover, scatterometer derived surface soil moisture estimates have proven their capability to monitor extreme hydrological events like droughts and floods, to improve runoff forecasts, support epidemiological predications and agricultural applications. In addition, the necessity of long-term global surface soil moisture observations was recognised for climate studies predicting climate changes or validating complex climate models.

With respect to the cryosphere, scatterometer data is used in the retrieval of several sea ice parameters, such as sea ice coverage, type and drift and long C-band data records are being generated since 1992.

In line with this, the main users of the SCA will be the NWP centres of National Meteorological Services and ECMWF, Operational Nowcasting services of National Meteorological and Hydrological Services or commercial weather providers are also users of SCA for marine services and hydrological warnings. The SCA mission is moreover very relevant to non-real-time users, such as oceanographic researchers and climate system modellers. The primary objectives of SCA are thus to support NWP, climate monitoring, nowcasting, and ocean state forecasts at regional and global scales, through the provision of oceanic surface wind vector measurements.

In addition the EPS/MetOp-SG scatterometer mission provides information on land surface soil moisture, vegetation water content, freeze/thaw state, and sea-ice to NWP, ocean and climate monitoring. Hydrology applications will benefit from observations of soil moisture and efforts now exist to derive accumulated rain measurements from scatterometer soil moisture.

The software, production, monitoring, calibration and validation are well documented through the EUMETSAT OSI, NWP and Hydrology SAFs and through the EU Copernicus Marine Environment Monitoring Service (CMEMS) Thematic Assembly Centres (TAC) on Wind and Sea Ice. It moreover describes scatterometer application in NWP, where user guides are developed in the context of the NWP SAF for wind data assimilation and bias correction, thus reaching out to the operational and scientific expert and user communities, and fostering mechanisms for innovative application research. These services are equipped with help desks. Visualisation sites of NRT data, on-line open and accessible NRT and archive data bases of scatterometer data and associated reference data are available.

Wider scientific elaboration and development of scatterometer processing or application is well facilitated through the visiting and associated scientist programmes of the EUMETSAT SAFs. Moreover, all scatterometer developments and standardization is well coordinated on an international level through the IOVWST and CEOS, for example.

Wind and wave marine training is taken up with NOAA and EUMETSAT, providing face-to-face training across the globe. In addition, on-line modules, case studies and training is provided and will be continued. Scatterometer winds are generally well used for hurricane forecasting, both in the tropics and in the extra-tropics, but also to monitor mesoscale wind features over sea, soil moisture conditions and sea ice extent, drift and type. Finally, as a further outreach, media interviews occur frequently, when scatterometer data depict extreme storms, draughts or minimum sea ice coverage. These activities will be continued for SCA.

Challenges in product development

Research and development needs for SCA focus on the two main user priorities of temporal coverage, of dynamical and extreme weather in particular, and of advanced high-resolution processing, particularly in coastal, land and sea ice applications. Besides direct use of scatterometer products, there is a clear tendency of further integration of the scatterometer products in nowcasting, NWP and reanalyses, which needs are further discussed in this Science Plan. Moreover, to benefit the user community, focus should be put on standardization.

Wind and stress in NRT and as CDR will be needed from SCA at all processing levels. At L4 combination with other active and also passive instruments is necessary, hence a focus on intercalibration of basic measurements and winds is required.

The existing NRT processing and monitoring is typically used for CDR development and the cone metrics approach guarantees inter-calibration of backscatter over the C-band missions. The absolute calibration of ASCAT has been possible through transponder campaigns, which will be continued for SCA.

The goal for SCA and ASCAT is to obtain full global coverage when possible at 9:30 and 21:30 Local Solar Time (LST), as increased spatial and temporal resolution is a key user requirement, e.g., for the nowcasting of hurricanes. Planning for such complete coverage, using both ASCAT and SCA instruments beyond 2023 will be required.

In order to develop standards, the international collaboration and representation in the IOVWST, IWW, CEOS and WMO is necessary, as well as dedicated resources to inter-compare products and to agree on algorithms and references. In addition to standard development, these fora set priorities and requirements for R&D needs and may embark on effective international collaboration schemes. These R&D priorities include typically Cal/Val, inter-calibration, coastal processing, resolution enhancement, dependency on sea state, SST, ocean current, vegetation, dependency on e.m. wavelength , extremes, etc.. In addition, requirement assessment, spatial and temporal coverage coordination, product format standardization, quality metrics, open (collocation) data bases, open tools and processing software are generally part of these international collaborative fora. For example, ASCAT has proven to be very important for other OVW-sensing instruments, due to its optimal geometry, all-weather capability and excellent stability. In the virtual constellation plentiful close collocations between ASCAT and RapidScat or ScatSat have been exploited to achieve better product consistency through adapting all product processing steps (Calibration, GMF, retrieval, QC and 2DVAR). With SCA, such exploitation will be continued and extended to VH, extreme winds, sea state, ocean currents, etc.. Lessons learned from ASCAT may be further exploited for other scatterometer systems, such as the application of cone metrics, the use of the MLE as a measure of wind variability and ASCAT-determined ECMWF error covariances in 2DVAR MSS.

We also note the possible convoy with SKIM, which would be very useful to better determine the dynamical aspects of air-sea interaction. SCA winds will be very useful for the success of SKIM, while SKIM measurements aid in the understanding of SCA backscatter and, possibly, Doppler measurements. Further synergy on MetOp-SG is obtained through MWI, which would probably impact both SKIM and SCA products.

Forthcoming improvements for ASCAT include coastal processing, using the L1B Land Contribution Ratio (LCR), and improved ship detection, which latter is particularly difficult for moderate ship corner reflections on moving ships at modal wind speeds, due to the on-board accumulation. With SCA, without on-board accumulation, advanced spatial processing near coastlines will be possible and better discrimination of ship echo's is expected, as well as enhanced possibilities for processing at higher spatial resolution or on user-defined grids over both land, sea and coasts.

For ASCAT transponder campaigns are held, which interrupt the surface backscatter measurements, resulting in a loss of data. For SCA the calibration mode is integrated in its normal duty cycle while surface backscatter measurements are made. The improved SCA coverage and radiometric performance will lead to higher quality winds in more places. Combining these measurements with the ongoing ASCAT missions will need investigation.

VH measurements will allow extreme wind measurements and will be very useful with complementary benefits over land and sea ice. A VH wind processing chain will be developed for day 1 and later on the VH and co-polarization processed winds will be merged into a single wind product. VH measurements from SAR have been exploited to develop a GMF, while VH campaigns in extreme winds collect further data to corroborate the SAR results. For lower signals, pure VH may be more difficult to obtain due to Faraday rotation and its effect on wind speed retrieval needs further elaboration.

A recently developed HH GMF confirms that HH is less sensitive to wind than VV and thus using all VV co-polarization maximizes sensitivity for ocean wind retrieval, amended by VH measurements for extreme winds.

Recent simulation work opens the possible exploration of SCA phase and Doppler information for ocean currents. Using an echo cancellation method, further signal quality enhancement is simulated. Without any further SCA design trade-offs, these concepts should be further investigated and tested in order to realize such capability with SCA, possibly in synergy with SKIM.

Application challenges

Nowcasters are faced with an enormous amount of satellite observations that contribute new information to their advisories. Commonly, large differences of the observations from NWP forecasts should alert nowcasters to revise these advisories. Such large differences may be automatically detected in the areas of interest from SCA observations, using the ECMWF forecast as reference. In addition, information on expected errors and local wind variability (MLE) can be provided.

The absence of an in-situ wind reference for high and extreme winds remains a concern for the calibration and validation of all ocean satellite wind retrievals, but also for the development of improved NWP model parameterizations in storm conditions.

For NWP wind data assimilation we suggest to distinguish developments in regional and global NWP. Aliasing of the scales well determined by the analysis from scatterometer observations with the underdetermined smaller scales over the seas should be avoided and techniques to avoid such detrimental effects of model noise should be further elaborated for regional NWP. Global NWP models generally avoid small-scale model noise (so far) and are much smoother than regional model wind fields. To deal with the relatively high density of SCA observations, thinning is currently practised, but should be avoided. Tests with error inflation to compensate for oversampling of the model analysis structures or “superobbing” are ongoing for global NWP.

A second main problem in NWP is that innovations due to ASCAT are substantially affected by systematic NWP model errors, which violate the BLUE paradigm in NWP data assimilation. Schemes for compensation (bias correction) of systematic model errors are sorely needed to

- Optimise the extraction of dynamical information observed by SCA;
- Provide an improved (corrected) forcing of ocean, wave and surge models.

Bias correction schemes are already in place for many other assimilated satellite retrievals.

Long (30 yr+) harmonized time series of satellite-derived winds, soil moisture and sea ice products have been produced in the context of the ESA-CCI programme and of the Copernicus Climate Change and Marine Environment Monitoring Services, where ASCAT data are a key component of these products.

For climate applications consisting in detecting trends in the seasonal variability of soil moisture, disentangling soil moisture and vegetation water content effects on the backscatter level is of key importance. Assessing properly the inter-annual variability of soil moisture is key, and new techniques able to account for changes in vegetation density from one year to another in the soil moisture retrieval algorithm have to be developed. This requirement is also valid for NWP applications, as seasonal biases in the assimilated soil moisture are detrimental to the quality of the assimilation results. Meteo-France plans to use its LDAS-Monde tool to produce global land reanalyses incorporating scatterometer CDRs together with other ECV products such as LAI. The use of SCA data in this context should be prepared, possibly through the development of an observation operator for sigma0. Apart from its use in the LDAS, the observation operator would allow the simulation of SCA sigma0 values over land. This would help assess the capability of SCA observations to monitor vegetation in addition to surface soil moisture.

The capabilities of SCA to provide a self-standing operational vegetation data product should also be assessed. The most promising vegetation variable to be retrieved by SCA is the vegetation optical depth (VOD) which has been shown to be indicative of vegetation water content and wet biomass. Hence, the VOD has significant potential to enrich the information about vegetation dynamics, complementing the vegetation data sets (LAI, NDVI, fAPAR) provided by optical sensors. This work will also have important benefits for the SCA soil moisture data services given that an improved parameterization of vegetation in the SCA backscatter models over land will lead to improved soil moisture retrievals.

Over land, the introduction of a SCA based rainfall product based on the SM2Rain method proposed by Brocca et al. (2014) shall be further developed. A recent EUMETSAT study conducted by Brocca and colleagues has shown that rainfall estimates derived from ASCAT soil moisture retrievals using the SM2Rain algorithm are comparable to, or even outperform, other existing rainfall data products (in situ, satellite, fused) in ungauged basins.

The Cal/Val of SCA could be an opportunity to address such issues. Long term field campaigns based on continuous backscatter observations made by portable simulators of SCA, associated with in situ soil moisture and vegetation biomass observations, are needed. ESA has experience in organizing such Cal/Val studies (e.g. the ELBARA programme in the framework of the SMOS Cal/Val). In addition, high-resolution SAR data are useful for the Cal/Val of SCA products, in particular from Sentinel-1 and RadarSat.

1 INTRODUCTION

1.1 Purpose

This document presents an overview of the high-level scientific aspects that support the implementation of the EPS/Metop-SG Scatterometer mission and thus provides a frame for scientific support and advice to ESA and EUMETSAT during its development from phase B up to D/E.

The document is written, owned and maintained by the Scatterometer Science Advisory Group (SAG), capitalising on the years-long developed expertise which is accumulated in the ASCAT SAG, in the areas of development, implementation and operations.[1]

1.2 Scope

The Science Plan details the scientific work and context needed to meet the scatterometer mission objectives, highlighting the research and development necessary to achieve those mission objectives and providing a framework for required scientific research and development activities.

This document is not intended as a review of the user or mission requirements outlined in the context of the EPS-SG Program Mission Experts Team (RD-1 and RD-2) but aims to provide a longer term outlook of the potential evolution of those objectives (i.e., emerging science and applications).

The views in this document are based on the state of the art in scatterometer science and applications, intended primarily for ESA, EUMETSAT and SAF mission scientists and engineers as a reference and guideline in the definition of the space and ground segments associated with the scatterometer mission, as well as their applications ground segment partners within the Satellite Applications Facilities (SAFs).

1.3 Document Overview

The EPS/MetOP-SG satellite series embarks on SAT-B the first-ever cross-polarisation scatterometer, which in this document is denoted as SCA. As described below, SCA moreover continues to fulfil and extends the ASCAT mission objectives that are successfully being accomplished during the first generation MetOp mission, which is currently ongoing and based on the European Remote-Sensing Satellite (ERS) scatterometer (ESCAT) heritage. This document describes this both useful and exiting perspective of the scatterometer mission on EPS/MetOp-SG.

The ASCAT heritage will first be described, followed by an outline of the advanced SCA instrument characteristics. The applications that are targeted are outlined subsequently, followed by a description of the data processing and products foreseen, including their monitoring.

---

[1] This document is not an EPS/MetOp-SG project document but aims at providing an independent advisory framework and a focus for the establishment of scientific research and development priorities.

Last, but not least, outreach needs and activities are suggested for the mission operation to be successful, as well as scientific requirements for research and development that would lead to advanced applications.

2 OBJECTIVES

The objectives and user requirements as collected by the Application Expert Groups (AEG, 2008) and endorsed in User Consultation Meetings (UCM, 2008) led to the definition and continuation of the EUMETSAT scatterometer mission.

Scatterometer instruments are part of so-called virtual constellations through international collaboration. The Committee on Earth Observation Satellites Ocean Surface Vector Wind Virtual Constellation (CEOS OSVW VC) agency working group, including EUMETSAT, is making steps to align requirements and standards to build a global constellation of scatterometers. A particularly pressing requirement at most participating CEOS OVW agencies is to obtain extreme winds in hurricanes (> 30 m/s) from scatterometers (CEOS, 2017).

Operational user requirements and capabilities in the EPS-SG era are discussed more broadly in the World Meteorological Organization (WMO) vision for the Global Observing System (GOS, 2010) in 2025. WMO works closely with the space agencies through the Coordination Group for Meteorological Satellites to fulfil its vision. Moreover, the observation requirements data base at WMO (OSCAR, 2017) provides a detailed account of current observing system capabilities and requirements, including surface vector winds over sea, soil moisture, accumulated rain and sea ice.

In the International Ocean Vector Wind Science Team meetings (IOVWST, 2017), the state-of-the-art in wind vector processing and the application of scatterometer winds is discussed. Moreover, ESA and EUMETSAT collect advice from the scatterometer expert and user community through the SCA Science Advisory Group (SAG). The international experts, scientists and users in these fora have been presented with the EPS SG SCA design options and have been requested to provide advice. Also, bilateral discussions with main users have been held. In this section the resulting discussions are briefly summarised.

Application	Ocean Vector Winds	Soil Moisture	Sea Ice
Global NWP	1	2	2
Regional NWP	1	2	2
Nowcasting	1		
Oceanography	1		1
Hydrology		1	
Climate	1	2	1

Table 2.1: AEG prioritisation, including feasibility, of the scatterometer mission parameters. Priorities range from 1 (prime) to 4 (low) (AEG, 2008).

2.1 The EPS/MetOp-SG Programme

The SCA user requirements have thus been assessed by the diverse AEGs before its design phase (AEG, 2008). This assessment is briefly recollected in table 2.1, for the application areas mandated to EUMETSAT and will serve as baseline in the following discussion. Since nearly a decade has passed since the assessment in 2008, a general revaluation by the AEG however is recommended, taking into account the latest scientific evidence.

A scatterometer mission is broadly supported in the diverse applications supported by the EUMETSAT mandate. The overall high priorities and feasibility warrant the continuation and advancement of the EUMETSAT scatterometer mission. Current general priorities are maintained through the aforementioned WMO OSCAR data base.

In addition to SCA, the MetOp-SG platform B will carry a MicroWave Imager, called MWI. Synergies between SCA and MWI will be further discussed in this document.

2.2 The Scatterometer Mission

The SCA instrument has a direct heritage from instruments such as the Advanced Scatterometer (ASCAT) flown on the Metop satellites and well established application areas (see table 2.1). Over ocean the SCA mission supports NWP, climate monitoring, nowcasting, and ocean state forecasts at regional and global scales, through the provision of oceanic surface wind vector measurements.

Over land the SCA mission provides information on land surface soil moisture, vegetation, snow and accumulated rain for NWP, climate monitoring and hydrology .

In the cryosphere the SCA mission provides information on sea-ice type and extent in support of ice charting applications and climate monitoring.

Variables to be derived from the SCA mission include

- Ocean surface wind vector and wind variability
- Land surface soil moisture, vegetation and accumulated rain
- Sea-ice type and extent
- Freeze/thaw state

In the EPS-SG Mission Requirements Document (MRD) a brief description of the scatterometer mission is given, which has been repeated here for convenience.

For the scatterometer mission the MRD clearly favours horizontal resolution above spatial coverage. Moreover, while the threshold coverage and resolution are very similar to ASCAT on MetOp, the breakthrough values allow an increased exploitation of the scatterometer measurements in more advanced future applications as detailed in next section.

In fact, the MRD addresses alternate cross polarisation (VH or HV) measurements for its higher sensitivity to extreme winds at all incidence angles and its straightforward implementation on the mid beam. VH is advantageous in soil moisture and sea ice observation as well, as further elaborated in next chapter. The current SCA design also supports horizontal (HH) polarisation, which is beneficial for soil moisture retrieval.

The SCA design represents three major innovations w.r.t. ASCAT and in this section the science objectives for these items are summarized in particular:

- The addition of a cross-polarisation (VH) channel;
- Enhanced spatial resolution;
- Enhanced spatial coverage.

Moreover, the option to implement an ocean Doppler capability to retrieve the ocean motion vector has been investigated in some detail and will be presented too.

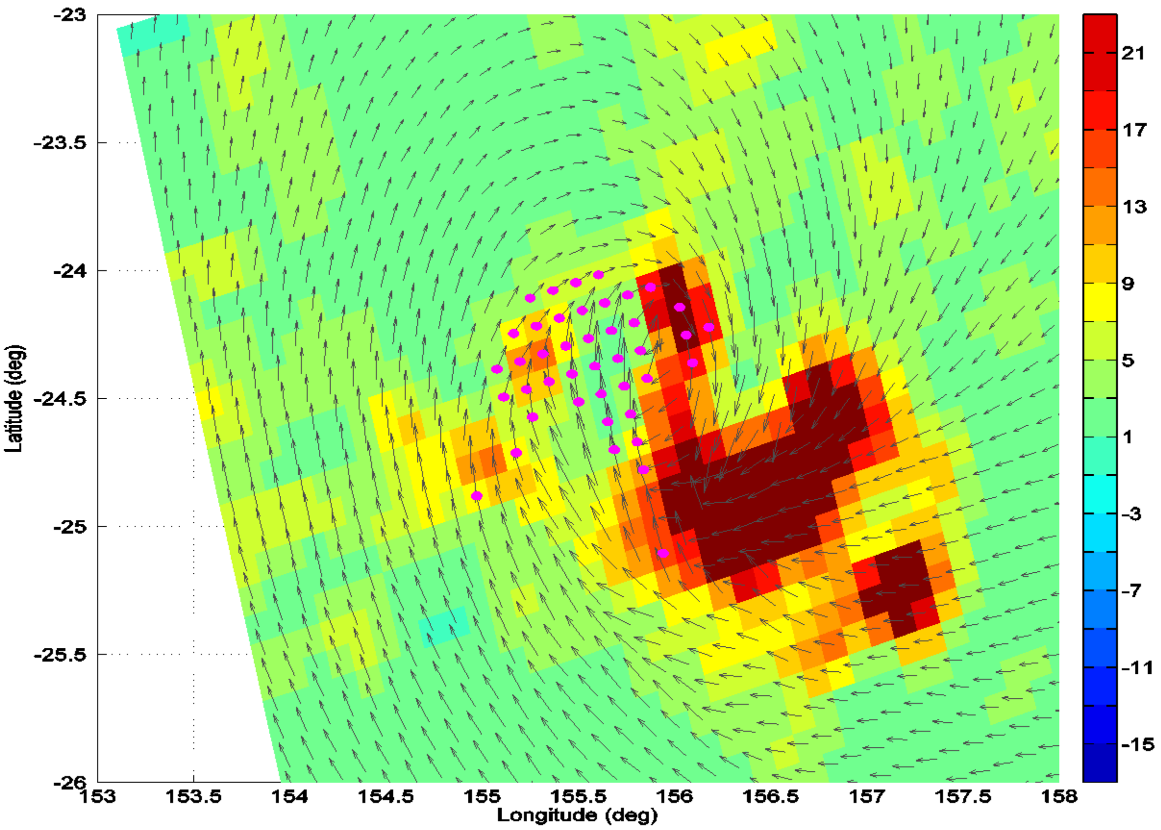

Figure 2.1: ASCAT innovations in wind inversion residual sign (MLE; colour) as a measure of local wind variability and in wind direction ambiguity removal (at the pink dots) for a dynamical mesoscale system in the southern Indian Ocean. Green MLE colours correspond to flow with low sub-WVC wind variability, while red colours indicate very large local wind variability, often due to wind downbursts in moist convective precipitation (Lin et al., 2015).

2.3 Innovative Objectives

ASCAT data has proven very useful in weather forecasting and is considered to be one of the most valuable observations for improving tropical cyclone forecasts. Improvements in processing and innovations in its use have been elaborated during its mission; see e.g. figure 2.1. For climate, marine applications and weather forecasting scatterometer requirements are consolidated and furthermore the community supports the desire to improve scatterometer technology to address the current known weaknesses of ASCAT:

- Wind vectors can be unreliable at wind speeds over 25m/s;
- Insufficient resolution for some processes (a 25 km product with 12.5 km spacing);
- Data coverage: key weather events can be missed due to incomplete coverage.

SCA addresses all three main areas, which are further discussed below.

Besides these main SCA innovations, two new additional capabilities of the MetOp-SG B platform are of interest to several scatterometer science objectives. The first is the potential Doppler capability, which could for example contribute to the simultaneous observation of the ocean surface wind and the ocean surface motion, but also be helpful in ambiguity removal in dynamical weather. The second is the availability of the synergistic MWI observations, potentially useful in atmospheric, ocean, land and cryospheric applications of the scatterometer.

General and unique measurement capabilities for scatterometer missions include the wind vector observations in tropical cyclones, polar lows and more in general the measurement of extreme winds in all weather conditions.

Increased spatial resolution allows in particular the monitoring of wind patterns associated with atmospheric convection, coastal flow, and furthermore of wind patterns transformed by temperature and motion of ocean eddies, which determine the mass, momentum, energy and gas fluxes at the air-sea interface. Wind information is not only essential to depict convection in the tropics, but also provides the Ekman ocean currents due to wind stress and an accurate view of the tropical circulation in the atmosphere, which is otherwise lacking. Besides wind benefits, scatterometers also provide soil moisture at high temporal and spatial coverage and enhanced sensitivity to thin sea ice, particularly in the melting season.

The three main SCA innovations thus have the following general effect:

- The alternate VH polarization on the mid beams improves the extreme wind speed range above 25 m/s, improves vegetation determination in conjunction with soil moisture retrieval and enhances sea ice detection;
- The breakthrough horizontal resolution of 25 km gives a better handle on physical processes such as turbulent flows, convective systems, tropical cyclones, polar lows, coastal phenomena, air-sea interaction, eddy-scale oceanography and tropical circulation. In addition, better resolved soil moisture, vegetation and temporal soil characterization will result over land. Over sea ice, it provides improved sea ice characterization and drift determination;

- The wider swath improves the ASCAT coverage (by 20%) and makes SCA more comparable to other scatterometers in this respect, but with improved accuracy.

3 HERITAGE

The first Active Microwave Instrument was launched on the European Remote Sensing satellite, ERS-1, in July 1991. When operated in Wind Scatterometer mode, the instrument acquired measurements of sea surface wind speed and direction. During the early days of ESCAT also unanticipated applications such as soil moisture (Wagner et al, 1999), land freeze/thaw (Pulliainen et al, 1998) and vegetation monitoring (Magagi and Kerr 1997) over land and sea-ice monitoring (Gohin and Cavanié, 1994) have been demonstrated and matured, though the instrument has not been designed and optimised for these applications. Altogether, ERS Scatterometer (ESCAT) data have been widely used for hurricane prediction, Numerical Weather Prediction, marine 'nowcasting', oceanography, hydrology and studies of the cryosphere, with societal and economic benefits in areas such as marine safety, offshore activities, ship routing, wind energy and climate change monitoring. Stoffelen and Wagner (2011) describe the ESCAT heritage at the celebration of its 20th anniversary.

However, initial comparisons of the ESCAT winds with other wind information showed large inconsistencies. This led to the development of novel analytical techniques using the measurement space of ESCAT, which confirmed the expected internal consistency of the ESCAT measurements and the low noise, but also provided an improved characterisation of the sensitivity to wind speed and direction, resulting in improved Geophysical Model Functions (GMFs). Moreover, the visualisation of the ESCAT measurement space provided insights into the non-linear wind retrieval problem, which has subsequently been improved, aided the discrimination of sea ice and water, and provided important insights into wind quality control.

The ESCAT wind Cal/Val also led to the development of the triple collocation methodology, which is now widely used in satellite algorithm development. The lessons learnt from ESCAT were readily applied to the NASA scatterometer missions at the Ku-band and provided similar benefits, leading to improved rain screening and wind datasets. ESCAT has also been successfully applied in soil moisture, sea ice and snow characterisation, leading to operational applications. ESCAT's heritage has also been important in the development of the Advanced Scatterometer (ASCAT) on MetOp for the EUMETSAT Polar System (EPS). The EPS Second Generation scatterometer (SCA) is now being build, where the ESCAT C-band static fan beam concept is being maintained due to its great success. This may well lead to over 40 years of C-band fan-beam scatterometer data, which will be a tremendous resource for climate applications for studying wind climatology, land surface hydrology, air–sea interactions, atmospheric and sea ice processes, etc. The demand for the unique ESCAT data and services will therefore remain high in the years to come (SCIRoCCo, 2017).

3.1 The first C-band fan-beam Scatterometer Instrument: ESCAT

During the Second World War, when radar was used to detect and track hostile vessels, it was noted that this detection was hampered at increasing wind speeds. Naturally, the idea of measuring wind near the sea surface by using microwaves, i.e. scatterometry (e.g. Moore & Pierson, 1967), was soon developed. Wind scatterometers measure the radar backscatter from wind-generated centimetre-sized gravity capillary waves and provide high-resolution vector wind fields over the oceans. All-weather scatterometer observations have proven accurate and important for the forecasting of dynamic and severe weather. Oceanographic applications have been developed since scatterometers provide unique forcing information on the ocean eddy scale. Although not designed for it, scatterometers also proved to contain useful information for land and cryosphere applications (see Fig. 3.1).

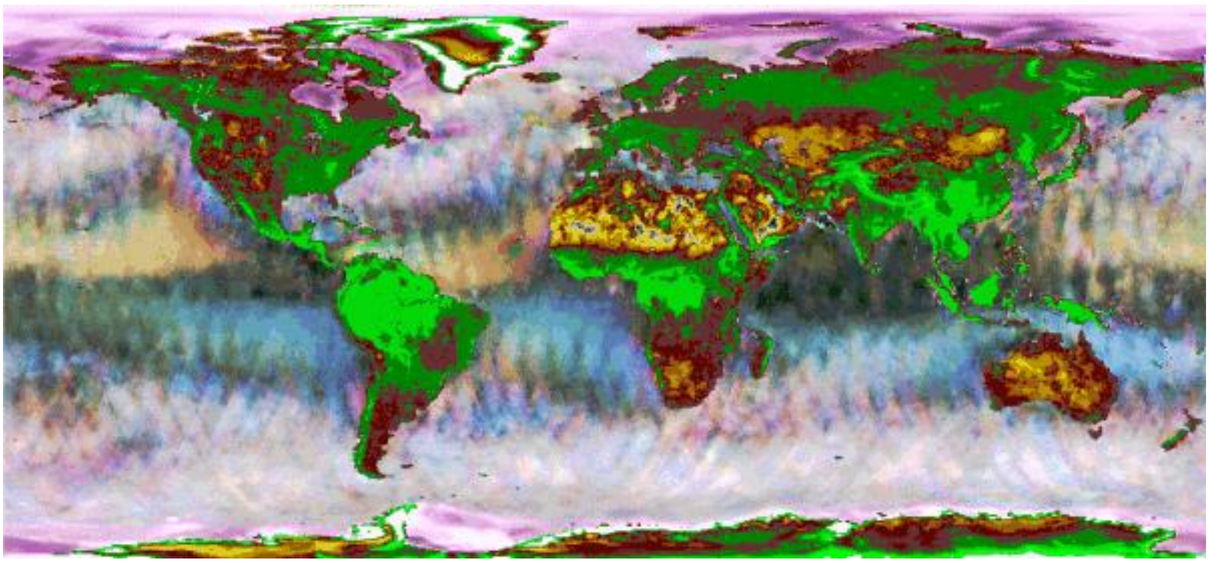

Figure 3.1. An 'impressionist' view based on the radar map of Earth's surface as observed by the ERS scatterometer. Sea ice is shown in violet, variable winds in grey and high winds in white, but with wind sensitivity depending somewhat on swath position. The yellow and blue in the northern and southern hemispheres indicate trade winds and correspond to higher signals in the fore and aft antennae, respectively, and thus indicate the directional stability of the wind in the intertropical regions. (Data processing by IFARS, Germany, for land surfaces, and by the ERS Product Control Service at ESRIN for oceans. (©ESA, 1998)

The design of all scatterometer missions was driven and optimised by the need to observe ocean winds. The first scatterometer in space was NASA's Seasat-A Scatterometer System (SASS), that flew for three months in 1978. SASS had four antennae, two on each side of the satellite (see e.g. Stoffelen, 1998). Each set of two antennae covered a swath – one to the right of the sub-satellite (ground) track and one to the left. In the horizontal plane, the fore and aft beams were pointing at 45° and 135° azimuth, respectively, with respect to the ground track. A location in the swath was first hit by the fore beam, and a few minutes later by the aft beam. Thus, each Wind Vector Cell (WVC) in the swath revealed two backscatter measurements obtained with a 90° difference in azimuth. Figure 3.2 illustrates the analysis of two such measurements. For each measurement it shows the wind speed solution as a function of all possible wind directions. Given the dependency of the backscatter signal on the basic harmonic wind direction, four solutions exist in this general case. This ambiguity poses a strong limitation on the usefulness of the SASS wind data, and extended manual efforts were needed to remove the ambiguity in order to obtain an acceptable wind product (Peteherych et al., 1984). The usefulness of this product has been demonstrated (see, e.g. Stoffelen & Cats, 1991).

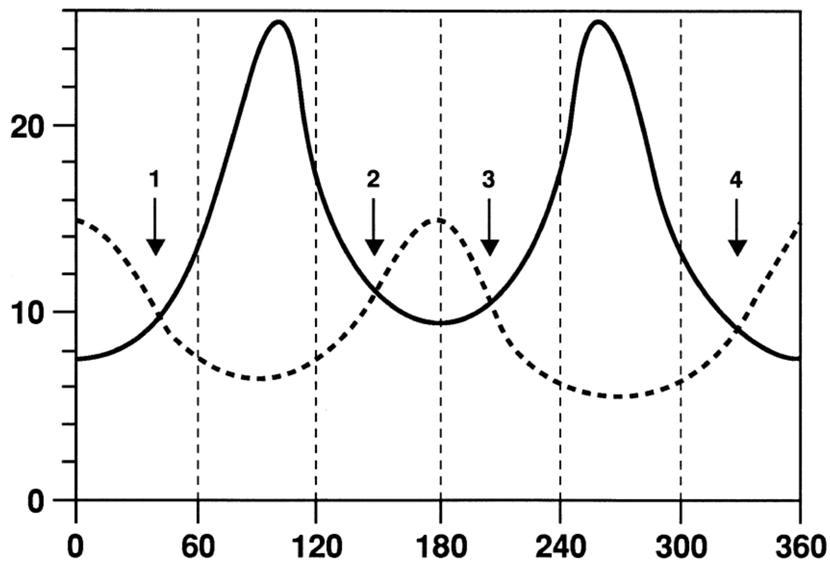

Figure 3.2. Wind speed as a function of wind direction for fore and aft beam measurements of backscatter from SASS data. The arrows indicate the four possible solutions for this typical case. (© Utrecht University, Stoffelen, 1998)

The scatterometers on ERS-1 and ERS-2 (here denoted ESCAT) were identical and each had three antennae that illuminated the ocean surface from three different azimuth directions (e.g. Stoffelen, 1998). A point on the ocean surface would be hit first by the fore beam, then by the mid-beam and soon after by the aft beam, see figure 3.3. Since this provided three measurements to determine two parameters, i.e., wind speed and direction, the ESCAT wind retrieval problem is overdetermined in principle. Moreover, the dominant harmonic azimuth dependence of the radar backscatter is a double harmonic (Long, 1986), which is ideally sampled by three azimuth angles 45° apart, enabling rather constant wind direction sensitivity of the ESCAT instrument (Stoffelen and Portabella, 2006). It was therefore anticipated (Attema, 1991) that this measurement geometry would generally result in (only) two opposite wind vector solutions and additional residual information (Maximum Likelihood Estimator or MLE), which could be used as measurement noise and/or quality indicator.

Based on the available technology, the C-band wavelength was chosen for the ERS microwave mission. With hindsight, this was a very fortunate choice as it provided sufficient wind sensitivity and little sensitivity to rain effects.

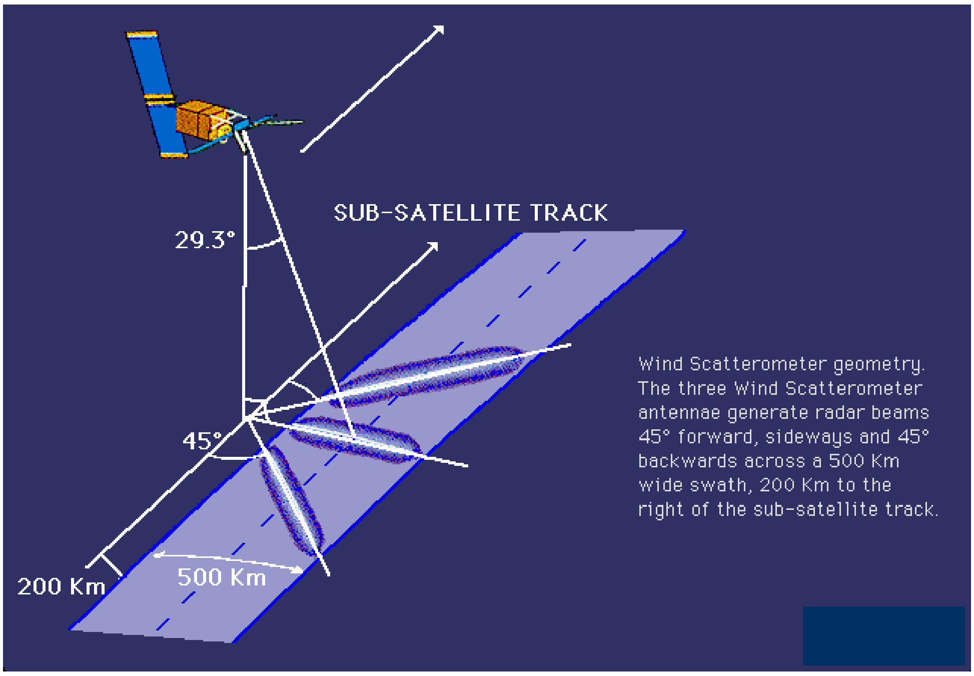

Figure 3.3: ESCAT wind scatterometer geometry (© ESA).

3.1.1 Measurement Space

At the launch of ERS 1, the European Centre for Medium-Range Weather Forecasts (ECMWF) model output was prepared to validate the ESCAT backscatter data and winds. However, comparisons of ESCAT and ECMWF backscatter and wind distributions, showed large differences depending on the radar beam, incidence angle, wind speed and wind direction. Since the ECMWF routinely monitors the quality of their winds and this had been intensified prior to the ERS1 launch, it was clear that there were some problems with the ESCAT winds. Since the bias patterns were very stable and repetitive, there was hope that they could be removed and NWP ocean calibration (NOC) was first used with success (Stoffelen, 1999). Remaining differences were subsequently investigated using the ESCAT measurement space.

Cavanié et al. (1986) made a 3D plot, where radar cross sections of the fore beam were plotted on the horizontal (*x*) axis, those of aft beam on the other horizontal (*y*) axis and mid-beam backscatter on the vertical (*z*) axis, as depicted in Fig. 3.4. They realised that due to wind speed and direction sensitivity, a two-parameter manifold or surface should emerge in such a 3D space. Stoffelen (1998) set out to make cross sections through this surface in order to observe whether the measured backscatter triplets would indeed follow a manifold and whether the manifold is well described by the C-band GMFs. This led to a true revolution in scatterometry, as described below.

The expected coherence in the measurement data was found and indeed the backscatter triplets are arranged in close proximity to a conical surface, as depicted in Fig. 3.4. The major axis of the 'cone' corresponds to variations in wind speed, whereas the minor axes represent changes in wind direction, confirming a basic sensitivity to the near-surface wind vector over the world's oceans (Stoffelen, 1997a, 1998).

The actual shape of the manifold has been characterised to high precision and the GMF has been improved accordingly (Stoffelen, 1998). The resulting C-band GMF, called CMOD5.N (Hersbach et al., 2007), is also used for Synthetic Aperture Radar (SAR; Portabella et al., 2002) and ASCAT wind retrieval (Stoffelen & Anderson, 1997a).

The measured triplets are spread across the ideal conical manifold and this spread has been characterised in detail by Stoffelen & Anderson (1997a). Later, Portabella & Stoffelen (2006) modelled this spread in the ERS data and found that at high winds it is mainly determined by radar (speckle) noise, but at low winds by local wind variability. Since the fore, mid and aft beams sample a WVC slightly differently, due to their different sampling sequences and footprint shapes, variable winds may cause the mean wind in the spatially integrated radar footprint over a WVC to be slightly different for each of the three beams. This effect is particularly relevant for low winds, as these generally show the highest relative variation in surface backscatter. The inconsistency in the spatial collocation of fore, mid- and aft beams and the resulting backscatter uncertainty due to local (sub-WVC) wind variability has been called 'geophysical noise' by Portabella & Stoffelen (2006).

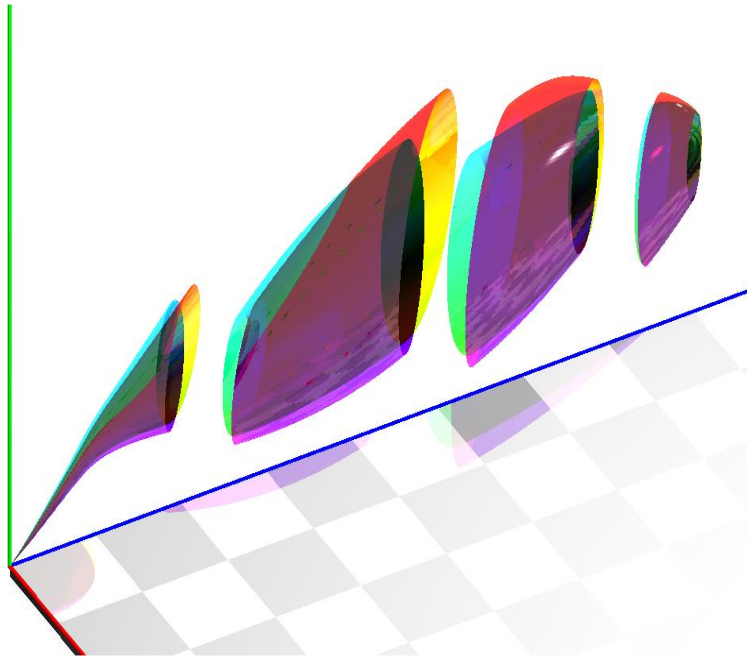

Figure 3.4. Depiction of the CMOD5.N GMF manifold at the outer ESCAT swath in measurement space spanned by the backscatter measurements of the fore antenna (red axis), the mid antenna (green axis) and the aft antenna (blue axis). The colours indicate the wind direction (red 0°, green 120°, blue 240°, all with reference to the mid-beam). The GMF is split at wind speeds of 10 m s^{-1}, 20 m s^{-1} and 30 m s^{-1}, respectively, to reveal its internal structure (Vogelzang & Stoffelen, 2012).

In the cross sections (as in Fig. 3. 5 occasional triplets are seen that lie almost in the middle of the cone (i.e. along its major axis) and rather far away from the wind GMF manifold (surface) as measured by the nominal noise parameters (Portabella & Stoffelen, 2006). These triplets do not correspond to good-quality winds and are rejected after wind retrieval by a Quality Control (QC) step. For ERS and ASCAT, about 0.5% of data over the open ocean (Portabella et al., 2012a) is rejected as being unlikely wind triplets. The same QC methodology has been applied to the NASA Scatterometer (NSCAT; Figa & Stoffelen, 2000) and SeaWinds instruments at the Ku-band with great success (Portabella & Stoffelen, 2001, 2002). At this wavelength about 5% of open-ocean WVCs are rejected by the QC procedure, most often due to rain clouds.

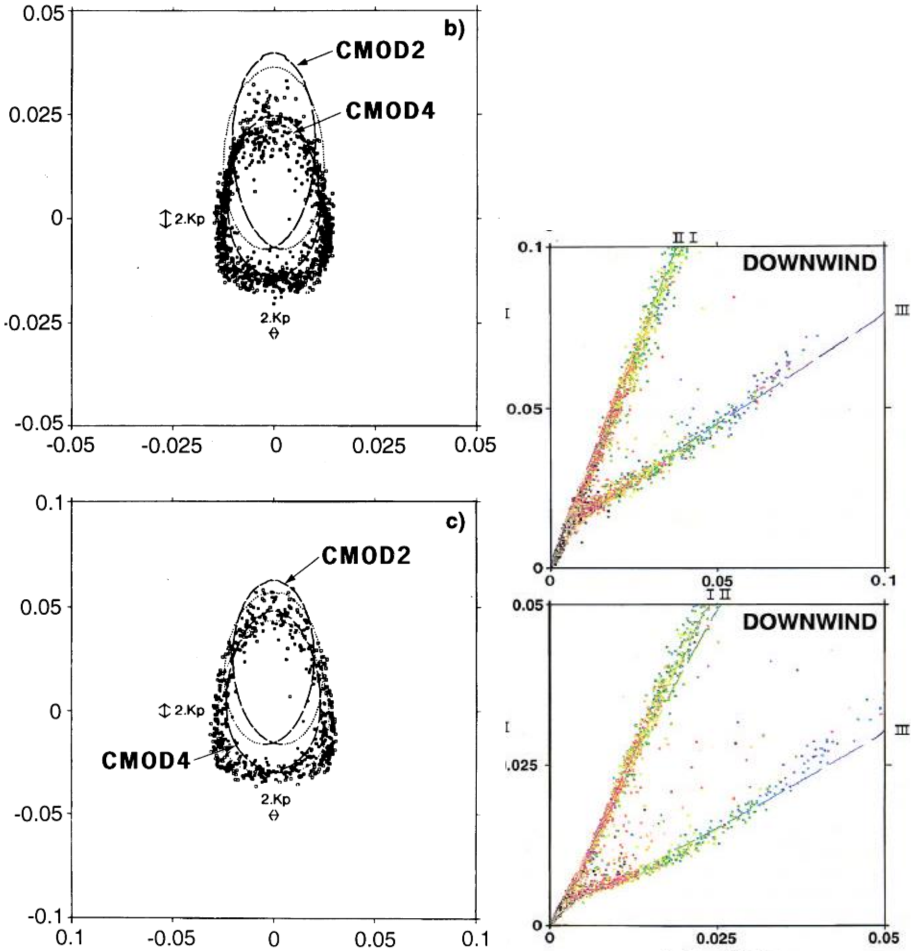

Figure 3.5. Cross sections through the manifold in the ESCAT measurement space (see Fig. 3.4) across the manifold (left panels) and along its main axis (right panels). (© AMS, Stoffelen & Anderson, 1997a)

It was also noted that in cross sections across the cone (Fig. 6, left panels) the measurements appear to be triangular in shape. Stoffelen & Anderson (1997a) realised that prior knowledge of this particular shape could be used in the wind retrieval in order to avoid irregularities (attractors) in the retrieved wind directions. They found a rather simple transformation of the backscatter measurement space that results in a circular manifold. A circular manifold has constant prior probability of each wind direction and is straightforward in the wind retrieval. Later, Stoffelen & Portabella (2006) noted that the wind retrieval in the transformed measurement space with a circular GMF manifold is regular since it results in a wind vector sensitivity that is rather smooth and constant. Lin et al. (2013) further refine the non-linear wind inversion by detecting and removing a few artificial high-rank wind solutions caused by cone geometry effects. However, while the transformation works well for ESCAT-type scatterometers, constant wind vector sensitivity cannot be obtained for rotating pencil-beam scatterometers. So, due to rain and measurement geometry rotating pencil-beam Ku-band scatterometers are difficult to handle, but the experiences with ESCAT resulted in unprecedented-quality retrievals for QuikScat and OceanSat-2 (Portabella &

Stoffelen, 2004; Vogelzang et al., 2011; Stoffelen et al., 2013). Table 1 provides evidence of the high accuracy of the C-band scatterometer products from ASCAT.

Table 3.1. Wind component error standard deviations with respect to the (different) scales resolved by the different scatterometer wind products as obtained by triple collocation. The lower the buoy error, the better the scatterometer product resolves the buoy scales, and thus the higher the resolution. (© AGU, Vogelzang et al., 2011).

Dataset	Buoy		ECMWF		Scatterometer	
	ε_v (m s^{-1})	ε_v (m s^{-1})	ε_v (m s^{-1})	ε_v (m s^{-1})	ε_v (m s^{-1})	ε_v (m s^{-1})
ASCAT-12.5	1.21	1.23	1.54	1.55	0.69	0.82
ASCAT-25	1.24	1.30	1.42	1.45	0.65	0.74
SeaWinds – KNMI	1.40	1.44	1.19	1.27	0.79	0.63
SeaWinds – NOAA	1.39	1.41	1.20	1.30	1.20	1.04

The final advance in the geophysical interpretation of the ESCAT backscatter data was its use to model sea ice and to discriminate between water and sea ice surfaces. Just like wind over water, sea ice has a very particular signature in the measurement space. Sea ice surfaces are generally isotropic with varying roughness. These features were first exploited by the group at IFREMER for ice type analysis (Gohin and Cavanié, 1994). It has further been developed for operational utilization in ice edge and ice type mapping in the context of the OSI SAF sea ice service (Breivik and Schyberg 1998; Breivik et al, 2001, 2012). Indeed, sea ice points lie on a line in measurement space, where the coordinate along the line depicts sea ice roughness (de Haan & Stoffelen, 2001). Subsequently, Bayesian methods were used to compute the probability of water in the WVC (Belmonte Rivas & Stoffelen, 2011). This method, first developed for ESCAT, is now also in use for the ASCAT, QuikScat and the OceanSat-2 scatterometers.

In summary, the advances inspired by the ESCAT measurement space revolutionised not only the ESCAT wind retrieval methodology, but also those of all other wind scatterometers.

3.1.2 Wind Quality

Besides the advances inspired by the ESCAT measurement space, the ERS era brought other innovations as well. The first was ocean calibration by NWP model wind fields (Stoffelen, 1999), which is still applied today to obtain inter-beam backscatter calibration and the highest-quality ASCAT winds (Verspeek et al., 2012). Another statistical assessment showing the high quality and consistency of the ESCAT and ASCAT instruments and wind retrievals was provided by Hersbach (2008); the plot in Fig. 3.6 was produced after calibrating both ESCAT and ASCAT data to the ECMWF model.

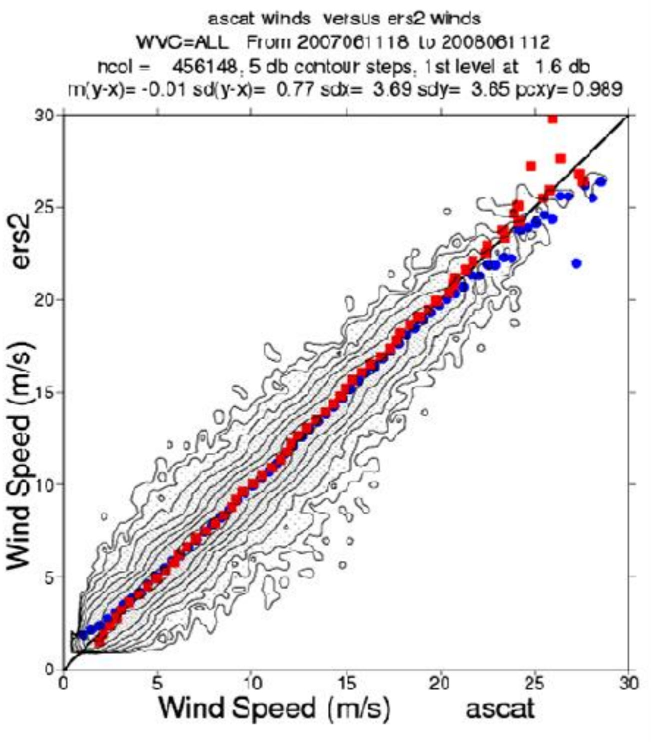

Figure 3.6. Joint distribution of collocated ESCAT and ASCAT winds with a Pearson correlation of 98.9% and standard deviation of differences of 0.77 m s^{-1}. The blue dots depict the average ERS2 wind speed in a 1 ms^{-1} ASCAT wind speed bin, conversely, blue dots are average ASCAT wind speeds in an ERS2 bin. (From Hersbach, 2008).

Another innovation was in triple wind collocation (Stoffelen, 1998), which is used today for ASCAT wind quality assessment (see Table 1), but also in several other Earth observation disciplines, such as quality assessments of soil moisture, sea surface temperature, sea ice drift, precipitation and altimeter wave height data.

Together, NWP Ocean Calibration (NOC) and triple collocation essentially tie the scatterometer winds to the global buoy wind network and at the same time provide statistical evidence of biases in the NWP model (e.g. ECMWF). NOC and triple collocation are performed routinely to assess the stability of scatterometer winds over time (see www.knmi.nl/scatterometer). Since the global moored buoy wind network is considered as an absolute reference, the combination of triple collocation and NOC may also be used to intercalibrate scatterometers, in particular ESCAT and ASCAT, with the objective of obtaining decadal scatterometer wind time series, soil moisture and ice products. These procedures are thus being applied to obtain a high-quality Fundamental Climate Data record for the ESCAT data.

Space-borne scatterometers provide unique global ocean surface vector wind products at high spatial resolution. Since they operate at microwave (radar) frequencies, these instruments are not hindered by cloud cover and hence are able to reveal phenomena such as polar front disturbances and tropical cyclone winds. Figure 3.7 shows mesoscale ESCAT winds (red) detected by the ESCAT instrument on ERS-2 and Numerical Weather Prediction (NWP) model winds (blue wind vectors). The ESCAT mesoscale wind details in the area where the cold northerly flow interacts with the warmer southerly flow line up well with the geostationary satellite cloud bands at the time of the ERS-2 overpass. The NWP winds describe only the larger scales well.

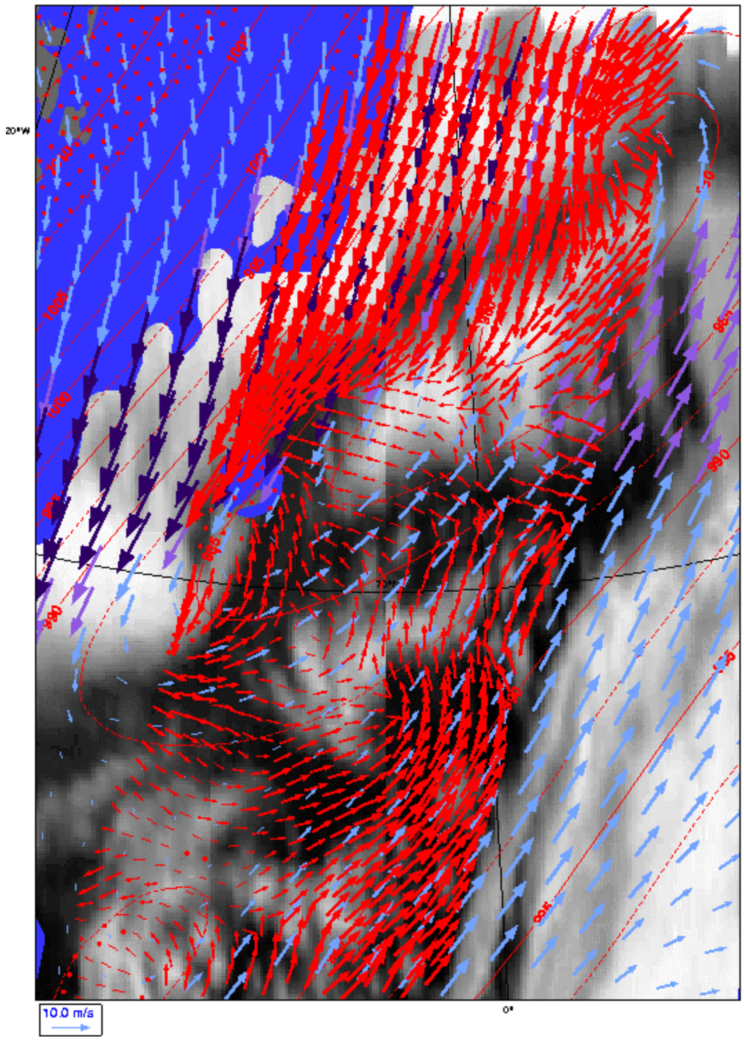

Figure 3.7. Scatterometer winds from ERS-2 at around 12:00 GMT on 24 Nov. 1999 at 70°N and 0°W (www.knmi.nl/scatterometer). The grey shading is a Meteosat IR image coherent with the scatterometer winds. Blue mask: areas where the sea surface temperature is below zero and sea ice is probable. Grey mask: land at 80°N and 20°W (top right). The red contours indicate surface pressure from the HIRLAM model at KNMI (3-h forecast). Blue and purple are the spatially smooth wind vectors from HIRLAM (the amount of purple increases with wind speed). The red wind vectors depict the spatially detailed ERS-2 winds. The red dots indicate where winds were rejected because of a confused sea state (bottom left) or the presence of sea ice (top left). Scatterometers reveal more coherent spatial detail than NWP winds. (© Eumetsat OSI SAF, 1999)

The excellent statistical verification of both ESCAT and ASCAT winds was corroborated by the inspection of wind maps such as the one shown in Fig. 3.7 (see www.knmi.nl/scatterometer). The spatially smooth wind vectors from the High-Resolution Limited Area Model, shown in blue and purple, depict a cold northerly flow on the left, adjacent to a warmer southerly flow on the right (the amount of purple increases with wind speed). The scatterometer winds from ERS-2 at around 12:00 GMT on 24 November 1999 in the Norwegian Sea (indicated in red) show much more structure and detail. Note that the grey-shaded Meteosat IR image is coherent with the scatterometer winds, with wind convergence patterns lining up well with cloud patterns, revealing details of the local meteorological conditions.

C-band scatterometer data are now widely used for hurricane prediction, Numerical Weather Prediction, marine nowcasting, oceanography, hydrology and studies of the cryosphere, providing societal and economic benefits in areas such as marine safety, offshore activities, ship routing, wind energy and climate change monitoring. The ESCAT research mission anticipated such a wide range of applications, with for example the near-real time availability of the scatterometer winds. The launch of ERS 1 inspired the development of novel analytical techniques using the measurement space of ESCAT, which confirmed the expected internal consistency of the ESCAT measurements and the low noise, but also provided improved characterisation of the sensitivity to wind speed and direction, resulting in improved GMFs. Moreover, the visualisation of the ESCAT measurement space provided insights into the nonlinear wind retrieval problem, which has subsequently been improved. It has also aided the discrimination of sea ice and water and has provided important insights into the wind retrieval quality control.

The ESCAT wind Cal/Val led to the further development of the triple collocation methodology that is now widely used in Earth observation. The lessons learnt from ESCAT were readily applied to the NASA scatterometer missions at the Ku-band and provided similar benefits, leading to improved rain screening and wind datasets. ESCAT has also been successfully applied in soil moisture, sea ice and snow characterisation, leading to operational applications. The ESCAT heritage has been important for the development of ASCAT on MetOp for the Eumetsat Polar System. The EPS Second Generation ASCAT is now being designed, where the ESCAT C-band static fan beam concept is being maintained due to its great success. This may well lead to over 40 years of C-band scatterometer data, which will be a tremendous resource for climate applications to study wind climatology, air–sea interactions, atmospheric processes, etc. The demand for the unique ESCAT wind, soil moisture, snow and sea ice data will therefore remain high in the years to come and continued ESA data and processing services would still provide great societal benefit.

3.1.3 ESCAT over land

European C-band fan-beam scatterometers are specifically designed for the monitoring of wind speed and direction over the oceans in support to operational applications. Over land surface, it was initially not clear if and how scatterometer observations might be useful. One particular concern was that the spatial resolution of scatterometers is simply too coarse to be of value for land applications due to the high heterogeneity of land surfaces. However, research carried out with ESCAT demonstrated the usefulness of scatterometer observations over land. The global systematic coverage achieved by ESCAT attracted several research groups who began to investigate the capabilities of ESCAT for mapping of vegetation (Frison & Mougin, 1996), soil moisture (Wagner et al., 1999b), freeze/thawing (Wismann, 2000) and snow (Drinkwater et al., 2001).

One of the scientific challenges faced by all initial land surface studies was the strong dependency of the backscattering coefficient on the incidence angle, which varies from 18° for the mid-beam in the near-range, to 59° for the fore and aft beams in the far range. Therefore, the backscattering coefficient changes significantly over the image swath, and from acquisition to acquisition, making the interpretation of the images, or time series, elusive without a prior correction or normalisation of the backscatter data. Thus many of the initial studies addressed this dependency by fitting a linear function to the backscatter measurements collected over a long period such as a month (Mougin et al., 1995; Schmullius, 1997), following a procedure previously developed for the SASS scatterometer by Kennett & Li (1989). This allowed studies of the relationship between the backscatter measurements and global land cover, and seasonal land surface dynamics due to vegetation phenology or freeze/thaw processes in high-latitude areas. Nevertheless, this monthly fitting procedure suppresses short-term signal fluctuations caused, for example, by changes in soil moisture, short-term freeze/thaw events, or changes in snow morphology, rendering a more physically based interpretation of the scatterometer data impossible.

More advanced modelling approaches have been developed in which the observed backscatter is decomposed into its different components taking advantage of the specific sensor geometry (providing measurements at different incidence angles), the physical properties of these components and the different temporal scales at which they act. One such approach is the method developed by Wagner et al. (1999b), where in one of the first processing steps the incidence angle dependency of σ^0 is determined for each land surface pixel and for each day of the year by comparing the quasi-simultaneous mid- and aft/fore beam backscatter measurements. This knowledge of the incidence angle behaviour then not only allows extrapolation of the backscatter measurements to a given reference angle (40°), but also separating the backscatter contributions due to seasonal vegetation growth and decay from the shorter-term soil moisture fluctuations (Wagner et al., 1999a). Furthermore, several semi-empirical backscatter models typically composed of bare soil backscatter- and volume scattering formulations for simulating backscatter of vegetation- and snow-covered surfaces have been developed (Magagi & Kerr, 1997; Pulliainen et al., 1998; Wen & Su, 2003; Woodhouse & Hoekman, 2000; Zribi et al., 2008). These semi-empirical models can be used to improve our theoretical process understanding and, at a more practical level, the simultaneous retrieval of soil moisture, vegetation and other land surface parameters (e.g. roughness) using iterative least-squares matching procedures. These models have been implemented over selected world regions with varying degrees of success, but not yet on a global scale.

3.1.4 ESCAT and sea ice

The extent of sea ice over the polar oceans is a critical parameter for understanding and forecasting ocean circulation and climate change. Further, updated sea ice information is crucial to NWP, globally as well as on regional scales at high latitudes. No satisfactory conventional observing system is available and sea ice is difficult to observe using satellite optical sensors because of the low level of illumination and the frequent cloud cover in polar regions.

Microwave instruments and in particular satellite-borne radars, such as scatterometers, are of great interest because of their large temporal and spatial coverage over the poles and their all-weather measurement capability.

The development of specific data analysis for scatterometer data led to several methods for detection of sea ice and to estimates of its extent, drift and age. A routine ESCAT processing was developed at the ERS Processing and Archiving Facility of the French Research Institute for Exploitation of the Sea (CERSAT/IFREMER) to produce fields of sea ice age, drift and extent, with polar coverage, on a weekly and monthly basis. Figure 3.8 shows an image of the ESCAT backscatter coefficient used to analyze the sea ice type in the Arctic Ocean.

The microwave backscatter over sea ice is dependent on the ice surface roughness and on the degree of volume scattering from brine pockets within the ice, both of which are related to the ice type and ice age. Sea ice which has survived at least one summer season is called multiyear ice and typically it has a rougher surface than first-year ice, and hence the backscatter is larger over multi-year ice. An exception to this, however, is ice in the marginal ice zone which, due to strong winds and waves, can appear very rough independent of ice type. Multi-year ice, in particular during winter, also has an additional backscatter signature compared to first-year ice as a result of volume scattering. Hence, scatterometer data are convenient for ice type classifications (Gohin and Cavanié 1994, Breivik et al. 2001). In the examples of ice type analysis from ESCAT backscatter data (Figure 3.8) the higher backscatter values (green-yellow) represented multiyear ice and the lower values (blue) represent first-year ice.

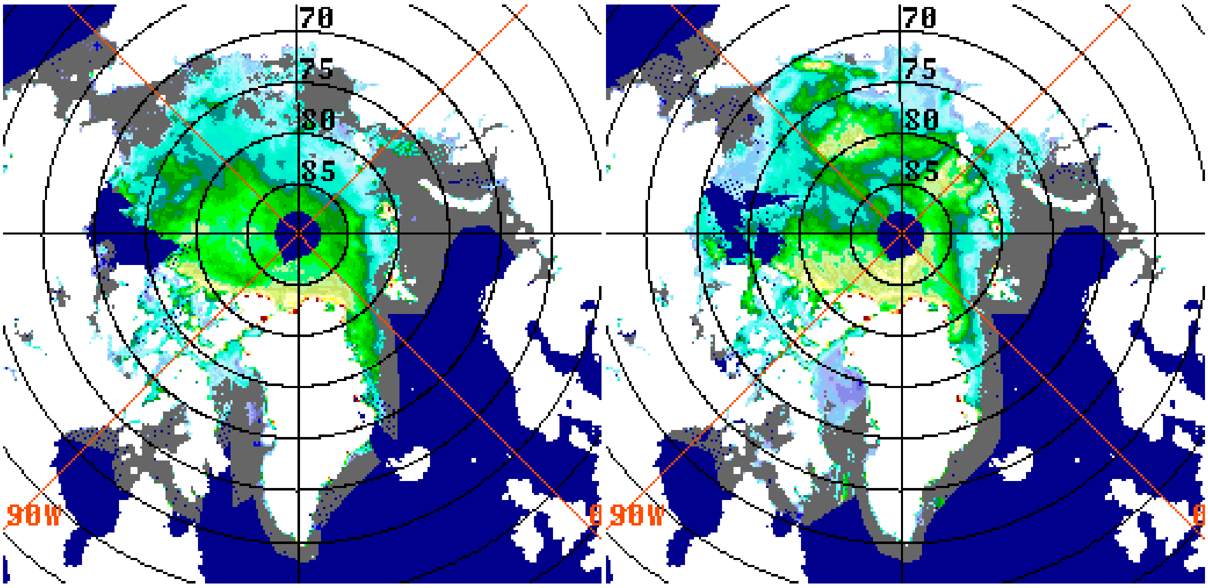

Figure 3.8. Images of the backscatter coefficient over the Arctic region, observed at an incidence angle of 40° during October 1995 (ERS-1, left) and October 1996 (ERS-2, right). Dark blue: unprocessed areas; grey: open water. The highest values of the backscatter coefficient are observed for multi-year ice, shown in green or yellow. This pair of images shows how the sea ice situation can differ from year to year. In 1996, new and multi-year ice covered the coastal zones of Siberia where large areas of open water were apparent in the 1995 image (CERSAT, 2011).

For the purpose of distinguishing sea ice from open water the measured backscatter cannot be used directly. However, the backscatter dependencies on the measurement geometry, which is also the basis for wind direction retrieval over the open ocean, can be utilized to distinguish sea ice from open water. Both the different viewing azimuth directions of the antennas (fore, mid, and aft) and their different incidence angles are used, see illustration of ESCAT measurement geometry on Figure 3.3. Firstly, backscattering is relatively isotropic over sea ice compared to the strong anisotropic behavior over open water. Secondly, the change of backscatter with incidence angle shows larger variation over water than over sea ice.

Pioneers in the field of utilization of C-band scatterometer data for sea ice detection were the group at IFREMER (Gohin&Cavanié 1994). Based on their suggestions the use of ESCAT data for operational sea ice monitoring was also demonstrated in the context of the OSI SAF project (Breivik et al. 2001; Breivik and Schyberg 1998).

It has also been shown, by de Haan and Stoffelen (2001) that over sea ice the scatterometer measurements are aligned along a line in the three dimensional backscatter space spanned by the three σ_0-measurements of the fore, mid and aft beam. An ice/water discrimination parameter is defined as the backscatter distance to this “ice-line”, reflecting the likelihood of a WVC to be sea ice, relative to the backscatter distance to the ocean model (cone) used for wind retrieval. Moreover, the position along the ice-line is related to ice age.

3.2 The Advanced Scatterometer (ASCAT)

Figa et al. (2002) describe the ASCAT scatterometer. ASCAT-A was launched in 2006, which mission was extended to a tandem ASCAT mission in 2011 with the launch of ASCAT-B. ASCAT-C has been launched in 2018. The main innovations of the ASCAT with respect to ESCAT are:

- Extended spatial coverage by a double swath, one on both sides of the sub-satellite track;
- A 10% increase in swath width;
- A move to higher incidence angles to enhance wind sensitivity;

Besides these instrumental changes, improvements were achieved in calibration, noise assessment, spatial resolution and geophysical processing as described below.

3.2.1 Calibration and ASCAT Performance

Anderson et al. (2012a) report on the validation of backscatter measurements from the ASCAT-A using a dedicated transponder facility in Turkey with three transponders. In the same year Anderson et al. (2012b) provided an analysis of ASCAT ocean backscatter measurement noise. The rain forest, ocean and sea ice are exploited to characterise the ASCAT-A and –B backscatter measurements, which are found to be accurate and stable, besides two small-amplitude ASCAT-A anomalies (Verspeek and Stoffelen, 2015).

This is confirmed on the cover of this report by cone metrics (Belmonte et al, 2017). The excellent calibration stability of both ESCAT and ASCAT make these instruments a reference for inter-calibration with Ku-band scatterometers and radiometers alike. Moreover, ERS- and ASCAT-based thematic climate data records (CDR) over land, ocean and cryosphere will be an excellent basis for the validation of climate data records based on model reanalyses, such as from ECMWF (ERA).

3.2.2 Spatial Resolution

Another major step forward is in the spatial processing of ASCAT products. It has been shown that box-car filtering results in improved products with winds in coastal areas, which were not possible with Hamming filtering as used in the day-1 ASCAT and ESCAT processing. Moreover, small-scale soil moisture and sea ice features are better preserved. Recently, much research has gone into the spatial processing of ASCAT data over sea

(Vogelzang&Stoffelen, 2017a,b), land (Hahn et al., 2014) and sea ice (Aaboe&Lavergne, 2016; Long, 2017), following research on ASCAT near-coastal winds (Verhoef et al., 2012), where improvements due to improved spatial filtering are found in all domains with respect to the nominal products. Moreover, taking into account the shape and orientation of the basic Spatial Response Functions (SRF) of ASCAT (Lindsley, 2016), and after a careful matching of the Cumulative SRFs (CSRF) of its three beams, a 5.6-km wind product with < 20 km spatial resolution has been constructed. A key asset for such resolution enhancement is the radiometric noise (Kp) (Vogelzang&Stoffelen, 2017b). Together with the SRFs it determines the maximum resolution achievable at an acceptable noise level. The on-board averaging for ASCAT severely limits the matching scenarios of aggregated backscatter measurements and should be avoided for SCA.

3.2.3 Wind Processing

Besides resolution enhancement, also much attention has been paid to GMF development, wind variability, spectra, moist convection and ambiguity removal for ASCAT wind processing.

Stoffelen et al. (2017b) describes the development of CMOD7, which is a VV GMF applicable for both ESCAT and ASCAT. It provides wind PDFs after the wind retrieval that do not depend on the across-swath position, nor on the instrument that provides the backscatter data, be it ESCAT or ASCAT. In addition, CMOD7 uses so-called stress-equivalent winds as input. Stress-equivalent winds are winds at 10m height that are corrected for both atmospheric stability and atmospheric mass density (de Kloe et al., 2017).

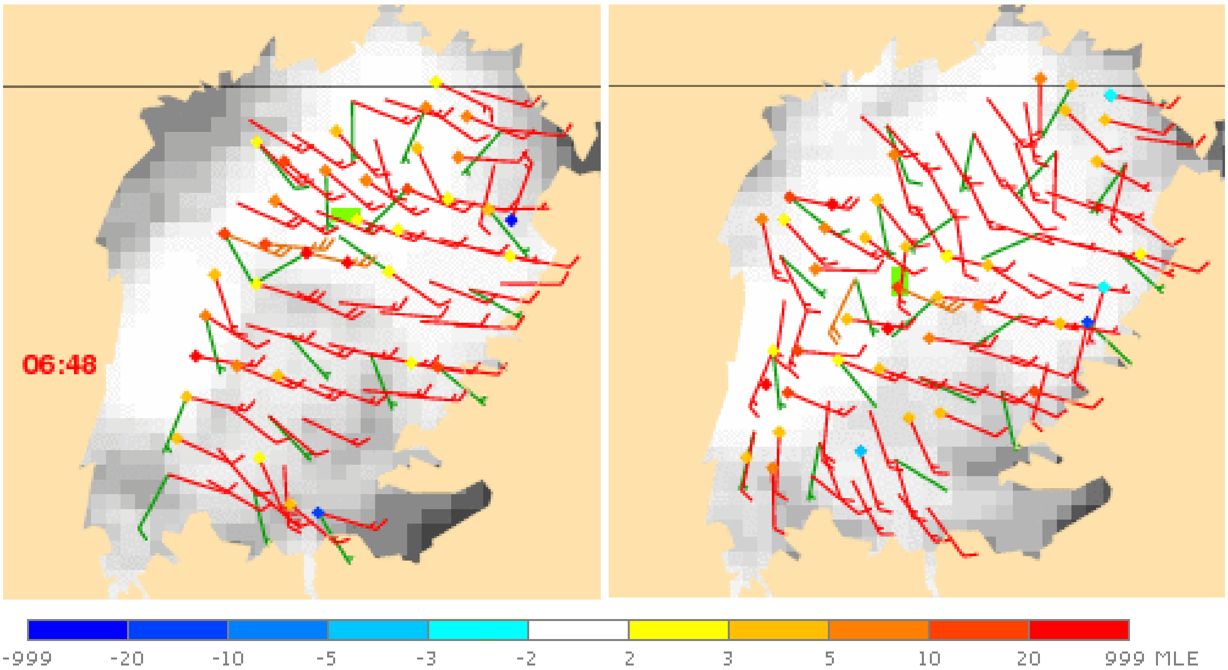

Figure 3.9. ASCAT (red arrows) and ECMWF (green arrows) wind fields together with collocated inverted MSG IR image (grey) and ASCAT wind variability (MLE color legend). ASCAT-A (left) on 8 Dec 2016 6:48 and –B (right) 50 min later.

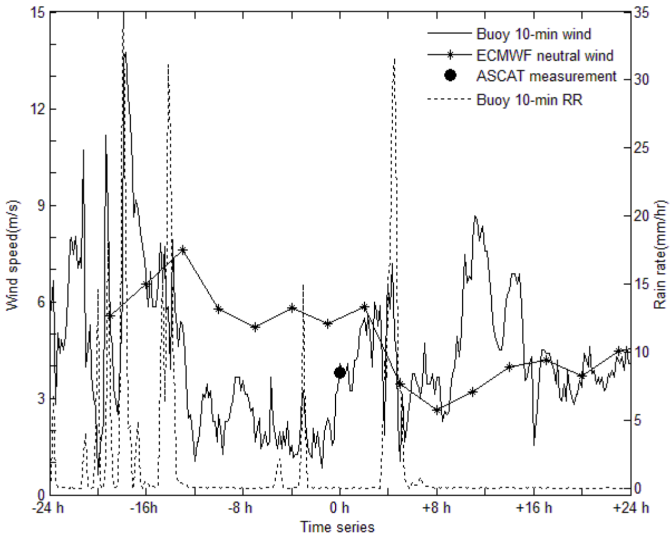

Figure 3.10. Wind speed (left axis) and rain rate (right axis) as functions of time at a rainy buoy location as explained in the legend. Time is centred around an ASCAT overpass (black dot) where the reference ECMWF forecast winds have base time at –25 h. (Portabella et al., 2012b)

Since C-band scatterometers are much less affected by rain than Ku-band scatterometers, the representation of deep tropical convection is better. While effects of splash, i.e., rain droplets roughening the sea surface, appear generally modest wind downbursts are widespread. The latter are due to air cooled by melting and evaporating precipitation, thus increasing its mass density and falling to the sea surface, where the air is deflected in the horizontal direction, often in a circular outflow pattern. The horizontal extent of downburst patterns is generally much larger than that of the associated rain patterns and changing fast (see Figure 3.9 for wind downbursts in Lake Victoria). Global models, such as ECMWF, generally lack these downburst. As a result, scatterometer winds can be much higher in areas with moist convection than NWP model winds as in figure 3.9.

Figure 3.10 shows a representative example of moored buoy winds in the tropics in the presence of rain. Wind shifts as large as 10 m s^{-1} are often associated with local rain. However, convective areas also show wind shifts when no rain is measured at the buoy. This is most likely due to the already mentioned horizontal extent of downburst areas being larger than those of rain areas. ASCAT winds are variable in convective areas, but prove a reasonable representation of the local buoy winds, given the rather high wind variance in the spatial representation difference of buoy and ASCAT. Triple collocation shows that the ECMWF model winds are clearly further away from the buoy winds, as expected, given the rather smooth wind fields in such convective areas (Portabella et al., 2012b; Lin et al., 2015). It may be clear that convective processes in the tropics have a rather large effect on the surface winds and air−sea interaction processes, but also on vertical exchange in the atmosphere and tropical circulation. It remains a challenge today to assimilate the full spatial detail as measured by a scatterometer into NWP models. Therefore, process studies using scatterometer data will remain necessary in order to exploit scatterometer data to the full.

3.2.4 Land

ESCAT research efforts led to the derivation of the first global long-term (1992−2000) soil moisture database from both ERS-1 and ERS-2 (Scipal et al., 2002; Wagner et al., 2003; see Fig. 10). Later on, this soil moisture retrieval model, initially tailored to ESCAT observations, was successfully transferred to the Advanced Scatterometer (ASCAT) on-board of the MetOp satellites (Bartalis, 2007; Naeimi et al., 2009) with a number of enhancements. Those datasets raised considerable interest and several validation studies carried out by independent research teams quickly demonstrated the high quality of the data (Albergel et al., 2012, Brocca et al., 2011, Dirmeyer et al., 2004; Drusch et al., 2004; Pellarin et al., 2006). This was unexpected because active C-band measurements had often been stated as sub-optimal for the retrieval of soil moisture. This was mainly because, first, active measurements are more sensitive to surface roughness compared with passive microwave measurements and, second, the C-band (λ = 3.8−7.5 cm) is less able to penetrate vegetation and the soil than the L-band (λ = 15−30 cm) (Wagner et al., 2007). However, it has been overlooked that scatterometers are well-calibrated space-borne instruments with a high radiometric accuracy and long-term stability. In retrospect, it can be said that this unexpected success was possible because of ESCAT and ASCAT unique characteristics:

- The multi-incidence angle viewing capability, which allows the separation of vegetation and soil moisture effects;
- The high temporal sampling rate, which allows researchers to exploit the advantages of change detection; and
- The excellent radiometric accuracy, which results in a suitable signal-to-noise ratio for the task of soil moisture retrieval.

3.2.5 Accumulated rain

The ASCAT soil moisture products inspired to develop products of accumulated rain (Brocca et al., 2014). The associated SM2RAIN algorithm delivered several rainfall products obtained from satellite soil moisture data, both from ASCAT and QuikScat (Brocca et al., 2015). The first rainfall datasets had daily temporal resolution, 1-degree spatial resolution and are available for the period 2007-2012 (Brocca et al., 2014). The more recent ASCAT datasets have improved spatial resolution at 12.5 km (hydrology.irpi.cnr.it/).

3.2.6 Cryosphere

The measure of the anisotropy and the change of backscatter with incidence angle can be derived and utilized for sea ice detection. In the context of the OSI SAF service, http://osisaf.met.no, these parameters were tested on ERS-1 data (Breivik and Schyberg, 1998). However, due to the limited ERS-1 and -2 data coverage, the method was never put into operational use. Ten years later this situation changed by the largely increased data coverage from ASCAT on Metop and ASCAT data has been in operational use in the OSI SAF for ice type and ice edge detection since 2009.

Compared to the traditional sea ice classification with low frequency passive microwave data, the scatterometer data results in more details along the ice edge and also captures better e.g. the multiyear ice outflow in the East Greenland Current. An important limitation in the algorithms based on scatterometer measurements is noise caused by certain wind directions leading to false sea ice detection. This can be compensated to some degree by using a multi-sensor approach adding information from other types of sensors, e.g. combining ASCAT data with observations from passive microwave like e.g. SSMIS or AMSR-2 (Breivik et al., 2012).

An extra ice/water discrimination capability is added by inclusion of dual polarization radars as provided by the Ku-band scatterometers NSCAT (1996–1997) and SeaWinds on QuikSCAT (1999–2010) both NASA/NOAA. Whereas the ESCAT and ASCAT C-band scatterometers operate in vertical polarization only (VV), the Seawinds Ku-band scatterometer had both HH and VV capability. The polarization ratio was defined and proved to be very sensitive to ice versus water. These data have been used for sea ice analysis with very good results (Remund&Long, 1999; Haarpainter et al. 2004). Belmonte and Stoffelen (2011) used the ice-line approach (see section 3.1), extended to utilize the dual polarization capability of the SeaWinds Ku-band scatterometer, and introduced the distance to an ice model as parameter in a Bayesian ice/water classification.

With the introduction of ASCAT, the coverage per day opened for utilization of backscatter data for ice drift detection. Low resolution ice drift datasets are computed on a daily basis from aggregated maps of passive microwave (e.g., SSMIS, AMSR2) or scatterometer (e.g. ASCAT) signals. The typical resolution/spacing of those input images is 12.5 km. Wide swaths, high repetition rates and independence with respect to the atmospheric perturbations permit daily coverage of most of polar sea ice. During fall, winter, and spring, the excellent coverage makes it possible to extract 48 hours global ice drift vectors at a spatial resolution of 62.5 km (Lavergne et al., 2010).

4 THE SCA INSTRUMENT

The C-band was chosen again because it provides good sensitivity, all-weather capability and continuity of the ESCAT and ASCAT series. Rotating pencil beam concepts were discarded due to poorer simulated performance, while rotating fan beam concepts were considered to be technically too complex, since ASCAT-SG would share a satellite platform with several other Earth-viewing microwave instruments (Lin et al., 2012; 2017).

Two technical limitations of the ASCAT instrument have been lifted in the design of the SCA mission. The first is an on-board along-track averaging, which currently reduces the resolution of the ASCAT backscatter data. The second is the merging of the transponder calibration signal in the SCA measurement cycle. Currently, transponder campaigns for ASCAT require switching off of the surface backscatter measurement mode and result in a reduction of spatial coverage near the Turkish transponder sites. The SCA instrument will thus provide more opportunity for spatial resolution enhancement and with less coverage gaps.

4.1 Technical summary

Measurement concept, principles, performances, including those expected from innovations w.r.t. heritage instruments.

In summary, concerning threshold and breakthrough requirements for cross polarisation, horizontal resolution and spatial coverage, the current MRD lists the following applicable SCA requirements:

MRD_SCA.001:
In any trade-off between horizontal resolution and spatial coverage the former shall have higher priority.

MRD_SCA.110:
The SCA shall provide:

- coverage ≥ 50% within 12 hours and 97% coverage within 48 hours (threshold);
- coverage ≥ 82% within 12 hours (breakthrough).

MRD_SCA.120:
The horizontal resolution shall be ≤ 25 km (breakthrough), ≤ 50 km (threshold).

MRD_SCA.130:
The horizontal sampling interval shall be ≤ 12.5 km.

MRD_SCA.190

The SCA shall operate, fulfilling the radiometric requirements, in VV polarisation as threshold and in VV and alternate polarisations as objective.

4.2 Scientific Challenges

The three SCA innovations correspond to scientific challenges in the area of GMF development, land and sea ice applications (Stoffelen et al., 2017). These challenges are elaborated below.

4.2.1 Cross polarization and HH co-polarization

The alternate VH polarization on the mid beams improves the extreme wind speed range and preliminary research has provided first empirical and theoretical insights on the VH and HV sensitivity at extreme winds (e.g., van Zadelhoff et al., 2014; Fois et al., 2015). Moreover, the NOAA hurricane hunters received a prototype SCA antenna panel that is being flown in their campaigns and compared to the on-board instrumentation, with proven capability in hurricane conditions (e.g., Esteban et al., 2006). Further elaboration of the VH GMF for wind, soil, and cryospheric applications will be necessary, as well as elaboration of the geophysical retrieval methodologies to include the VH and possibly HH sensitivity.

VH polarization measurements are very important for weather forecasting because they have the potential of extending the useful range of SCA wind speeds to 40m/s, or higher (Fig 4.1). Like for many others, it is a key part of the European Centre for Medium-range Weather Forecasts (ECMWF) strategy to improve forecasts of severe weather (Belmonte-Rivas et al., 2017) and for tracking severe tropical and extra-tropical storms an accurate analysis of extreme winds is important. Whilst extreme winds are relatively rare, their impact on economy and society is enormous and, due to increasing population and infrastructure, increasing over time.

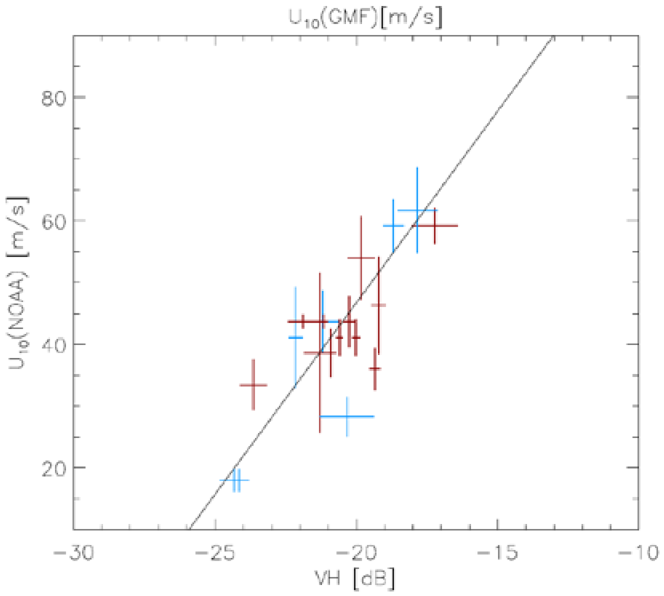

Figure 4.1. Extreme 1-minute sustained 10m wind speed gusts, derived from RadarSat VH-polarization and compared to air-based wind data from NOAA, cf. (van Zadelhoff et al, 2014).

In addition to extending the wind range, VH is expected to improve vegetation determination in conjunction with soil moisture retrieval (McColl et al., 2014). For example, Aquarius VH-polarized and VV-polarized backscatter observations at L band were compared to existing vegetation datasets (Hahn et al, 2015). The cross-/co-pol ratio captures vegetation dynamics over most vegetation zones well. Interestingly, differences in dynamics are observed between vegetation products from active and passive microwave measurements. VH is also expected to lead to an improved characterization of volume scattering effects by the vegetation, (dry) snow, and soil. This demonstrates that valuable information can be gained from vegetation products of scatterometers at VV, HH and VH (Hahn et al, 2015).

VH will help to better distinguish open water surfaces from surrounding land surface areas. Additionally, the higher sensitivity of VH to volume scattering in snow and sea ice is expected to further progress the monitoring of freeze/thaw processes and detection of open water surfaces versus sea ice. Experiences with cross-polarization C-band channels used for detecting sea ice are more developed with data from Synthetic Aperture Radar (SAR), which also measures the radar backscatter. Modern SAR systems, such as RADARSAT-2 and Sentinel-1, use a C-band radar and provide data at different pre-selected polarizations. In the ice charting community the HH- and HV-polarizations are often used for sea ice monitoring. The contrasts between ice and water are higher in HH-polarized images than in VV images (Partington et al., 2010). However, over open water and high winds, the co-polarized backscatter from both HH and VV is similar to that of sea ice, such that the separation of ice and water may be difficult (Belmonte-Rivas et al., 2011). The cross-polarized (HV or VH) backscatter is much lower and therefore better suited for ice-water discrimination in regions of strong winds (De Abreu et al., 2003). The additional polarization channels on SCA are therefore expected to provide very useful contribution to sea ice detection.

Over water surfaces VH signals are about 15 dB lower than VV. This may possibly pose measurement limitations, due to the 1-3 degrees Faraday polarization rotation in the ionosphere (Burn, 1966), causing an emitted pure vertical polarization (V) signal to become partially horizontal polarization (H) and vice versa. This implies that emitted vertical polarization results in HH scattering off the ocean surface, which in turn contaminates the VH measurement, since it implies the measurement of H. Van Zadelhoff et al. (2014) used combined satellite VV and VH measurements in hurricanes and found little angular dependence of the VH measurements, implying little contamination by HH as this has strong angular dependency. It should be noted, however, that those measurements (cf. fig. 4.1) were taken during a period of solar inactivity and thus reduced Faraday rotation. A main investigation for SCA will remain in the characterization of this effect. In particular, spatial and geographical variations will be of interest, as well as the capability to forecast the Faraday rotation.

At the extreme winds, the difference between VV and VH is much reduced and Faraday rotation effects on VH thus limited; hence, this is not compromising the main SCA mission of measuring extreme winds where VV and HH polarization measurements are saturated.

The required SCA VH capability implies HH measurements become possible too. Over the ocean HH sensitivity is lower than VV sensitivity and thus replacing VV with HH is tested to be generally not beneficial. However, over land surfaces the new co-polarization (HH) channel will in particular help to improve the quality of the soil moisture retrievals due to the reduced sensitivity of HH (compared to VV) to vertically oriented vegetation elements over grassland and agricultural areas (e.g., see Fig. 4.2).

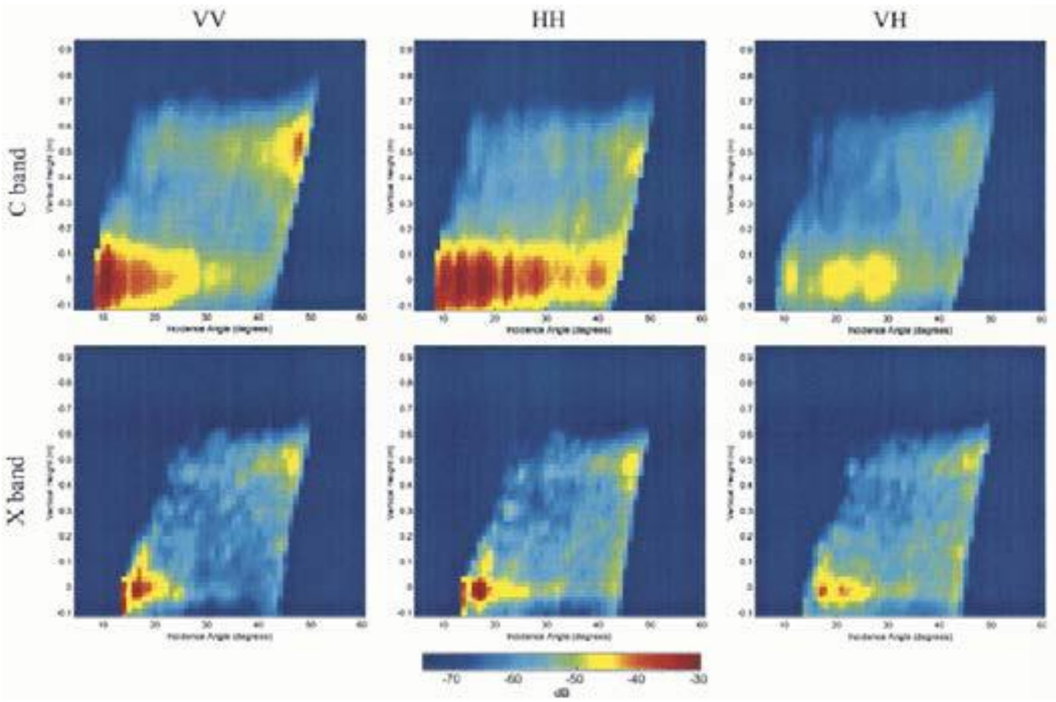

Figure 4.2. Radar cross section images of a green and 58 cm tall wheat canopy acquired by an experimental profiling radar at C- and X-bands at VV, HH, and VH polarizations. Horizontally the incidence angle ranges from 5 to 60 degrees and vertically height from -11 to 93 cm. Soil returns appear most dominant in C band, whereas HH shows the strongest soil signal due to the reduced extinction of horizontally oriented waves by the predominantly vertically oriented vegetated elements. From (Brown et al., 2003).

Taking note of the scientific advances in our understanding of the interaction of microwaves with the land surface, one can confidently predict that SCA will not only allow for improved soil moisture and freeze/thaw retrievals, but also for delivering several novel data products, including but not limited to vegetation water stress (Steel-Dunne et al., 2012; Frolking et al., 2011; Schroeder et al. 2016), vegetation optical depth (Vreugdenhil et al, 2016), and aerodynamic roughness [46]. Over land, renewed efforts in building advanced backscatter models (Quast&Wagner, 2016) and new experimental approaches (e.g., Morrision, 2013) are needed to better disentangle the backscatter contributions from different parts of the vegetation canopy and the soil profile. This will improve not only the quality of the soil moisture retrievals, but will at the same time allow the development of new land data products for SCA. Moreover, for semi-arid regions there is a strong need for further research to understand the co- and cross-polarization scattering contributions from the stratified upper soil layers and their dependence on environmental conditions.

4.2.2 Spatial Resolution

Many users cry out for increased spatial resolution products, but producers need to strike a complex balance between technical feasibility, spatial coverage, spatial resolution, noise and achievable information content.

Over the ocean, the SCA breakthrough horizontal resolution of 25 km will give a better handle on physical processes such as turbulent flows, convective systems, tropical cyclones, polar lows, coastal phenomena, air-sea interaction, eddy-scale oceanography and tropical circulation. In particular, improvements in the coastal region brought by increased resolution will be beneficial for many weather and climate applications.

Over land, the higher resolution of SCA will result in better resolved soil moisture and temporal soil characterization. For soil moisture many geophysical applications such as hydrology and agriculture request high spatial resolution and there is no satellite mission proposed that fully meets all requirements. Whilst instruments like SMOS and SMAP operate at a longer wavelength (L-band) to enhance their sensitivity to soil moisture under vegetation, as compared to C-band (Kerr et al., 2001; Brown et al, 2013), their spatial resolution remains rather coarse, leading to adverse error properties (Miyaoka et al., 2017). Also Sentinel-1, which like ASCAT provides C-band VV+VH backscatter observations, albeit at a much increased spatial resolution (20 m), is very promising (Hornácek et al., 2012). However, its temporal sampling rate varies from bi-weekly in well sampled areas such as Europe to bi-monthly for most of the global land surface.

Over sea ice, the higher SCA resolution will provide improved sea ice characterization and drift determination. High-resolution twice-daily and improved-sensitivity measurements will aid in the development and understanding of, e.g., dynamical sea ice models, particularly in the marginal sea ice zones. If scatterometer observations are indeed available at much higher spatial resolution they can add significant new information. Recently, much research has gone into the spatial processing of ASCAT NRCS data over sea (Vogelzang and Stoffelen, 2017a; b), land (Hahn et al., 2014) and sea ice (Aaboe&Lavergne, 2016; Long, 2017), following research on ASCAT near-coastal winds, where improvements due to improved spatial NRCS filtering are found in all domains with respect to the nominal products. Moreover, taking into account the shape and orientation of the basic Spatial Response Functions (SRF) of the ASCAT NRCS (Lindsley, 2015; 2016), and after a careful matching of the Cumulative SRFs (CSRF) of its three beams, a 5.6-km wind product with < 20 km spatial resolution has been constructed. A key asset for such resolution enhancement is the radiometric noise (Kp) (Vogelzang and Stoffelen, 2017a). Together with the SRFs it determines the maximum resolution achievable at an acceptable noise level. For land and sea ice applications, further resolution enhancement is possible in principle for ASCAT by combining the SRFs of the three beams for different azimuths and times, as these targets are less anisotropic and more stable (Long, 2017). Yet, ambiguities will remain, particularly in case of mixed pixels (e.g. mixture of wet snow, standing water and thawed ground). Therefore, approaches like the one proposed by who combined the backscatter data with auxiliary data set (like air temperature) for freeze/thaw detection should be further investigated.

As compared to ASCAT, SCA will have a reduced size of the SRF by a factor of two, improved radiometric noise and no on-board averaging, all of which will help in achieving increased resolution over sea, land and ice, to the benefit of the SCA product users.

4.2.3 Coverage

Coverage matters due to the fast evolution of small-scale atmospheric processes and a scatterometer constellation is needed for dense time coverage over land and oceans. Soil moisture evolution and the extraction of precipitation estimates from it, similarly critically depends on complete coverage (Brocca et al., 2017). Frustratingly, frequently key weather events are missed due to incomplete coverage by ASCAT. The wider swath will improve the ASCAT coverage (by 20%) and makes SCA more comparable to existing Ku-band scatterometers in this respect. Another aspect is to ascertain that we do gain more impact in NWP if there is less overlap between the successive scatterometer swaths, i.e., increasing the total spatial coverage.

With more agencies now building and operating scatterometers (e.g., the Indian ScatSat, the future HY and FY Chinese satellites and the Chinese-French CFOSAT scatterometer), a multi-agency constellation is being progressively built to better address spatio-temporal coverage. EPS Metop-SG will have a consolidated mid-morning orbit position in this constellation (CEOS, 2017).

Given the launch schedule of Metop/Metop-SG satellites and the typical lifetime of scatterometers, a tandem SCA configuration may be offered for the benefit of all scatterometer applications. This may provide almost complete coverage in a single pass of the tandem, when the tandem is optimally separated by a quarter orbit length, as illustrated in Fig. 4.3. For ASCAT the 50 minute separation for Metop-A and Metop-B has not been optimal since this leaves significant coverage gaps in the tropics and the overlapping data are fairly close in time (Cotton, 2013). Depending on the end of life scenario for Metop-A, there may be an opportunity to compare the impact of two ASCAT's at 50 min separation (e.g., ASCAT-B/A) with two ASCAT's at 30/70 minute separation (e.g., ASCAT-B/C). With three Metop's in orbit at the same time one could obtain a direct comparison of these configurations through conducting observing system experiments within NWP.

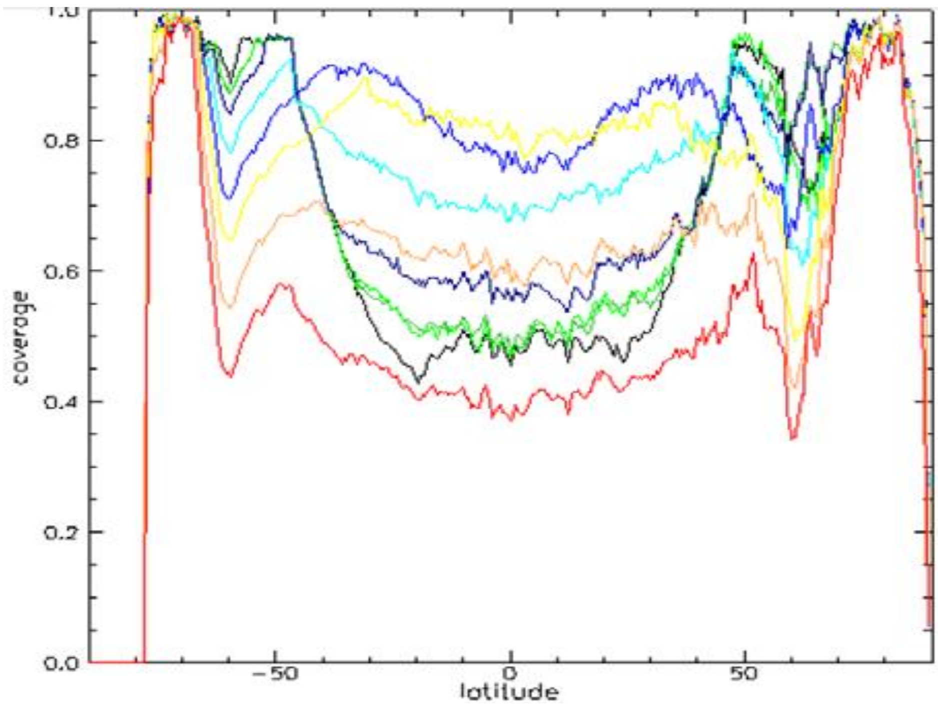

Figure 4.3. Tandem coverage over sea for different ASCAT-A and ASCAT-B orbit phase separations (Verspeek and Stoffelen, 2009). SCA's tandem coverage will be larger.

4.2.4 Potential Doppler Capability

A SCA Doppler capability would offer several opportunities for improving scatterometer products. Recently, over ocean, C-Band Doppler shift measurements as obtained with SAR revealed that the geophysical contribution to the Doppler shift includes ocean surface currents, sea-state and local wind-induced ocean surface velocity contributions. Chapron et al. (Chapron et al., 2005) (qualitatively) and then Rouault et al. (2010) (quantitatively) show how the ocean current contribution to the Doppler shift can be measured after a careful correction of the sea state contribution, based on ancillary information on the wind vector, which is the prime SCA mission. Furthermore, on a global scale and at 10 km resolution, wind can be used as a proxy for ocean motion (Chapron et al., 2005). This leads Mouche et al. (2012) to propose a first forward GMF that relates wind speed and direction (with respect to antenna look direction) as a function of incidence angle (17°-42°) for both VV and HH to a geophysical Doppler shift. They show for SAR how Doppler helps to constrain the wind retrieval (Fig. 4.4). In particular, it helps the wind direction retrieval in complex situations such as atmospheric fronts and low pressure systems. Moreover, for extreme winds, the Doppler wind direction sensitivity could be very complementary to the cross-polarization radar cross-section, since cross-polarization has no sensitivity to wind direction (Lindsley, 2016). Therefore, Doppler information may enhance scatterometer wind retrieval and ambiguity removal, and improved wind vector information will in turn enhance ocean surface current determination. Scatterometer winds are measured relative to the moving ocean surface, which wind vector frame is often most relevant for operations at sea. However, buoy and NWP model winds are provided with reference to a fixed Earth reference. Comparison of scatterometer and buoy and NWP datasets therefore require that ocean currents are known (Belmonte and Stoffelen, 2019). Direct eddy-scale current measurements would greatly improve ocean modeling, particularly in the tropics. After a first simulation study, Fois et al. (2015) showed the potential of SCA to determine ocean currents. This potential is currently further elaborated taking the specific SCA design into consideration and in particular investigating if the required performance can be achieved in practice (Hoogeboom et al., 2018).

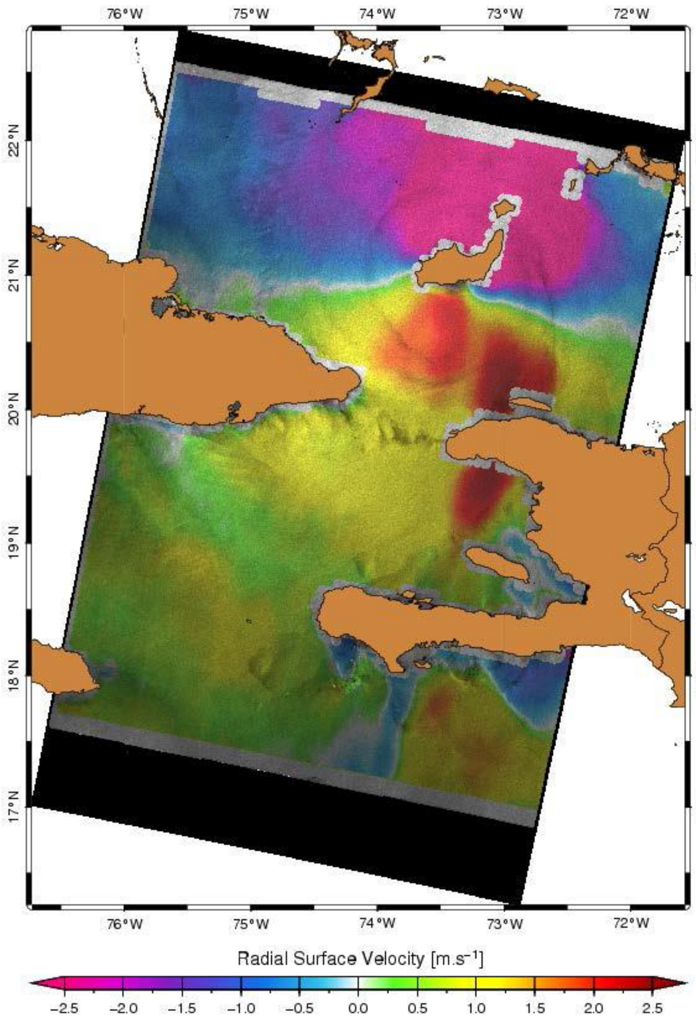

Figure 4.4. Radial surface velocity as measured in hurricane Ike on 8 September 2008 14:53 UTC by ESA ENVISAT Doppler capability. Ocean motion in excess of 2 m/s is seen towards (red) and away (purple) from the SAR, which provides essential wind direction information.

5 SCIENTIFIC PROSPECTS FOR SCA APPLICATIONS

Following the above-noted enhancements offered by the SCA instrument, due progress in scatterometer applications is elaborated below. Such anticipated progress is associated with the SCA innovations and therefore necessary for maximal operational SCA benefit in the application areas.

5.1 Using SCA Wind Variability

Stoffelen (1998), and Portabella and Stoffelen (2001) found that the normalized inversion residual, called MLE, is well capable of removing cases with extreme wind variability (at fronts or centers of lows), or with other geophysical variables affecting the radar backscatter. Recently, further progress has been made in the quality assessment of ASCAT winds near rain (Portabella et al. 2012; Lin et al., 2015; Lin et al., 2016) and it is confirmed that the MLE mainly represents enhanced wind variability. Generally, the MLE is positive and large when there is substantial wind variability within the cell, see e.g., Figure 2.1. Negative MLEs occur for stable flows.

Enhanced positive MLE corresponds to wind shifts due to convective downbursts, fronts and other dynamical phenomena. Such phenomena may span several Wind Vector Cells (WVC) and a local spatial analysis of MLE and singularity exponents (SE) provides an effective Quality Control (QC) (Lin et al., 2015). Singularity exponents are obtained from singularity analysis (SA), a spatial image processing technique, effective in detecting local decorrelation in a field. Also, such measures of wind variability are much desired in scatterometer applications, such as nowcasting and NWP.

5.2 Improving Land Applications

As mentioned above, scatterometers have a high potential for monitoring vegetation dynamics due to the fast revisit time and the VH cross-polarization measurement at high radiometric accuracy. This allows the depiction of seasonal and intra-annual changes in the incidence angle behavior of the backscatter measurement with high accuracy. This may be highly valuable information for monitoring of vegetation dynamics by the vegetation optical depth (Figure 5.1), which is closely related to vegetation water content and height (Vreugdenhil et al., 2016). By averaging backscatter measurements over longer time intervals, information about vegetation characteristics can also be estimated from averaged backscatter measurements (Schroeder et al., 2016) or by comparing diurnal differences in backscatter (Steele-Dunne et al., 2012). Such information will improve the retrieval of soil moisture but can also be exploited as a self-standing product.

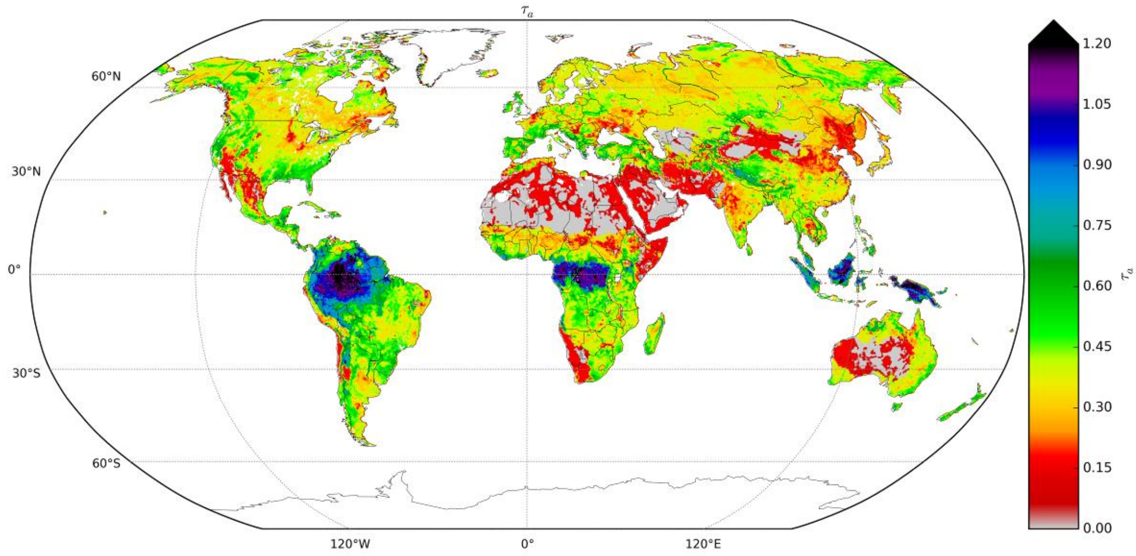

Figure 5.1: Global map of average vegetation optical depth τ_a retrieved from ASCAT.

Additional improvements in the soil moisture product are expected from a better characterization of scattering in arid and semi-arid environments. Backscatter from vegetated and bare soil is in general positively correlated with soil moisture. However, over some arid and semi-arid environments, an inverse relationship is observed (Figure 5.2). Wagner et al. (2013) hypothesized that this phenomenon is caused by the high penetration of microwaves into dry soil and the presence of strong sub-surface scatterers in line with recent experiments (Morrison et al., 2012; Liu et al., 2016). Potentially, extension of this research may lead to a better understanding of land degradation and desertification processes.

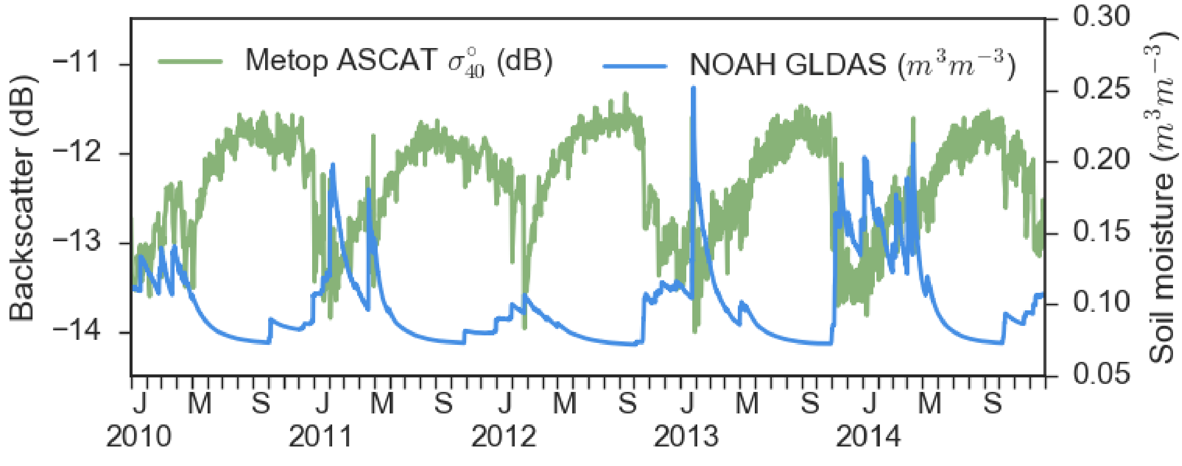

Figure 5.2: ASCAT backscatter time series (normalized to 40° incidence angle) over a desert area in Saudia Arabia (30.72°N, 40.85°E). The backscatter time series shows an inverse behaviour as the soil moisture time series modelled by NOAH GLDAS (Rodell et al., 2004).

5.3 Sea Ice Application Evolution

The microwave backscatter over sea ice is dependent on the ice surface roughness and on the degree of volume scattering from brine pockets within the ice to which VH is sensitive.

Current experience has been gained with classification of sea ice from the Sentinel-1 satellites. As an input to manual ice charting the Sentinels are great both in terms of quality and coverage. However, when it comes to automatic ice classification there are considerable challenges, mainly due to processing artifacts in the SAR image such as scalloping and gain-shift, particularly at low winds over water. The largest differences between SAR and scatterometer are the higher resolution of SAR, the multiple viewing directions of a scatterometer, and the superior calibration stability of a scatterometer. Because of the SCA calibration stability and accuracy we expect to see an improved objective classification based on the SCA VH, albeit at coarser resolution. Therefore, the prospect of combining the measurement from Sentinel-1 and SCA, which are otherwise very similar, are indeed very promising. In the context of the Copernicus Marine Environment Monitoring Service (CMEMS) work is ongoing to combine Sentinel-1 data with passive microwave data. SCA and MWI will simultaneously provide the synoptic full polarimetric capability at both poles. The potential areas of usage range from high resolution automatic ice charting for tactical navigation to large-scale sea ice analysis to support, e.g., climate models.

5.4 Backscatter Assimilation over Land.

Today, a number of users (e.g., ECMWF, Météo-France, UKMO) assimilate the ASCAT surface soil moisture product. Over vegetated areas, this product is affected by the vegetation structure and water content and this may impact the amplitudes of seasonal and inter-annual variability. As a result, a complex seasonal rescaling has to be performed before the integration of this product into Land Surface Models (LSMs). Some LSMs have a representation of plant growth (above-ground biomass, vegetation type, LAI). Potentially, such models could provide the missing information about vegetation. At the same time, the backscatter signal could help analyzing vegetation biomass together with soil moisture. An interesting development would be to develop (simple, e.g., quasi-linear) observation operators in land surface models giving the LSM the capability to simulate backscatter. This would, in the future, allow the assimilation of multi-angle and/or resolution-enhanced backscatter products over land.

A driver for improvements to the global observing system for LSM is an increasing need for information on the 10-km scale, as global and regional NWP models move to ever higher horizontal resolutions. In the next few years global weather forecasting will explore LSM resolutions below 10 km, e.g. ECMWF anticipates a resolution of 5-km (T3999) around 2020. With sub 10-km grid lengths we would expect LSM to resolve much smaller scales, e.g., coastal effects, and other sharp LSM gradients, probably associated with the presence of extreme weather conditions.

5.5 Wind Assimilation

For wind data assimilation we may identify the deterministic scale, which is the scale supported by observations in both space and time to deterministically initialize the smallest (short-lived and small-amplitude) evolving scales in weather models (Abdalla and DeChiara, 2017). These scales will remain larger than 100 km over sea due to persisting lack of temporal wind observation coverage (Stoffelen et al., 2018a). In addition, the effective dynamical model resolution may be defined, which is 5-10 times the grid length (Marseille and Stoffelen, 2017) and smaller than the mentioned deterministic scale. The ongoing challenge will be to maximize the benefit from higher resolution observations to help support small-scale structures, whilst the temporal coverage over sea remains limited (CEO, 2017). This means that model scales smaller than the deterministic scale, essentially weather model noise, need to be accounted for in data assimilation for the first time. For regional NWP, very-high horizontal resolution models with grid lengths of 300 m or less are anticipated at the Met Office and elsewhere. For fine-scale model grid lengths it will be important to take into account the scatterometer footprint to reduce the representativeness errors and take account of the deterministic scales (Marseille and Stoffelen, 2017). With increased supercomputer resources, mesoscale model improvements can be expected from the use of rapidly updating 4D-Var assimilation schemes, resolving the temporal and spatial scales of convection. Further research will be needed to develop more realistic, situation-dependent model and observation error schemes (based for example on the wind variability within the resolution cell (Lin et al., 2014)) that can improve the balance in the weight given to observations and background and provide the optimal spatial filtering in the analysis.

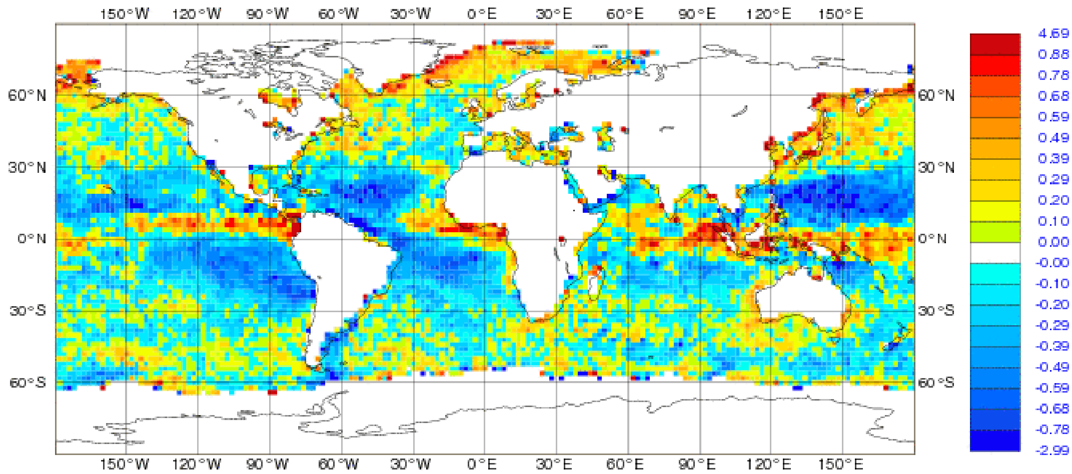

Figure 5.3. Accumulated statistics for 10-m equivalent-neutral mean wind speed differences between ASCAT-A and ECMWF first guess for the period from 21:00 UTC on 31 October 2015 until 9:00 UTC on 5 December 2015 in boxes of 2 by 2 degrees in ms^{-1}.

NWP data assimilation is based on a Best Linear Unbiased Estimate (BLUE), and generally bias correction schemes are used to remove observation minus model biases. Figure 5.3 shows typical NWP model biases against scatterometers. We note that the largest differences between scatterometer and ECMWF model winds appear in regions near the ITCZ, regions with ocean currents and near land masses or sea ice. These areas correspond to areas with large atmospheric dynamics and extensive moist convection. Besides substantial speed biases, substantial systematic wind direction biases also exist (Sandu et al, 2011; Belmonte&Stoffelen, 2019). NWP biases occur in all NWP models and are due to fast or mesoscale processes resolved by the scatterometer, but not by models, such as (moist) convection (Lin et al., 2016), atmospheric turbulence (King et al., 2014), gravity waves and systematic errors in boundary layer parameterizations or the lack of ocean currents. These biases tend to persist over time (not shown). The occurrence of these spatial biases is however ignored in data assimilation and their existence prevents the correct assimilation of observed dynamical weather features, following BLUE, and it thus may be worthwhile to develop local bias reduction schemes for scatterometers (Stoffelen&Vogelzang, 2018).

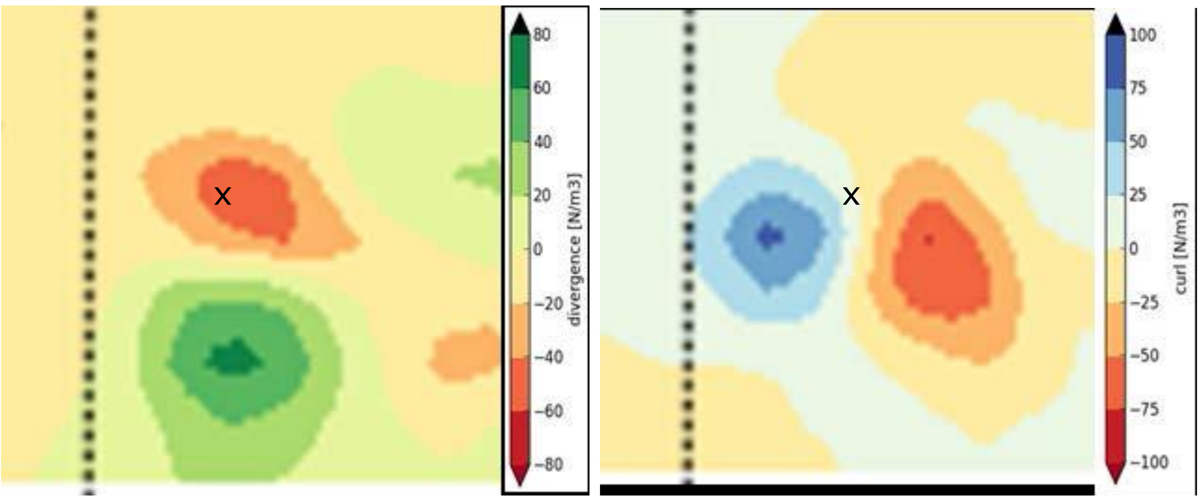

Figure 5.4. Characteristic depiction of a single deep moist convective cell in the tropics by ASCAT-A wind derivatives at 12.5 km sampling of divergence (left) and curl (right) over a 250 km by 250 km area on 4 Feb '14 near 0E (dotted line), 3N. The cross (x) indicates the precipitation centre in the collocated KNMI Meteosat rain product. The cell convergence, shear and wind downburst divergence are clearly visible, depicting the intense air-sea interaction of tropical moist convection.

5.6 Convection

The next grand challenge in NWP and climate prediction is to better understand the role of clouds in atmospheric circulation. In particular, cloud parameterizations are difficult to verify and new observations, e.g. that depict convection, are welcome. Convection is also associated with air downbursts that substantially affect air-sea interaction, another not well-understood aspect of climate change. Figure 5.4 shows an example of scatterometer-derived curl and divergence near a moist convective cell over ocean. The wind downburst divergence is clearly visible and coincides exactly with the precipitation cell as observed by a geostationary satellite (not shown). Moist convection is widespread in the tropics and results in intense air-sea interaction. Further research in wind derivatives of tandem scatterometers, such as ASCAT-A and –B in association with geostationary time loops of precipitation may shed further light on the dynamical aspects of moist convection and the related physical parameterizations (Holbach and Bourassa, 2017; King et al., 2017).

5.7 Coupled Atmosphere-Ocean-Land Assimilation

NWP centres are currently devoting a significant effort to increase the level of coupling between different components of the Earth System (Atmosphere, Ocean, and Land) in both global and regional models. The ambition is to move as close as possible to fully coupled models and data assimilation systems. The first weakly coupled data assimilation systems are already under development (Laloyaux et al., 2016; Lea et al., 2015; Saha et al., 2010). While they rely on coupled models, part of the data assimilation process is still performed separately for the individual components of the Earth system. Developing stronger coupling within the data assimilation process is the next challenge. These future systems will allow more effective exploitation of near-surface observations such as scatterometer winds, soil moisture, and sea ice, that have an impact on both atmosphere and surface, provided that the above-mentioned biases are resolved (see end of section 5.5).

5.8 Extreme Wind Speeds

With SCA we expect accurate winds over a larger dynamical range compared to ASCAT (Zadelhoff et al, 2014; Belmonte-Rivas et al., 2014). This opens the opportunity for NWP centers to exploit the data up to higher wind speed thresholds (current upper thresholds for ASCAT are 25 m/s at the Met Office [63] and 35 m/s at ECMWF [3]). How high can the thresholds go? To a large extent this will depend on how good the model winds are under extreme conditions. If the model winds are not accurate, it will be difficult to assimilate the information. This is because if the difference between the model and the scatterometer is too large then the observation will likely be rejected. Moreover, an aliasing problem often occurs in cases with fast moving storms or tropical cyclones, when the storm center is misplaced in the model background. Therefore, an active area of research remains, on the one hand, to improve model parameterizations at extreme winds and, on the other hand, the quality control and weights applied in variational assimilation (VarQC) so that observations with larger departures can be given a higher or non-zero weight in forming the analysis (De Chiara et al., 2015). We further note that in-situ wind measurements do not provide a continuous reference standard for high and extreme wind calibration. An in-situ reference is however needed for both satellite wind calibration and NWP model parameterization development (Stoffelen et al., 2018b).

5.9 Doppler Scatterometer

Scatterometer winds are measured relative to the ocean, whereas buoy and NWP model winds are provided with reference to a fixed Earth reference. Comparisons of these datasets therefore require that mean ocean currents are known. Direct current measurements would greatly improve ocean modelling, particularly in the tropics (Belmonte&Stoffelen, 2019). ESA launched a project that aims to assess the potential of earth-observation instruments for sea surface current retrieval in addition to surface wind vector estimation. Besides new products and ideas, the GlobCurrent project provides recommendations on signal processing techniques and GMF development for surface current retrieval from the Doppler estimates. Since ocean waves cause motion, the Doppler capability will also depend on forcing wind information in order to obtain reasonable estimates of the ocean currents (see http://www.globcurrent.org/ for more details). Ardhuin et al. (2018) propose to combine the best satellite available wind measurements from SCA with Doppler capability on SKIM for the ESA Earth Explorer programme. SKIM has narrow-swath Doppler capability, which may be extended with SCA Doppler capability with less accuracy, but over the broader SCA swath (Hoogeboom et al., 2018).

6 DATA PROCESSING AND PRODUCTS

EUMETSAT produces for ASCAT the full resolution and 12.5 and 25 km sampled Normalized Radar Cross Section, NRCS, or backscatter products. For SCA, products at higher resolution and on different grids will emerge. These are the basis of the geophysical products on stress-equivalent 10m wind, U10S, soil moisture, vegetation, precipitation or sea ice and snow quantities. Both the backscatter and the backscatter variability in a WVC contain useful geophysical information (Anderson et al., 2012). The different levels of processing are discussed below.

6.1 Near-Real Time and Quasi-Real Time

Near-Real Time (NRT) services are very relevant for surface winds, as surface winds are responsible for much of the weather-related damage and losses on the earth. This motivated EUMETSAT to set up an Early Advanced Retransmission Service to provide timeliness of ERS and ASCAT winds of about 30 minutes around Europe. This Quasi-Real-Time (QRT) service is being extended and integrated with the regular NRT services to avoid duplication of products.

6.1.1 Level 1b

For ASCAT enhanced spatial processing has been well elaborated in all application fields as recently, much research has gone into the spatial NRCS processing of ASCAT data over sea (Vogelzang and Stoffelen, 2017a; b), land (Hahn et al., 2014) and sea ice (Aaboe and Lavergne, 2016; Long, 2017), following beneficial research on ASCAT near-coastal winds [58]. Moreover, taking into account the shape and orientation of the basic Spatial Response Functions (SRF) of the ASCAT NRCS (Lindsley, 2015; 2016), and after a careful matching of the Cumulative SRFs (CSRF) of its three beams, a 5.6-km wind product with < 20 km spatial resolution has been constructed. One detrimental aspect of ASCAT, in this respect, is its on-board averaging, which will be omitted for SCA. This opens the possibility of more advanced spatial processing for ASCAT. Over sea, it would allow improved coastal wind processing, while over land and ice surfaces resolution enhancement is feasible.

In addition, the accuracy of cone metrics may allow enhanced pointing monitoring by following deviations from the cone shape in the WVCs on the left and right swath. Also other EPS-SG instruments may profit from this (TBC).

6.1.2 Level 2 Wind

The wind scatterometer is an instrument that provides information on the wind field near the ocean surface, and the knowledge of extracting this information from the instrument's output is dealt with in this section. The first level of wind and sea ice products are swath based and referred to as Level 2 (L2).

In Europe scatterometer processing software is put available through the EUMETSAT Numerical Weather Prediction Satellite Application Facility (NWP SAF), whereas operational wind processing is performed in the Ocean and Sea Ice SAF (OSI SAF; see www.knmi.nl/scatterometer). KNMI has a long experience in scatterometer processing and is developing generic software for this purpose. Processing systems have been developed for ESCAT on ERS, ASCAT on MetOp, NSCAT on the Japanese ADEOS-I platform, SeaWinds on ADEOS-II and QuikSCat, the Indian OceanSat-2 scatterometer (OSCAT), RapidSCat on the International Space Station (ISS), the Chinese HY2A scatterometer (HSCAT), and will be further developed for future scatterometers such as the rotating fan-beam scatterometer on the Chinese-French Ocean Satellite (CFOSAT) or the dual-frequency scatterometer on the Chinese FY-3 satellite (WindRad).

KNMI was and is involved in the EUMETSAT Advanced Retransmission Service (EARS) ERS and ASCAT service as the centre where the Level 1b to Level 2 processing is carried out. The wind products are distributed in the BUFR and NetCDF CF compliant formats that are also used for the ASCAT wind data and other scatterometers. Therefore, the ERS data stream can be ingested by the user using the same interfacing as for the European ASCAT and other scatterometer wind products. Besides wind data, the KNMI processing services offer additional quality control and monitoring (Quality Assurance) ensuring that only reliable data will be made available. See also www.knmi.nl/scatterometer/ for real-time graphical examples of the products and up-to-date information and documentation on all scatterometer products processed at KNMI. Last, but not least, service messages are provided to keep professional users up-to-date on the satellite and ground segment performance.

6.1.2.1 Theoretical and Practical Background

Wind scatterometry was developed heuristically. It was found experimentally that the sensitivity to wind speed and direction describe well the changes in backscatter over the ocean at moderate incidence angles due to changes in surface roughness, as depicted in figure 6.1. In return, backscatter measurements can be used to determine the wind speed and wind direction in a Wind Vector Cell (WVC).

Measured backscatter appears indeed primarily due to surface roughness. One may then define the air-sea interaction and the associated temporal evolution of the ocean topography in a mathematical approximation and further assume e.m. scattering of microwaves on gravity-capillary waves in order to obtain a theoretically-based relationship between wind-induced ocean surface roughness and radar backscatter. In fact, it has been experimentally established that first-order Bragg scattering appears a main contribution, but theoretically-based models do not provide a description to within the precision of the scatterometer measurement. Some critical assumptions in describing ocean microwave scattering are:

- Electromagnetic (e.m.) closure;
- Isotropic Bragg scattering: are breaking and wind-reinforced cm-waves really the same in all directions?
- Roughness spectrum: different spectra provided widely different backscatter; are spectra always the same?
- Foam coverage, particularly at strong winds;

More advanced theoretical development remains useful, in particular to design new mission to effectively obtain simultaneous information on the ocean winds (backscatter) and on the ocean motion (Doppler), probably exploiting new wavelengths and new polarizations (e.g., Fois et al., 2014).

Nevertheless, for wind retrieval, we describe below the empirical developments in geophysics that led to the current state-of-the-art scatterometer wind retrieval. We first describe the stress-equivalent 10-meter wind that is retrieved from wind scatterometers.

6.1.2.2 Stress-equivalent 10m Wind

A scatterometer measurement relates to the ocean surface roughness (see figure 6.1), while the scatterometer product is represented by the wind at 10m height over a WVC. It is important to realize that in the approach followed here, the radar backscatter measurement σ^0 is related to the wind at 10 meter height above the ocean surface, simply because such measurements are widely available for validation. This does not mean that any effect that relates to the mean wind vector at 10 meter height is incorporated in the backscatter-to-wind relationship. In particular, air stability and mass density are not directly sensed by the wind scatterometer and should not appear in the derived 10m wind. Moreover, in buoy and NWP model validation sources, the 10m wind may be corrected for air stability and mass density with good precision. Therefore, scatterometer winds are given as so-called stress-equivalent 10m winds, abbreviated as U10S (de Kloe et al., 2017).

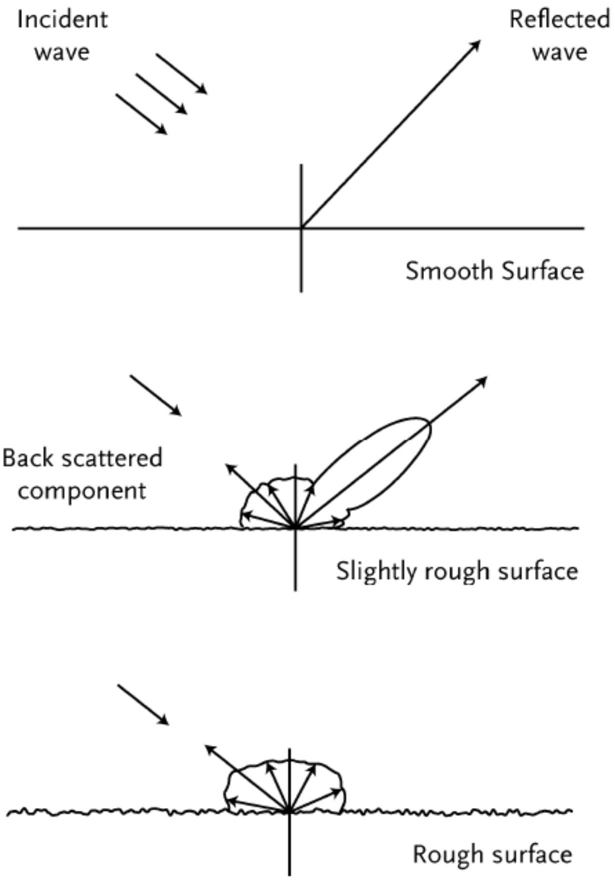

Figure 6.1: Schematic representation of microwave scattering and reflection at a smooth (a), rough (b) and very rough (c) ocean surface. As the roughness increases more microwave power is returned towards the direction of the microwave source.

To avoid atmospheric stability effects, we define the 10-m equivalent neutral wind vector, $\mathbf{U}_{10N}$, rather than the actual 10-m wind vector $\mathbf{U}_{10}$. To obtain $\mathbf{U}_{10}$ from $\mathbf{U}_{10N}$ one needs information on the stability of the atmospheric boundary layer, which may be obtained from buoys or NWP models with sufficient precision (Portabella and Stoffelen, 2009). Using Monin-Obukhov similarity scaling, the equivalent neutral wind vector amplitude is simply given by

$$U_{10N} = \frac{u_*}{\kappa}\ln\left(\frac{10}{z_0}\right) \tag{6.1}$$

where z_0 is the aerodynamic roughness length, the friction velocity is defined by the equation for the kinematic wind stress $u_*^2 = \boldsymbol{\tau}/\rho$ and κ is von Karman's constant. The aerodynamic roughness length

$$z_0 = \frac{0.11\nu}{u_*} + \alpha\frac{u_*^2}{g} \tag{6.2}$$

is approximated from the known geophysical variables ν, kinematic viscosity of the air (1.5x10-5 m^2/s), α, (dimensionless) Charnock parameter (see Charnock, 1955) and g is the gravitational constant of the Earth (9.81 m/s^2). The Charnock value, which is a sea-state parameter, varies substantially for different surface layer schemes, i.e., from 0.011 to around 0.018.

For the same $\mathbf{U}_{10N}$, cold heavy air will produce more stress (and roughness) than lighter (warmer or dryer) air. This effect is expressed by the surface stress equation. The surface wind stress $\boldsymbol{\tau} = \rho\, u_*^2$ indeed depends on the air density ρ. Assuming that σ^0 measurements are more a measure of $\boldsymbol{\tau}$ than U_{10N}, the ρ correction for NWP and buoy winds to U_{10N} takes the form

$$U_{10S} = \sqrt{\frac{\rho}{\langle\rho\rangle}}U_{10N} \tag{6.3}$$

where $\boldsymbol{U}_{10S}$ denotes the current set of 10m-height stress-equivalent scatterometer wind vector retrievals and $<\rho>$ is the average air density as defined in a standard atmosphere (≈1.225 kg/m^3). ρ variations, which depend on surface pressure, air temperature, and humidity, are generally small (1-2%) and can exceptionally increase locally in cases such as cold air outbreaks (de Kloe et al., 2017).

Based on

$$\boldsymbol{\tau} = \langle\rho\rangle U_{10S}\left(\frac{\kappa}{\ln\left(\frac{10}{z_0}\right)}\right)^2 \cdot \mathbf{U_{10S}} \tag{6.4}$$

we note the following:

1. When computing stress from U_{10S}, one should multiply by the globally average air density as opposed to using an air density value at the location of the measurement that one might get from a numerical model. The reason for this is that $\mathbf{U}_{10S}$ already includes the effect of varying air density;
2. Further guidance to compute stress from $\boldsymbol{U}_{10S}$ is being developed.

However, wind scatterometers may be sensitive to more parameters than only those that relate (correlate) with $\mathbf{U}_{10S}$. For example, the appearance of surface slicks, suppressing the amplitude of gravity or longer ocean waves and thus microwave roughness, is associated with low winds and depends to some degree on the strength of the wind and may, to the same degree, be fitted by a GMF (Stoffelen, 1998; Chapter I). However, abundant surfactants, generated by natural or human causes, may render the nominal wind-to-backscatter relationship, as captured by the GMF, less accurate. Other variable effects, such as rain (mainly for Ku-band scatterometers), extreme wind variability, complex sea states, SST, etc., may affect GMF accuracy too. Stoffelen (1998; Chapter IV) discusses a unique method to determine the accuracy of scatterometer, buoy, and NWP model $\mathbf{U}_{10S}$ winds: triple collocation, which will be discussed later on. First we discuss the geophysical relationship between $\mathbf{U}_{10S}$ and backscatter.

6.1.2.3 Geophysical Model Function

For the ERS wind product the CMOD7 GMF for calculating stress equivalent winds is used (Stoffelen et al., 2017). This model function enables the calculation of wind speeds meeting the product requirements between 0 and 25 m/s. CMOD7 is based on CMOD5.n (Verhoef et al., 2008) and CMOD5 (Hersbach et al., 2007; Portabella&Stoffelen, 2007). CMOD6 has been adapted taking into account the incidence-angle dependent ASCAT transponder calibration (Verspeek et al., 2012) and CMOD7 provides improved low winds and more uniform $\mathbf{U}_{10S}$ wind PDFs over the ASCAT and ERS swaths.

At low wind speeds, the wind direction and speed may vary considerably within the WVC. Locally, below a speed of roughly 2 ms^{-1}, calm areas are present where little or no backscatter occurs, perhaps further extended in the presence of natural slicks that increase the water surface tension (Donelan&Pierson, 1987). However, given the variability of the wind within a footprint area of 25 km it is, even in the case of zero mean vector wind, very unlikely that there are no patches with roughness in the footprint. As the mean vector wind increases, the probability of a calm patch will quickly decrease, and the mean microwave backscatter will increase. Also, natural slicks quickly disappear as the wind speed increases, and as such the occurrence of these is correlated to the amplitude of the mean vector wind over the footprint, as modelled by the GMF. Low scatterometer wind speeds are thus providing useful information on the surface wind condition.

At high wind speeds wave breaking will further intensify, causing air bubbles, spume and spray at the ocean surface, and a more and more complicated and heterogeneous ocean topography will appear. Although theoretically not obvious, it is empirically found that VV and HH σ^0 keep increasing for increasing wind speed from 25 m/s to 40 m/s (although at a smaller rate than for moderate winds), and that a useful wind direction dependency remains (Donelly et al., 1999). For SCA, the reduced sensitivity at extreme winds will be boosted by the use of cross-polarization (Zadelhoff et al., 2013).

6.1.2.4 Wind Retrieval

KNMI has an operational processing chain running in near real-time with ASCAT data, including visualisation on the web. This processor is based on the NWP SAF software and runs in the KNMI operational environment. The processing includes monitoring and archiving functionalities. A global overview of the modules of the ERS scatterometer processor is given below.

A schematic illustration of the processing is given in figure 6.2.

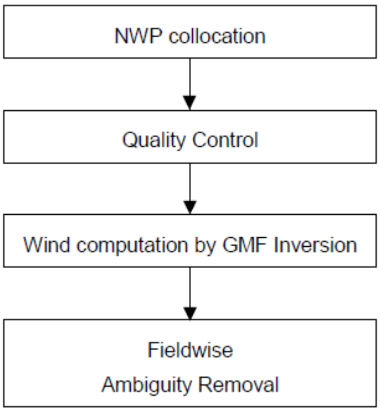

Figure 6.2: Overview of scatterometer wind retrieval algorithm.

The GMF has two unknowns, namely wind speed and wind direction, so, if more than two backscatter measurements are available, then these two unknowns may be estimated using a maximum-likelihood estimator (MLE) as the objective function for determining wind vector solutions, following a Bayesian approach (Pierson, 1989). The MLE is defined by (Stoffelen, 1998; Chapter II)

$$MLE = \left[z_{Oi} - z_M\left(u_i, \phi_i, \theta_i\right)\right]^2 \tag{6.4}$$

where $\boldsymbol{z}$ = $(\boldsymbol{\sigma}^0)^{0.625}$ are the transformed backscatter data, z_{Oi} are the backscatter measurements, $z_M(u_i, \phi_i, \theta_i)$ are the modelled backscatter values through the GMF after trial wind (u_i, ϕ_i) and incidence angle input θ_i. The well-defined local minima of the *MLE* correspond to wind vector solutions. The three independent measurements (fore, mid and aft beam) well sample the azimuth variation of the GMF in order to resolve the wind direction, albeit ambiguously (Stoffelen&Portabella, 2006).

6.1.2.5 Ambiguity Removal

ERS scatterometer wind inversion generally leads to two ambiguous wind solutions in each WVC on the earth's surface. These ambiguities are removed by applying constraints on the spatial characteristics of the output wind field, such as on rotation and divergence. Several ambiguity removal (AR) schemes were evaluated for ERS data (Stoffelen et al., 2000). In the OSI SAF Initial Operations Phase some schemes that were developed for ESCAT were compared. In addition to the subjective comparison of AR schemes, a method for the objective comparison of AR performance among the different schemes was used. By tuning 2DVAR, the strengths of these different schemes were combined. At KNMI this evolved version of 2DVAR is used (Vogelzang, 2007).

As 2DVAR is a simplified version of meteorological 3D-var and 4D-var variational data assimilation methods, adaptive versions of 2DVAR are being developed to guide meteorological data assimilation of ambiguous scatterometer winds (Lin et al., 2016).

6.1.2.6 Quality Control

Since the scatterometer wind retrieval problem is overdetermined, this opens up the possibility of quality control (QC) by checking the inversion residual MLE. If the MLE is normalised by the expected isotropic error variance then it is in theory inversely proportional to the log probability (that a node is affected solely by a uniform wind). The measurement variances, $Var(\sigma_m)_i = (K_{pi}^2\sigma_{oi}^2)$, are estimated to compute the norm of the inversion residual (Stoffelen, 1998). Generally the normalised MLE is substantial and, as a consequence, the inferred probability low, when there is substantial wind or sea state variability within the cell. As such, Stoffelen (1998) found that the inversion residual is well capable of removing cases with extreme variability (at fronts or centres of lows), or with other geophysical variables affecting the radar backscatter. Recently, further progress has been made in the quality assessment of ASCAT winds near rain (Portabella et al., 2012b; Lin et al., 2014; 2015).

Moreover, the concept of normalised MLE has also been applied to Ku-band scatterometers by Portabella and Stoffelen (2001), where it proves very effective to flag rain contamination.

6.1.2.7 Validation

Each step in the processing is validated separately by a quality control and monitoring scheme. The product validation step is controlled by visual inspection, and a statistical analysis is performed to control the validation steps. The inversion step is controlled in the same way. For ambiguity removal schemes an objective scheme exists that relies on initialisation with a one-day lead NWP forecast and validation of the ambiguity selection against independent NWP analyses, as in Stoffelen et al., (2000). Moreover, de Vries et al. (2005) describe subjective comparison of the 2D-VAR by routine operational meteorologists.

Moored buoys are the absolute calibration reference for scatterometer winds and triple collocation (Stoffelen, 1998) is used to estimate and verify bias and random errors (Vogelzang et al., 2009), see, e.g., table 6.1.

Table 6.1. Triple collocation results for KNMI scatterometer winds in subsequent months of November, December and January, starting in 2007 for ASCAT, 2015 for RapidScat, and 2009 for OSCAT and QuikScat. The zonal (u) and meridional (v) wind component error standard deviations are provided on the scatterometer scale (e.g., Verhoef et al., 2015).

Product	Scatterometer		Buoys		ECMWF	
	σ_U [ms^{-1}]	σ_V	σ_U [ms^{-1}]	σ_V	σ_U [ms^{-1}]	σ_V
12.5 km ASCAT	0.7	0.8	1.2	1.2	1.7	1.7
25 km ASCAT	0.6	0.7	1.2	1.2	1.6	1.6
25-km QuikScat	0.6	0.5	1.4	1.4	1.3	1.3
25-km RapidScat	0.6	0.7	1.3	1.4	1.2	1.2
50-km RapidScat	0.6	0.5	1.4	1.5	1.1	1.1
50-km OSCAT	0.7	0.5	1.5	1.6	1.0	1.1

6.1.3 Level 2 Soil Moisture

With respect to soil moisture retrieval, TU Wien has become a European competence centre for soil moisture retrieval from C-band fan-beam scatterometers. TU Wien is developing soil moisture retrieval algorithms since the late 1990s (Wagner et al., 1999c), implemented in a software package referred to as soil Water Retrieval Package (WARP). An operational soil moisture processing software for ASCAT was developed by EUMETSAT in cooperation with TU Wien, which is fully operational since December 2008 (Bartalis et al., 2007; Wagner et al., 2010). The objective of this software (WARP NRT) is to provide soil moisture products in near-real time (NRT) in the same orbit grid geometry as the Level 1b input. Product generation and archiving is done in the framework of the EUMETSAT Satellite Application Facility on Support to Operational Hydrology and Water Management (H-SAF). NRT soil moisture products produced by H-SAF are disseminated via EUMETCast and are offline available via FTP or the EUMETSAT Data Centre.

6.1.3.1 Theoretical and Practical Background

The soil moisture retrieval developed at TU Wien is a physically motivated empirical change detection method. The advantage of change detection over a radiative transfer model is that soil moisture can be directly retrieved from the backscatter measurements without the need of an iterative adjustment process. On the other hand, the change detection approach cannot directly separate the different contributions from soil, vegetation and soil-vegetation interactions to the observed total backscatter as in the case of the radiative transfer model. As a consequence, a multi-year radar backscatter archive is required to calibrate model parameters, used in the change detection approach, to implicitly account for land cover, surface roughness and many other effects. Therefore, full advantage is taken of the multi-incidence angle and multi-beam viewing capability of the European C-band scatterometers ESCAT and ASCAT in order to characterise backscatter variations of the Earth's land surface.

For an in-depth discussion and further details about the TU Wien soil moisture model, the reader is referred to Wagner et al., (1999c) and Naeimi et al. (2009). Variations of the backscatter coefficient σ^0 are related to surface roughness, changes in vegetation and to variations in the soil water content. An important fact is that each of these factors acts on a different spatial and temporal scale. With respect to these aspects, the TU Wien model allows the determination of model parameters from multi-year backscatter time series to gain essential knowledge on scattering effects taking place on a certain location on the Earth's land surface. The underlying physical assumptions and empirically observed evidences can be summed up as follows:

- The incidence angle has a strong impact on the backscatter coefficient σ^0 of natural targets. This dependency is a characteristic for roughness and vegetation, but soil moisture changes are not or only minimally affected by this circumstance.
- The incidence angle dependent backscatter coefficient $\sigma^0(\theta)$ is decreasing or increasing with vegetation growth, whether the contribution of the soil on the ground is higher than the contribution of the vegetation canopy or conversely. Hence, the $\sigma^0(\theta)$ time series is changing in accordance to the vegetation phenology over time.
- The vegetation phenology cycle influences σ^0 on a seasonal scale and local short-term variabilities are negligible due to the low resolution of the sensor.
- The relationship between soil moisture and σ^0, expressed in dB, is considered to be linear.
- There are certain incidence angles θ_{dry} and θ_{wet} at which σ^0 is rather stable in face of vegetation changes. These so called "crossover angles" are assumed to be 25° for the dry reference and 40° for the wet reference.
- The coarse resolution of the scatterometer admits the assumption that roughness and land cover are temporally invariant.

With respect to these physical assumptions, model parameters are calibrated by making use of a multi-year radar backscatter archive and the offline software package WARP. WARP NRT implemented at EUMETSAT is derived from and depends on the model parameters estimated by WARP. The key equation of the TU Wien model relates the observed backscatter observations at a given location at day t to the normalised the normalised backscatter at 40° incidence angle $\sigma^0(40,t)$, the vegetation state at day t mediated by the so called slope and curvature parameters $\sigma'(40°,t)$ and $\sigma''(40°,t)$, respectively, and the incidence angle θ:

$$\sigma^0(\theta,t) = \sigma^0(40°,t) + \sigma'(40°,t)(\theta - 40°) + \frac{1}{2}\,\sigma''(40°,t)(\theta - 40°)^2 \tag{6.5}$$

assuming a second order polynomial dependency. The slope and curvature parameters, which determine the effect of vegetation on the backscatter, are estimated using the multi-incidence angle capability of the scatterometers. Instantaneous backscatter measurements $\sigma^0(\theta, t)$ are first mapped to a reference incidence angle (at 40°) by inversion of Eq. (6.5). The measurements are then expressed relative to the historically highest and lowest backscatter values (the so called wet $\sigma_{wet}(40°, t)$ and dry $\sigma_{dry}(40°, t)$ references) at the given location.

$$sm(t) = \frac{\sigma^0(40,t) - \sigma^0{}_{dry}(40,t)}{\sigma^0{}_{dry}(40,t) - \sigma^0{}_{wet}(40,t)} \tag{6.6}$$

A simplified flowchart of the near-real-time processing chain is illustrated in Figure 6.2. As depicted, Level 1b input data are pre-processed by applying a calibration correction if required before the data stream is injected into the WARP NRT processor. Furthermore, offline estimated model parameter are used to normalise the backscatter measurements to account for different observation geometries. Finally, normalised backscatter measurements are scaled between the driest and wettest backscatter observation in history to retrieve relative surface soil moisture values by applying Eq. (6.6).

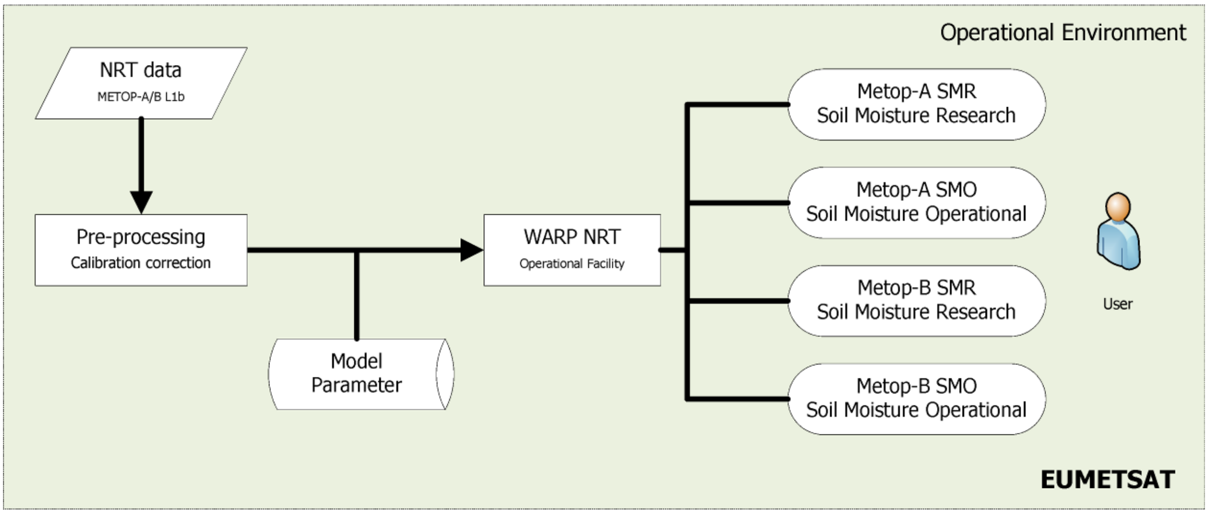

Figure 6.3: Flowchart of the near-real-time soil moisture product processing chain.

6.1.3.2 Surface soil moisture product

Level 2 soil moisture products generated in NRT are available in various data formats and resolutions. All products are disseminated as orbit images with samples on an instrument specific orbit grid. An overview of the generated NRT products in the framework of H-SAF is given at http://hsaf.meteoam.it/soil-moisture.php.

6.1.3.3 Validation

The ASCAT-derived SSM product was compared with in situ soil moisture observations and with independent SSM products by many authors (e.g. Albergel et al., 2012).

The EUMETSAT H-SAF has implemented an operational validation scheme based on in situ observations in Europe. The ASCAT-derived SSM values are compared with local in situ SSM observations. The correlation between the local and the satellite time series is the main indicator used to assess the quality of the product.

6.1.4 Level 3 and Level 4

Earth grid representations of scatterometer data are more convenient for users than swath grid representations. These are produced for a single instrument (called Level 3, L3) or for multiple instruments and/or combinations of model and observation based information (called Level 4, L4).

6.1.4.1 Wind and wind stress

Currently, the Copernicus Marine Environment Monitoring Service (CMEMS) produces L3 and L4 products resp. based on interpolation and a Kriging analysis of satellite and ECMWF winds (http://marine.copernicus.eu/).

The requirement for these products in the ocean community is immense, as it provides spatial information on air-sea interaction and thus exchanges of heat, momentum, water vapor, gasses and aerosol through processes of mixing, upwelling and downwelling in both the atmosphere and the ocean. Moreover, this highly dynamic interface covers about 70% of the earth's surface and thus determines climate dynamics to a large degree.

CMEMS products are critically important for determining the large-scale ocean circulation and transport. Vector winds are also needed to estimate the ageostrophic (Ekman) component of ocean currents, and consequently are linked to coastal upwelling, primary productivity, cross shelf transport, ice transport, mixed layer evolution, and deep-water formation. Accurate wind speeds are moreover essential for reliable computations of air/sea heat fluxes (sensible and latent heat fluxes) as well as mass fluxes (e.g. CO_2 and H_2O), making surface winds critically important for budgeting energy, moisture and Carbon, and for studies of ocean acidification and fish stocks. OSVW and surface stress are linked to ocean, atmospheric, cryospheric and terrestrial climate change and listed as Essential Climate Variable.

The CMEMS products contain L3 global daily gridded scatterometer observations relying on upstream Near-Real-Time or reprocessed L2 scatterometer products from the EUMETSAT Ocean and Sea Ice Satellite Application Facility (OSISAF) Wind Centre at KNMI. Data from ascending and descending passes are gridded into separate files.

The CMEMS L3 global wind product also contains gridded model U10s background winds from ECMWF, either from the operational NWP model in NRT or the ECMWF ERA winds when reprocessing. This model wind information is first stored in the OSISAF upstream L2 wind product. The model wind in the CMEMS L3 global wind product is then sampled and processed in exactly the same way as the scatterometer winds, so subject to identical space and time sampling errors. Comparing scatterometer-sampled ECMWF winds with uniformly-sampled ECMWF winds over a period of interest, reveals these spatio-temporal scatterometer sampling errors, which are substantial on time scales smaller than a month.

The variables provided are not limited to the stress-equivalent wind vector, but also include wind curl and divergence, wind stress curl and divergence, and wind stress magnitude. IFREMER is combining scatterometer and radiometer winds with ECMWF winds in order to produce space and time continuous wind and stress fields at L4, based on the Kriging approach. Future approaches will address the different physical error characteristics of scatterometer and ECMWF U10S, which affect the spatial and temporal integrity of the merged L4 products. Moreover, more advanced methods need to be developed to allow locally unbiased hourly wind and stress fields (see, e.g., the biases in Figure 7.2), but without the introduction of the satellite sampling patterns (Belmonte&Stoffelen, 2019).

6.1.4.2 Surface soil moisture

In the framework of the Copernicus Global Land Service (http://land.copernicus.eu/global/), the ASCAT SSM product is used to produce estimates of soil moisture for deep soil layers using an exponential filtering technique. A Land Data Assimilation System (LDAS) is used for the cross-cutting quality monitoring of the soil moisture product, together with LAI surface albedo, FAPAR and land surface temperature (LST) is performed (i.e., the simulated values are compared with the satellite products). Within the EUMETSAT Satellite Application Facility on Support to Operational Hydrology and Water Management (H-SAF) project, a root zone soil moisture product has been developed based on the level 2 surface soil moisture data assimilation in the ECMWF land data assimilation system. The obtained ASCAT root zone soil moisture product is provided for four vertical soil layers (from surface to root zone down to 3 meters) generated in NRT by ECMWF for H-SAF at 24 hour time steps, with a global daily coverage, at a resolution of 25 km. The analysed soil moisture fields are based on a modelled first guess, the screen-level temperature and humidity analyses, and the ASCAT-derived surface soil moisture. Consistent with the level 2 soil moisture, the ASCAT root zone soil moisture (SM-DAS-2/H14) it expressed as an index by normalizing by the saturated soil moisture value as a function of texture soil type. This product has been operational since July 2012. Validation studies showed very good quality of the ASCAT root zone product compared to ground stations (Albergel et al., 2012). From 2019 the ASCAT root zone soil moisture product will be provided at 10 km resolution (H26).

In addition to the previous mentioned Level 3 soil moisture products, H-SAF is hosting a time-series product referred to as H25-offline georeferenced on a equidistance global grid (WARP5 grid). This product is generated/updated in regular time intervals by TU-Wien as an extension to the latest available H25 Data Record.

6.1.4.3 Sea Ice

As part of their wind processing and to allow NRT sea and ice discrimination, KNMI processes L3 sea ice extend and type from single instruments, such as ASCAT-A/B/C, SeaWinds, OSCAT and other pencil-beam scatterometers (http://projects.knmi.nl/scatterometer/ice_extents/). Multi-instrument, including ASCAT, extend and products are available from the EUMETSAT OSI SAF Ice Centre (http://osisaf.met.no/p/ice/edge_type_long_description.html).

6.1.4.4 Daily rain

Daily accumulated rain products are under development in the EUMETSAT Hydrology SAF (see, e.g., http://hydrology.irpi.cnr.it/download-area/sm2rain-data-sets/).

6.2 Climate data records

Monitoring of climate change requires the production of transparent and consistent Climate Data Records (CDRs). For winds, climate scientists require an accuracy in the global wind trend of 0.1 m/s per decade. Using the analysis tools developed for NRT data, such accuracy appears possible for scatterometer wind data (Verhoef et al., 2017; Wentz et al., 2017; Belmonte et al., 2017; Stoffelen et al., 2017).

The current non-uniform distribution of moored buoys makes them rather unsuitable for global change metrics. The geographical distribution of moored buoys points to a glaring hole in the southern hemisphere, where the monitoring of atmospheric and ocean dynamics is poor. This while the vulnerability of the Antarctic region is particularly important in the global climate system. With the equivalent of 60m of global ocean water level stored on Antarctica, scientific misjudgement of changes in the Antarctic warming may have rather drastic consequences on climate projections. However, buoy monitoring in the SH extra-tropics is essentially missing and should be recommended in our view. It would be much appreciated if (particularly southern hemisphere governments) would take responsibility in this area. Moored buoy winds are of high quality and are our only absolute reference for satellite wind calibration and monitoring.

Triple collocation (TC) is essential as satellite wind instruments and General Circulation Models (GCMs) lack absolute calibration otherwise. Maintaining a globally representative long-term data record of surface wind measurements is thus critical to the cross-calibration of satellite winds from different satellite missions and different satellite sensor types (e.g., the SSM/I series microwave radiometers, Ku- vs C- vs L-band scatterometers).

It is observed that different global metrics provide different trends though, as they cover different spatio-temporal domains, e.g., at all global buoy measurement positions (as in TC), at model grid positions (either regular or uniformly spaced), or at all satellite measurement points (after QC usually). The satellite or GCM representations of the global waters appear clearly the most faithful representation of the mean integrated global wind change over water.

In situ data, moored ocean buoys for winds, are not uniformly distributed over the earth's oceans and large local decadal circulation changes make it impossible to achieve a globally representative trend with the above accuracy. Satellite wind CDRs are thus immensely important to monitor global climate change.

For surface soil moisture consecutive Climate Data Records are being produced at ECMWF by the H-SAF, by reprocessing the root zone soil moisture product to cover the ERS-ASCAT period. It is produced using consistent version of the ECMWF assimilation system and using the reprocessed version of the level 2 surface soil moisture product. This root zone soil moisture CDR (H27) is of high interest for hydrological applications as well as for NWP and climate models validation purposes. It provides a consistent quality product of root zone soil moisture for 1992-2014 (Albergel et al., 2015). In addition, a number of CDRs representing surface soil moisture are produced by TU Wien on behalf of H-SAF. The CDRs are derived from calibrated Level 1b input data to achieve best possible consistency within the data.

Furthermore, the ESA SCIRoCCo project (SCIRoCCo, 2017) reworked the ERS data in the context of the ESA Long-Term Data Preservation program. The ESCAT data has beenmade mutually consistent (notably, ERS1 and ERS2) and made consistent with the ASCAT data record. All progress made on ASCAT wind, ice and soil moisture processing is employed in order to produce calibrated ESCAT geophysical CDRs from the Fundamental Climate Data Record (FCDR) of backscatter values (Belmonte et al., 2017). Similarly, noted instrument anomalies should be corrected for in the ASCAT FCDR and improved geophysical processing, which has been deployed over time in NRT, be run on it, in order to produce state-of-the-art CDRs.

CDRs will be formatted as NetCDF Climate-Format (CF) convention and associated with a Digital Object Identifier (DOI).

Low resolution ice drift datasets are computed on a daily basis from aggregated maps of scatterometer (e.g. ASCAT) signals. During fall, winter, and spring, the excellent coverage makes it possible to extract 48 hours global ice drift vectors at a spatial resolution of 62.5 km (Lavergne et.al 2010).

With the prospect of having scatterometer data, continuously available from 1991, and further with the forthcoming SCA in EPS-SG, reprocessing of scatterometer data in support of climate monitoring is very relevant. It will, however demand careful treatment of inter-sensor variations which is obtained with cone metrics. The dynamical tie point approach utilized in the operational OSI SAF ice type processing will be one method that will be compared. In addition, by relating roughness to sea ice age and thickness, more information about multi-year sea ice and sea ice volume trends may be obtained since 1991.

6.3 Future developments

Future developments include improved spatial and temporal resolution, near-coastal processing, user-defined grids and cloud processing.

Concerning increased spatial resolution and near-coastal processing, the exact knowledge of the Spatial Response Functions (SRF) is important, as well as the availability of full-resolution (non-accumulated) samples. For wind processing it is essential that the fore, mid and aft beams view the same area on the ocean surface, i.e., view the same area-mean wind vector. If the Cumulated SRF (CSRF) is different for the fore mid and aft beams, then the consistency of the backscatter values with the GMF will be degraded. Matching CSRFs is challenging for the smaller footprints, due to the different basic sampling of the three beams.

For soil moisture and sea ice, a different opportunity occurs, as the signal levels are high and the response is azimuthally isotropic. This offers the possibility of resolution enhancement when the three beams do not exactly overlap over land and sea ice areas (Lindsley et al., 2015).

Increased temporal resolution will be achieved by the CEOS virtual constellation, as concrete plans exist in India, China and Russia to launch scatterometers in complementary orbit planes, thus covering several times of day.

The scatterometer sampling is quite uniform and the geophysical processing allows processing on user-defined grids in principle. This could in principle prevent interpolation errors when transforming L2 to L3 or L4 products.

Finally, scatterometer winds are useful in combination with other geophysical observables and synthesis in different application areas, in particular in air-surface interaction processes, as outlined in this report. The scatterometer wind processors are publicly available through the NWP SAF and may be extended to allow their use in cloud computation and data infrastructures.

7 PERFORMANCE MONITORING

Long-term absolute stability of the scatterometer backscatter properties at L1b may be locally monitored by transponders.

For shorter-term (NRT to months) and long-term, more detailed relative monitoring, e.g., as a function of WVC, geophysical monitoring and monitoring along the orbit, well-established and reliable methods are in place, as described below.

7.1 Near-Real Time

NRT monitoring provides an essential assurance for the NRT application of scatterometer winds, in particular for automatic ingestion in NWP data assimilation, since the assimilation of large quantities of erroneous data could impede forecast skill. Since NWP provides global short-range forecasts of ocean surface vector winds at all scatterometer WVCs, these are used extensively in the product monitoring. Further monitoring is moreover carried out daily by the users, who report artefacts at the helpdesk scat@knmi.nl .

Currently, mean MLEs and short-range ECMWF forecasts are used for monitoring, see, e.g., projects.knmi.nl/scatterometer/ascat_osi_co_prod/ascat_app.cgi?cmd=monitoring&period=week&day=0&flag=yes, where a product flag is raised when anomalous values appear in an orbit above a threshold probability of 1/10,000. This safeguards the use of erroneous products.

For off-line validation the moored buoy network is used as an absolute reference for the scatterometer and NWP winds (projects.knmi.nl/scatterometer/ascat_osi_co_prod/ascat_app.cgi?cmd=buoy_validations&period=week&day=0&flag=yes). A method called triple collocation has been developed to provide a comprehensive error analysis and calibration of these error sources as described in section 6. Validated algorithms are used for higher level processing and the use of critically monitored L2 products is generally sufficient to warrant the stable quality of L3 and L4 products. Nevertheless, this is checked by regular off-line validations.

7.1.1 NWP collocation

ECMWF wind forecasts are available twice a day (from 00 and 12 GMT analysis times) with hourly forecast time steps, such that KNMI receives NWP model data twice a day through the Regional Meteorological Data Communication Network (RMDCN). For reprocessing, the ECMWF archive is used, which contains reanalysis data, such as ERA-interim and ERA5 (Dee et al., 2011; Belmonte&Stoffelen, 2019). At KNMI $\mathbf{U}_{10S}$ is extracted from the full resolution ECMWF fields and interpolated to the time and location of the scatterometer WVCs and stored in the scatterometer output products as value-added variables. NWP model sea surface temperature and land-sea mask data are used to provide information about possible ice or land presence in the WVCs. WVCs with a sea surface temperature below 272.16 K (-1 °C) are assumed to be covered with ice and no wind information is calculated. At SSTs above -1 °C a Bayesian scheme is used for the discrimination of water and ice (Belmonte et al., 2012; Otasaka et al., 2017). Land presence within each WVC is determined by using the land-sea mask available from ECMWF. The weighted mean value of the land fractions of all model grid points within 80 km of the WVC centre is calculated. The weight of each grid point scales with $1/r^2$, where r is the distance between the WVC centre and the model grid point. If this mean land fraction value exceeds a small threshold, no wind retrieval is performed. Land fraction should ideally be provided in the L1B products for each basic measurement.

7.1.2 Calibration

While scatterometer systems have generally excellent calibration stability, their absolute calibration level is difficult to determine. For fan-beam scatterometers, the beam patterns of the three beams determine the relative calibration of the backscatter values in a measured triplet for a particular WVC. This relative calibration is of utmost importance and determines the general wind retrieval quality. The different WVCs and beams experience a very similar wind climatology over a year. This is being exploited in a NWP ocean calibration (NOC) procedure, which determines a calibration value for each WVC and beam that provides statistical consistency between the calibrated backscatter triplets, the GMF and the ECMWF winds. NOC is essentially used for all scatterometers to optimise wind performance by balancing the beams for each WVC in a consistent manner. NOC diagnostics have provided excellent feedback to instrument anomaly monitoring, both in the ERS and ASCAT ERA. In turn, both ERA-interim and scatterometer winds are being monitored and verified against buoy measurements. Using NOC, KNMI reported anomalies in scatterometer L1 processing on several occasions, including for ASCAT, and provided corrections to the backscatter data (Figure 7.1).

Belmonte et al. (2017) present cone metrics as the most sensitive tool for relative calibration of all C-band scatterometer missions and for each individual radar beam, independent of NWP. In addition, the accuracy of cone metrics may allow enhanced pointing monitoring by following deviations from the cone shape in the WVCs on the left and right swath. Also other EPS-SG instruments will profit from this .

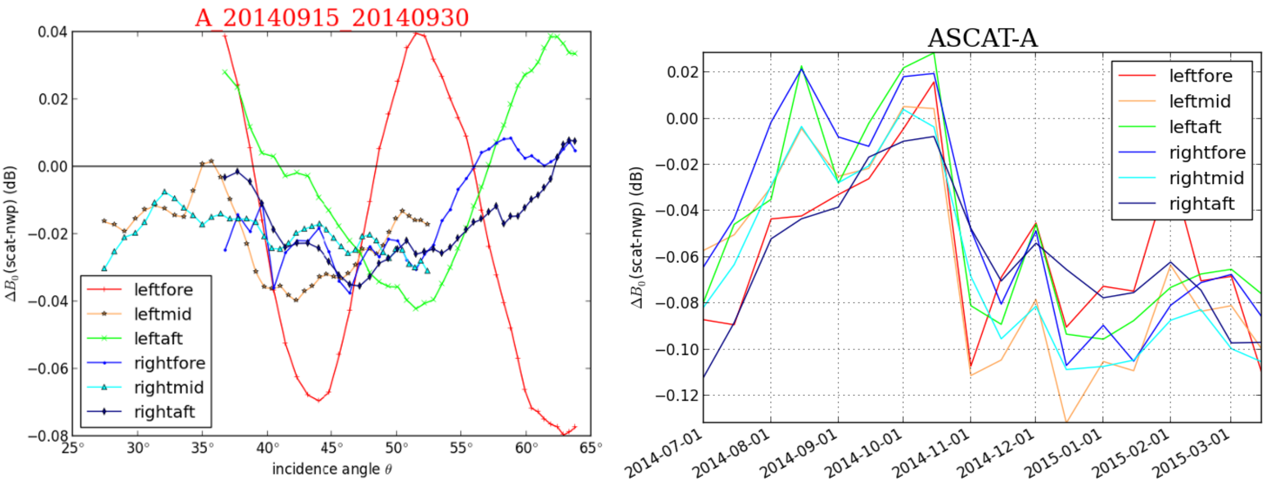

Figure 7.1: Two ASCAT-A anomalies in autumn 2014 detected by NWP ocean calibration and later confirmed by cone metrics.

Moreover, cone metrics has been proven useful to inter-calibrate scatterometers, linking ECMWF ERA-interim winds to both the ERS and ASCAT scatterometers through the GMF, but also providing a close link between concurrent scatterometers, such as ASCAT-A and ASCAT-B.

7.1.3 Quality Control and Monitoring

In each WVC, the σ^0 data is checked for quality and completeness and the inversion residual (see section 6.1.2.6) is checked. Degraded WVCs are flagged and the flag bits stored in a flag variable (see ASCAT Wind Product User Manual, 2013). The quality of the delivered products is controlled through an ad hoc visual examination of the graphical products and the automatic production of control parameters. The examination of the products is done at KNMI by experts. Specific tools have been developed to help this analysis. User queries obviously lead to the inspection of suspect products. The ad hoc and user queried inspections are used for quality assurance. An information file is made for each product. The content of the file is identical whatever the product and results from a compilation of all the global information concerning this product. From these files, various graphs are produced to visually display the confidence levels of the products and their evolution with time. These graphs are available on the KNMI website.

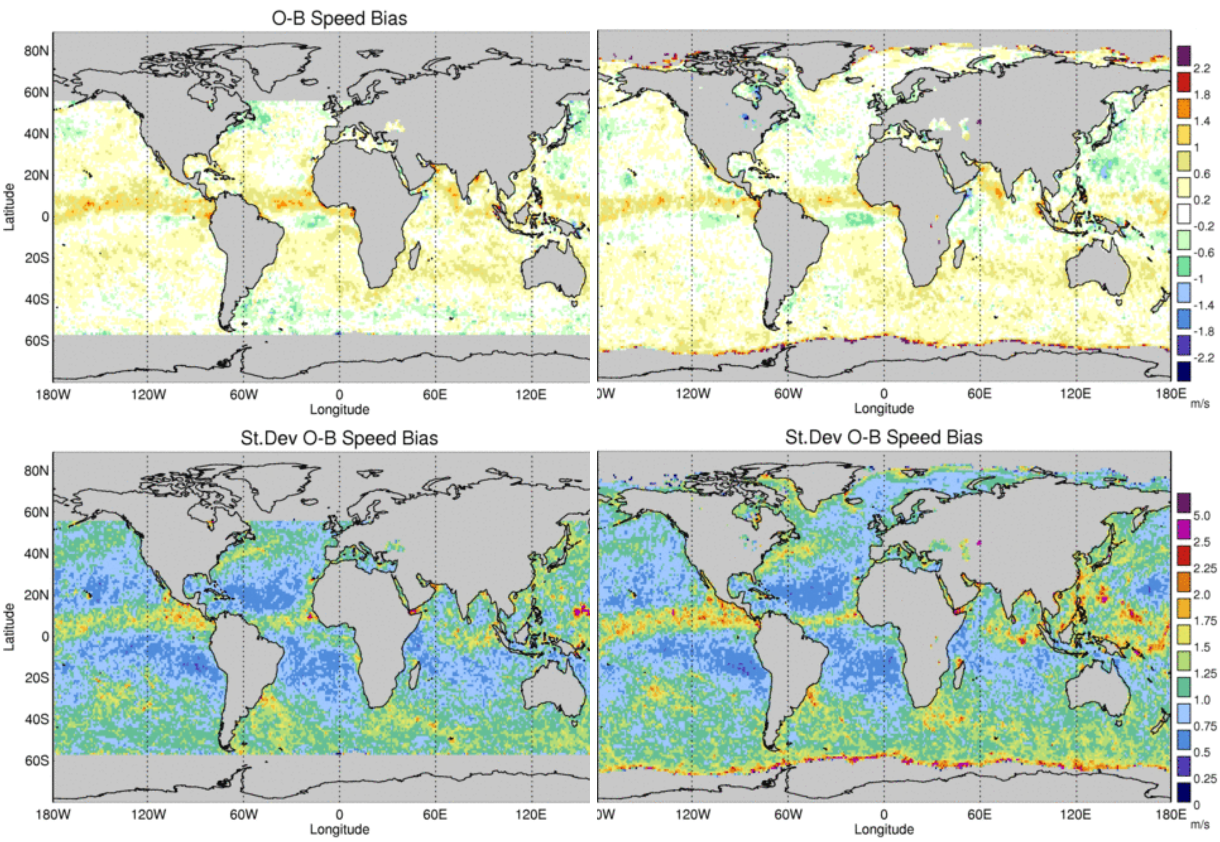

Figure 7.2: Speed bias of scatterometer winds with respect to the Met. Office global model for RapidScat on ISS (left) and ASCAT-A on MetOp (right) for July 2015. Different scatterometers produce similar local mean and variability of differences with respect to GCMs.

The NWP SAF moreover monitors scatterometer winds in various representations against volunteering global NWP model outputs, revealing differences between these models and the scatterometer products and their evolution over NWP model cycles (NWP SAF, 2017).

7.2 Climate data records

The reprocessing of scatterometer data profits from the strict automated monitoring developed in NRT; the same procedures are implemented for reprocessing. In addition, NOC, cone metrics and TC are used for long-loop instrument and parameter performance monitoring (e.g., calibration stability, etc.) on a monthly and yearly basis.

TC with moored buoys, scatterometers and GCMs is performed to establish the accuracy and calibration of the scatterometer winds and the GCMs at the available moored buoy positions. By physical inference, it is assumed that the spatial sample of buoys is sufficient to obtain a globally representative absolute scatterometer calibration. This can obviously not be proven, as no globally representative in situ wind network is available (Stoffelen et al., 2015). However, given such plausible inference, it appears possible to reach the 0.1 m/s per decade stability in a representative global metric from scatterometers (Verhoef et al., 2017; Wentz al., 2017).

8 OUTREACH NEEDS

This Science Plan describes the heritage, background, processing and control of scatterometer data. The software, production, monitoring, calibration and validation are well documented through the EUMETSAT OSI, NWP and Hydrology SAFs and through the EU Copernicus Marine Environment Monitoring Service (CMEMS) Thematic Assembly Centres (TAC) on Wind and Sea Ice. It moreover describes scatterometer application in NWP, where user guides are developed in the context of the NWP SAF for wind data assimilation and bias correction, thus reaching out to the operational and scientific expert and user communities, and fostering mechanisms for innovative application research. These services are equipped with help desks.

Sections 6 and 7 moreover contain visualisation sites of NRT data, on-line open and accessible NRT and archive data bases of scatterometer data and associated reference data. In particular, KNMI developed recently a multi-platform scatterometer winds viewer that is suitable for many local weather forecasters across the globe (projects.knmi.nl/scatterometer/tile_prod/tile_app.cgi).

Wider scientific elaboration and development of scatterometer processing or application is well facilitated through the visiting and associated scientist programmes of the EUMETSAT SAFs. Moreover, all scatterometer developments and standardization is well coordinated on an international level through the IOVWST and CEOS, for example.

Wind and wave marine training has been taken up with NOAA and EUMETSAT for many years now, providing face-to-face training across the globe. In addition, on-line modules, case studies and training is provided (see, e.g., projects.knmi.nl/scatterometer/training_material/). Scatterometer winds are generally well used for hurricane forecasting, both in the tropics and in the extra-tropics, but also to monitor mesoscale wind features over sea, soil moisture conditions and sea ice extent, drift and type.

Finally, media interviews occur frequently, when scatterometer data depict extreme storms, draughts or minimum sea ice coverage.

9 RESEARCH AND DEVELOPMENT NEEDS

Research and development needs focus on the two main user priorities of temporal coverage, of dynamical and extreme weather in particular, and of advanced high-resolution processing, particularly in coastal, land and sea ice applications. Additional efforts are needed to transfer emerging science products into operational applications. Besides direct use of scatterometer products, there is a clear tendency of further integration of the scatterometer products in Nowcasting, NWP and reanalyses, which needs are further discussed here. To benefit the user community, focus should be put on standardization.

9.1 SCA and the constellation

Wind and stress in NRT and as CDR will be needed from SCA at all processing levels. At L4 combination with other active and also passive instruments is necessary, hence a focus on intercalibration of basic measurements and winds is required.

The existing NRT processing and monitoring is typically used for CDR development and the cone metrics approach guarantees intercalibration of backscatter over the C-band missions. For ASCAT absolute calibration has been possible through transponder campaigns and which will be continued for SCA.

The goal for SCA and ASCAT is to obtain full global coverage when possible at 9:30 and 21:30 LST, as increased spatial and temporal resolution is a key user requirement, e.g., for the nowcasting of hurricanes. Planning for such complete coverage, using both ASCAT and SCA instruments beyond 2023 will be required.

In order to develop standards, the international collaboration and representation in the IOVWST, IWW, CEOS and WMO is necessary, as well as dedicated resources to intercompare and agree on algorithms and references. In addition to standard development, these fora set priorities and requirements for R&D needs and may embark on effective international collaboration schemes. These R&D priorities include typically Cal/Val, intercalibration, coastal processing, resolution enhancement, dependency on sea state, SST, ocean current, vegetation, dependency on e.m. wavelength , extremes, etc.. In addition, requirement assessment, spatial and temporal coverage coordination, product format standardization, quality metrics, open (collocation) data bases, open tools and processing software are part of these international collaborative fora.

ASCAT has proven to be very important for other OVW-sensing instruments, due to its optimal geometry, all-weather capability and excellent stability. In the virtual constellation plentiful close collocations between ASCAT and RapidScat or ScatSat have been exploited to achieve better product consistency (Wang et al., 2019). ASCAT and later ESCAT have been exploited to determine:

- The calibration stability of other active and passive wind-sensing instruments (Ricciardulli&Wentz, 2013);
- SST-sensitivity of Ku-band backscatter (Wang et al., 2017);
- Rain sensitivity and QC of Ku-band scatterometers;
- Wind direction sensitivity (Wang et al., 2019);

- ECMWF background error covariances for use in 2DVAR (Vogelzang&Stoffelen, 2018).

With SCA, such exploitation will be continued and extended to VH, extreme winds, sea state, ocean currents, etc..

In this section, we also note the possible convoy with SKIM (Ardhuin et al., 2018), which would be very useful to better determine the dynamical aspects of air-sea interaction. SCA winds will be very useful for the success SKIM, while SKIM measurements aid in the understanding of SCA backscatter and, possibly, Doppler measurements. Further synergy on MetOp-SG is obtained through MWI, which would probably impact both SKIM and SCA products.

Finally, lessons learned from ASCAT may be further exploited for other scatterometer systems, such as the application of cone metrics, the use of the MLE as a measure of wind variability and ASCAT-determined ECMWF error covariances in 2DVAR MSS (Vogelzang &Stoffelen, 2018).

Forthcoming improvements for ASCAT include coastal processing, using the L1B Land Contribution Ration (LCR), and improved ship detection, which latter is particularly difficult for moderate ship corner reflections on moving ships at modal wind speeds, due to the on-board accumulation.

9.2 SCA advances

For ASCAT transponder campaigns are held, which interrupt the surface backscatter measurements, resulting in a loss of data. For SCA the calibration mode in integrated in its normal duty cycle while surface backscatter measurements are made.

With SCA, without on-board accumulation, advanced spatial processing near coastlines will be possible and better discrimination of ship echo's is expected, as well as enhanced possibilities for processing at higher spatial resolution or on user-defined grids over both land, sea and coasts.

The better coverage and radiometric performance will lead to higher quality winds in more places. Combining these measurements with the ongoing ASCAT missions will need investigation.

VH measurements will allow extreme wind measurements and will be very useful with complementary benefits over land and sea ice. A VH wind processing chain will be developed for day 1 and later on the VH and co-polarization processed winds will be merged into a single wind product. VH measurements from SAR have been exploited to develop a GMF, while VH campaigns in extreme winds collect further data to corroborate the SAR results. For lower signals, pure VH may be more difficult to obtain due to Faraday rotation and its effect on wind speed retrieval needs further elaboration.

Zhang et al. (2019) develop an HH GMF and confirm that HH is less sensitive to wind than VV and thus using all VV co-polarization maximizes sensitivity for ocean wind retrieval, amended by VH measurements for extreme winds.

Hoogeboom et al. (2018) simulate the exploration of SCA phase and Doppler information for ocean currents. Using an echo cancellation method, further signal quality enhancement is simulated. Without any further SCA design trade-offs, these concepts should be further investigated and tested in order to realize such capability with SCA, possibly in synergy with SKIM.

9.3 Nowcasting, NWP and reanalyses needs

Nowcasters are faced with an enormous amount of satellite observations that contribute new information to their advisories. Commonly, large differences of the observations from NWP forecasts should alert nowcasters to revise these advisories. Such large differences may be automatically detected in the areas of interest from SCA observations, using the ECMWF forecast as reference. In addition, information on expected errors and local wind variability (MLE) can be provided.

The absence of an in-situ wind reference for high and extreme winds remains a concern for the calibration and validation of all ocean satellite wind retrievals, but also for the development of improved NWP model parameterizations in storm conditions.

For NWP wind data assimilation Stoffelen et al. (2018a) suggest to distinguish developments in regional and global NWP. Aliasing with the underdetermined scales over the seas should be avoided and techniques to avoid effects of model noise should be further elaborated for regional NWP, such as "supermodding". Global models generally avoid model noise (so far) and are much smoother than regional model wind fields. To deal with the relatively high density of SCA observations, thinning is currently practised, but should be avoided. Tests with error inflation to compensate for oversampling of the model analysis structures or superobbing are ongoing for global NWP.

Another problem in global NWP is that innovations due to ASCAT are substantially affected by systematic model errors, which violates the BLUE paradigm in NWP data assimilation. Schemes for compensation (bias correction) of systematic model errors are sorely needed to

- Optimise the extraction of dynamical information from SCA;
- Provide an improved forcing of ocean, wave and surge models.

Bias correction schemes are already in place for many other assimilated satellite retrievals.

For climate applications consisting in detecting trends in the seasonal variability of soil moisture, disentangling soil moisture and vegetation water content effects on the backscatter level is of key importance. Assessing properly the inter-annual variability of soil moisture is key, and new techniques able to account for changes in vegetation density from one year to another in the soil moisture retrieval algorithm have to be developed.

This requirement is also valid for NWP applications, as seasonal biases in the assimilated soil moisture are detrimental to the quality of the assimilation results.

Long (30 yr+) harmonized time series of satellite-derived surface soil moisture estimates have been produced in the context of the ESA-CCI programme and of the Copernicus Climate Change service, where ASCAT data are a key component of these products. Meteo-France plans to use its LDAS-Monde tool (Albergel et al., 2017) to produce global land reanalyses incorporating such data records together with other ECV products such as LAI. The use of SCA data in this context should be prepared, possibly through the development of an observation operator for sigma0. Apart from its use in the LDAS, the observation operator would allow the simulation of SCA sigma0 values over land. This would help assess the capability of SCA observations to monitor vegetation in addition to surface soil moisture.

The capabilities of SCA to provide a self-standing operational vegetation data product should also be assessed. The most promising vegetation variable to be retrieved by SCA is the vegetation optical depth (VOD) which has been shown to be indicative of vegetation water content and wet biomass. Hence, the VOD has significant potential to enrich the information about vegetation dynamics, complementing the vegetation data sets (LAI, NDVI, fAPAR) provided by optical sensors. This work will also have important benefits for the SCA soil moisture data services given that an improved parameterization of vegetation in the SCA backscatter models over land will lead to improved soil moisture retrievals.

Over land, the introduction of a SCA based rainfall product based on the SM2Rain method proposed by Brocca et al. (2014) shall be further developed. A recent EUMETSAT study conducted by Brocca and colleagues has shown that rainfall estimates derived from ASCAT soil moisture retrievals using the SM2Rain algorithm are comparable to, or even outperform, other existing rainfall data products (in situ, satellite, fused) in ungauged basins.

The Cal/Val of SCA could be an opportunity to address land issues. Long term field campaigns based on continuous backscatter observations made by portable simulators of SCA, associated with in situ soil moisture and vegetation biomass observations, are needed. ESA has experience in organizing such Cal/Val studies (e.g., the ELBARA programme in the framework of the SMOS Cal/Val). In addition, high-resolution SAR data are useful for the Cal/Val of SCA products, in particular from Sentinel-1 and RadarSat.

10 REFERENCES

10.1 Literature

Aaboe, Signe, and Thomas Lavergne (2016), Cooperation on assessing the impact of different sigma0 re-sampling on OSI SAF sea ice products using ASCAT data, EUMETSAT and OSI SAF Federated Activity, Version 1.1, Norwegian Meteorological Institute.

AEG, 2008, Position Papers of User Needs:
- Requirements for Operational Atmospheric Chemistry Monitoring in the Post-EPS Time Frame beyond 2020;
- Requirements for Ocean Observations relevant to POST-EPS;
- Post-EPS Developments on Atmospheric Sounding and Wind Profiling;
- Post-EPS: Generic Requirements on Climate Monitoring;
- Cloud, Precipitation and Large Scale Land Surface Imaging (CPL) Observational Requirements for Meteorology, Hydrology and Climate

References at www.eumetsat.int/Home/Main/Satellites/EPS-SG/Resources/index.htm?l=en.

Albergel, C., S. Munier, D. J. Leroux, H. Dewaele, D. Fairbairn, A. L. Barbu, E. Gelati, W. Dorigo, S. Faroux, C. Meurey, P. Le Moigne, B. Decharme, J.-F. Mahfouf, J.-C. Calvet: Sequential assimilation of satellite-derived vegetation and soil moisture products using SURFEX_v8.0: LDAS-Monde assessment over the Euro-Mediterranean area, Geosci. Model Dev., Geosci. Model Dev., 10, 3889–3912, https://doi.org/10.5194/gmd-10-3889-2017, 2017.

Albergel C., P. de Rosnay, C. Gruhier, J. Muñoz Sabater, S. Hasenauer, L. Isaksen, Y. Kerr and W. Wagner: Evaluation of remotely sensed and modelled soil moisture products using global ground-based in-situ observations, Remote Sensing of Environment, 118, pp215-226, 2012, doi: 10.1016/j.rse.2011.11.017

Albergel C., P. de Rosnay, G. Balsamo, E. Dutra, T. Kral, J. Munoz-Sabater, L. Isaksen, S. Boussetta, C. Massari, and L. Brocca: "Long term global scale root zone soil moisture monitoring at ECMWF using a surface-only land data assimilation system". (EGU2015-9561), European Geosciences Union (EGU) General Assembly, Vienna, 12 April - 17 April 2015

Anderson, C., Bonekamp, H., Figa-Saldana, J., Wilson, J., Verspeek, J., Stoffelen, A., and Portabella, M., 2012a, Validation of Backscatter Measurements from the Advanced Scatterometer on MetOp-A, J. of Atm. And Ocean. Techn. 29(1), 77-88, doi:10.1175/JTECH-D-11-00020.1.

Anderson, C.; Bonekamp, H.; Duff, C.; Figa-Saldana, J.; Wilson, J.J.W., 2012b, "Analysis of ASCAT Ocean Backscatter Measurement Noise", *Geoscience and Remote Sensing, IEEE Transactions on* , vol.50, no.7, pp.2449,2457, doi:10.1109/TGRS.2012.2190739.

Ardhuin, Fabrice, et al. (2018), SKIM, a candidate satellite mission exploring global ocean currents and waves, ESA Earth Explorer candidate SKIM: the Sea surface KInematics Multiscale monitoring satellite mission, preprint for OceanObs'19, DOI: 10.13140/RG.2.2.35397.29927.

ASCAT Wind Product User Manual, ASCAT coastal product, 2013, Ocean and Sea Ice SAF, SAF/OSI/CDOP/KNMI/TEC/MA/126, Version 1.13, May 2013. www.knmi.nl/scatterometer/publications/pdf/ASCAT_Product_Manual.pdf.

ATBD (2015), EPS-SG SCA Level 1 Algorithm Theoretical Baseline Document (ATBD), EUMETSAT Doc: EUM/LEO-EPSSG/SPE/14/739659, v1.

Attema, E.P.W. (1991). The Active Microwave Instrument on-board the ERS-1 satellite. *Proc. IEEE* **79**(6), 791–799. doi: 10.1109/5.90158.

Bartalis, Z., Wagner, W., Naeimi, V., Hasenauer, S., Scipal, K., Bonekamp, H., Figa, J. and Anderson, C. (2007). Initial soil moisture retrievals from the MetOp-A Advanced Scatterometer (ASCAT). *Geophys. Res. Lett* **34**, L20401.

Belmonte Rivas, Maria, Ad Stoffelen (2019), Characterizing ERA-interim and ERA5 surface wind biases using ASCAT, Ocean Sci. Discuss., under review, DOI: doi.org/10.5194/os-2018-160.Belmonte, M., J. Verspeek, A. Verhoef and A. Stoffelen, 2012, *Bayesian sea ice detection with the Advanced Scatterometer*, IEEE Transactions on Geoscience and Remote Sensing, **50**, 7, 2649-2657, doi:10.1109/TGRS.2011.2182356.

Belmonte Rivas, M. & A. Stoffelen, 2011, New Bayesian algorithm for sea ice detection with QuikSCAT. *IEEE Trans. Geosci. Rem. Sens.* I **49**(6), 1894–1901. doi:10.1109/TGRS.2010.2101608.

Bidlot J., D. Holmes, P. Wittmann, R. Lalbeharry, and H. Chen, 2002, Intercomparison of the performance of operational ocean wave forecasting systems with buoy data, *Wea. Forecasting*, vol. **17**, 287-310.

Blanke, B., Speich, S., Bentamy, A., Roy, C. & Sow, B. (2005). Modelling the structure and variability of the southern Benguela upwelling using QuikSCAT wind forcing. *J. Geophys. Res.* **110**, C07018. doi: 1029/2004JC002529.

Bourassa et al., 2009, Remotely Sensed Winds and Wind Stresses for Marine Forecasting and Ocean Modelling, OceanObs'09 coaps.fsu.edu/scatterometry/reports/docs/OceanObs09_Winds_White_Paper.pdf

Breivik L.A., S. Eastwood, Ø. Godøy, H. Schyberg, S. Andersen, R.T. Tonboe, 2001, "Sea Ice Products for EUMETSAT Satellite Application Facility." Can. J. Remote Sensing. Vol. 27. No. 5, pp 403 – 410

Breivik L.A., H. Schyberg, 1998, Scatterometer Data for SAF Sea Ice Products. In Proc. Joint ESA-Eumetsat Workshop on Emerging Scatterometer Applications –From Research to Operations, 5-7 October

Breivik, L.-A.; Eastwood, S.; Lavergne, T.; , Use of C-Band Scatterometer for Sea Ice Edge Identification, Geoscience and Remote Sensing, IEEE Transactions on , vol.50, no.7, pp.2669-2677, July 2012.

Brocca, L., Ciabatta, L., Massari, C., Moramarco, T., Hahn, S., Hasenauer, S., Kidd, R., Dorigo, W., Wagner, W., and Levizzani, V. (2014), Soil as a natural rain gauge: Estimating global rainfall from satellite soil moisture data, J. Geophys. Res. Atmos., 119, 5128– 5141, doi:10.1002/2014JD021489.

Brocca, L., Melone, F., Moramarco, T., Wagner, W. (2013). A new method for rainfall estimation through soil moisture observations. Geophys. Res. Lett., 40(5), 853-858.

Brocca, L., S. Hasenauer, T. Lacava, F. Melone, T. Moramarco, W. Wagner, W. Dorigo, et al. "Soil Moisture Estimation through ASCAT and AMSR-E Sensors: An Intercomparison and Validation Study across Europe." Remote Sensing of Environment 115, no. 12 (2011): 3390–3408. doi:10.1016/j.rse.2011.08.003.

Brocca, L., Massari, C., Ciabatta, L., Wagner, W., Stoffelen, A. (2016). Remote sensing of terrestrial rainfall from Ku-band scatterometers. IEEE Journal of Selected Topics in Applied Earth Observations and Remote Sensing, 9(1), 533-539, doi:10.1109/JSTARS.2015.2508065. http://dx.doi.org/10.1109/JSTARS.2015.2508065.

BUFR, 2007, ADDITIONS TO BUFR/CREX TABLES FOR PRE-OPERATIONAL IMPLEMENTATION ENDORSED BY CBS for full operational status on 7 November 2007 (updated 04/01/07), pp55-60, available on
www.wmo.int/web/www/WMOCodes/Updates/BUFRCREX/Preoperational050107.doc

Cavanié, A., Demurger, J. & Lecomte, P. (1986). Evaluation of the different parameters in Long's C-band model. *Proc. Workshop on ERS-1 Wind and Wave Calibration,* Schliersee, Germany. ESA SP-262, European Space Agency, Noordwijk, the Netherlands, pp.47-51.

Center for Ocean-Atmosphere Prediction Studies (COAPS). COAPS Scatterometry. 2017. http://www.coaps.fsu.edu/scatterometry/.
Accessed April 2017.

CEOS, 2017, Ocean Surface Vector Winds - Virtual Constellation,
ceos.org/ourwork/virtual-constellations/osvw/

Chelton, D.B., Schlax, M.G. Freilich, M.H. & Milliff, R.E. (2004). Satellite measurements reveal persistent small-scale features in ocean winds. *Science* **303**, 978–983.

De Abreu R, Flett D, et al. 203 Operational sea ice monitorng with RADARSAT-2 a glimpse into the future Geosci. Remote Sens. Symposium, 203. IGARS '03 Proceedings. 1308-1310

Dee, D. P., S. M. Uppala, A. J. Simmons, P. Berrisford, P. Poli, S. Kobayashi, U. Andrae, M. A. Balmaseda, G. Balsamo, P. Bauer, P. Bechtold, A. C. M. Beljaars, L. van de Berg, J. Bidlot, N. Bormann, C. Delsol, R. Dragani, M. Fuentes, A. J. Geer, L. Haimberger, S. B. Healy, H. Hersbach, E. V. Hólm, L. Isaksen, P. Kållberg, M. Köhler, M. Matricardi, A. P. McNally, B. M. Monge-Sanz, J.-J. Morcrette, B.-K. Park, C. Peubey, P. de Rosnay, C. Tavolato, J.-N. Thépaut and F. Vitart, 2011, The ERA-Interim reanalysis: configuration and performance of the data assimilation system, Quarterly Journal of the Royal Meteorological Society **137 (656),** 553–597, April 2011 Part A, DOI: 10.1002/qj.828.

De Haan, S. & Stoffelen, A. (2001). *Ice Discrimination using ERS Scatterometer.* Document external project: 2001, SAF/OSI/KNMI/TEC/TN/120, Eumetsat. *www.knmi.nl/publications/fulltexts/safosi_w_icescrknmi.pdf*

De Lannoy, G. J. M., P. de Rosnay, and R. H. Reichle: "Soil Moisture Data Assimilation" In: Handbook of Hydrometeorological Ensemble Forecasting, edited by Q. Duan, F. Pappenberger, J. Thielen, A. Wood, H. Cloke, and J. C. Schaake, Springer Verlag, New York, in press, 2015.

de Rosnay P., A. Fouilloux, M. Dahoui, I. Mallas, E. Fucile, C. Albergel, J. Muñoz Sabater, E. Dutra, G. Balsamo, P. Lopez, L. Isaksen, J.-N. Thépaut: "ECMWF land data assimilation system: Recent improvements and impact on Numerical Weather Prediction", 7th International Scientific Conference on the Global Energy and Water Cycle, The Hague, 14-17 July 2014

de Rosnay P., M. Drusch, D. Vasiljevic, G. Balsamo, C. Albergel and L. Isaksen: A simplified Extended Kalman Filter for the global operational soil moisture analysis at ECMWF, Q. J. R. Meteorol. Soc., 139(674):1199-1213, 2013, doi: 10.1002/qj.2023

de Rosnay, P.: Sensitivity of ASCAT soil moisture first guess departure to incidence angle, ECMWF Research department memorandum 0953, July 2009

De Wit, A. & Van Diepen, C. (2007). Crop model data assimilation with the ensemble Kalman filter for improving regional crop yield forecasts. *Agric. Forest Meteorol.* **146**(1–2), 38–56.

Dharssi, I., Bovis, K. J., Macpherson, B., and Jones, C. P.: Operational assimilation of ASCAT surface soil wetness at the Met Office, Hydrol. Earth Syst. Sci., 15, 2729-2746, doi:10.5194/hess-15-2729-2011, 2011.

Dierking, W. 2013. Sea ice monitoring by synthetic aperture radar. Oceanography 26(2):100–111, http://dx.doi.org/10.5670/oceanog.2013.33.

Dirmeyer, P.A., Guo, Z.C. & Gao, X. (2004). Comparison, validation, and transferability of eight multiyear global soil wetness products. *J. Hydrometeorol.* **5**(6), 1011–1033.

Donelan, M. A., and W. J. Pierson, 1987, Radar scattering and equilibrium ranges in wind generated waves with application to scatterometry, *J. Geophys. Res.* **92**, 4971-5029.

Donelly, William J., James R. Carswell, and Robert E. McIntosh, 1999, Revised ocean backscatter at C and Ku band under high wind conditions, *J. Geophys. Res.* **104**, 11,485-11,497.

Dorigo, W.A., Scipal, K., Parinussa, R.M., Liu, Y.Y., Wagner, W., de Jeu, R.A.M. & Naeimi, V. (2010). Error characterisation of global active and passive microwave soil moisture datasets. *Hydrol. Earth Syst. Sci.* **14**(12), 2605–2616.

Drinkwater, M.R., Long, D.G. & Bingham, A.W. (2001). Greenland snow accumulation estimates from satellite radar scatterometer data. *J. Geophys. Res. D: Atmospheres* **106**(D24), 33 935–33 950.

Drinkwater, M.R., and C.C. Lin. 2000. Introduction to the special section on emerging scatterometer applications. *IEEE Transactions on Geoscience and Remote Sensing* 38(4): 1763-1764.

Drusch, M., Wood, E., Gao, H. & Thiele, A. (2004). Soil moisture retrieval during the Southern Great Plains Hydrologic Experiment 1999: A comparison between experimental remote sensing data and operational products. *Water Resources Res.* **40**(W02504). doi:10.1029/2003WR002441.

Entekhabi, D., Njoku, E.G., Houser, P., Spencer, M., Doiron, T., Yunjin, K., Smith, J., Girard, R., Belair, S., Crow, W., Jackson, T.J., Kerr, Y.H., Kimball, J.S., Koster, R., McDonald, K.C., O'Neill, P.E., Pultz, T., Running, S.W., Jiancheng, S., Wood, E. & van Zyl, J. (2004). The Hydrosphere

State (Hydros) satellite mission: An Earth system pathfinder for global mapping of soil moisture and land freeze/thaw. *IEEE Trans. Geosci. Rem. Sens.* **42**(10), 2184–2195.

ERS, 2001, ERS PRODUCTS – WMO FM94 BUFR FORMAT, ER-IS-UKM-GS-0001, Version 4, Issue 2, 16 February 2001.

ERA-interim, 2015, www.ecmwf.int/en/research/climate-reanalysis/era-interim

ESA (1998). *Proc. Emerging Scatterometer Applications Workshop,* ESTEC. ESA SP-424, European Space Agency, Noordwijk, the Netherlands.

ESA (1999). *Atmospheric Dynamics Mission: Core Earth Explorer Mission Selection Report.* ESA SP-1233(4), European Space Agency, Noordwijk, the Netherlands.

Eumetsat OSI SAF (1999). *www.knmi.nl/scatterometer/ers_prod/*

EURD, 2013

European Space Agency. "Scatterometer design." Earthnet Online (2004). http://earth.esa.int/ers/instruments/.
Accessed December 2004.

Fernandez, D. E., J. R. Carswell, S. Frasier, P. S. Chang, P. G. Black, and F. D. Marks, 2006, Dual-polarized C- and Ku-band ocean backscatter response to hurricane-force winds, J. Geophys. Res., 111, C08013, doi:10.1029/2005JC003048.

Figa-Saldaña, J., J.J.W. Wilson, E. Attema, R. Gelsthorpe, M.R. Drinkwater, and A. Stoffelen (2002). The advanced scatterometer (ASCAT) on the meteorological operational (MetOp) platform: A follow on for European wind scatterometers. *Canadian Journal of Remote Sensing* 28(3): 404-412.

Figa, J. & Stoffelen, A. (2000). On the assimilation of Ku-band scatterometer winds for weather analysis and forecasting*, IEEE Trans. Geosci. Rem. Sens.* **38**(4), 1893–1902.

Fois, F.; Hoogeboom, P.; Le Chevalier, F.; Stoffelen, A., Future Ocean Scatterometry (2015), On the Use of Cross-Polar Scattering to Observe Very High Winds, Geoscience and Remote Sensing, IEEE Transactions on, vol.PP, no.99, pp.1,12, doi: 10.1109/TGRS.2015.2416203.

Fois, Franco, Peter Hoogeboom, Francois Chevalier, Ad Stoffelen, Alexis Mouche (2016), "DopSCAT: a Mission Concept for Simultaneous Measurements of Marine Winds and Surface Currents", accepted for publication in Journal of Geophysical Research – Oceans, Paper #2015JC011011RR

Frison, P.L. & Mougin, E. (1996). Monitoring global vegetation dynamics with ERS-1 wind scatterometer data. *Int. J. Rem. Sens.* **17**(16), 3201–3218.

Frolking, S., T. Milliman, K. McDonald, J. Kimball, M. Zhao, and M. Fahnestock. (2006). Evaluation of the zea winds scatterometer for regional monitoring of vegetation phenology, *J. Geophys. Res. Atm.*, **111**(17): 1–14.

Gohin, F. and Cavanié, A. (1994) A first try at identification of sea ice using the three beam scatterometer of ERS-1” Int. J. Remote Sensing, Vol. 15, No. 6, pp. 1221 — 1228

GOS, 2010, WMO Vision for the Global Observing System,
www.wmo.int/pages/prog/www/OSY/gos-vision.html

Hahn, S., A. Plocon, S. Hasenauer, A. Verhoef, A. Stoffelen, J. Figa-Saldaña, C. Anderson (2014), Effects on Level 2 Soil Moisture using Level 1b sigma0 re-sampled with a circular top-hat window and exploration of the Level 1b full-resolution sigma0 product, Federated activity report EUMETSAT Hydrology SAF, TU Wien, EUMETSAT, KNMI, Version 0.9, 16 December.

Hahn S., C. Notarnicola, S. Paloscia, F. Greifeneder, E. Santi, M. Vreugdenhil, C. Reimer, W. Wagner, and A. Gruber (2015), "Technical Report 3 - Algorithm description, implementation and validation," TU Wien, Vienna, Austria, Technical Report.

Henderson, F.M., and A.J. Lewis, eds. 1998. *Principles & applications of imaging radar*. Manual of Remote Sensing Third Edition, Volume 2. New York: John Wiley & Sons, Inc.

Hersbach, H. (2008). The usage of scatterometer data at ECMWF. *OVWST meeting,* Seattle. *http://coaps.fsu.edu/scatterometry/meeting/docs/2008/othersci/hersbach.pdf*

Hersbach, H., Stoffelen, A. & de Haan, S. (2007). An improved C-band scatterometer ocean geophysical model function: CMOD5. *J. Geophys. Res.* **112**. doi:10.1029/2006JC003743.

Hollmann, R., C.J. Merchant, R. Saunders, C. Downy, M. Buchwitz, A. Cazenave, E. Chuvieco, P. Defourny, G. de Leeuw, R. Forsberg, T. Holzer-Popp, F. Paul, S. Sandven, S. Sathyendranath, M. van Roozendael, W. Wagner (2013), The ESA Climate Change Initiative: satellite data records for essential climate variables, Bulletin of the American Meteorological Society, doi: http://dx.doi.org/10.1175/BAMS-D-11-00254.1

Hoogeboom, Peter, Ad Stoffelen, Paco Lopez Dekker (2018), DopSCA, Scatterometer-based Simultaneous Ocean Vector Current and Wind Estimation, Proc. Conference: 2018 Doppler Oceanography from Space (DOfS), DOI: 10.1109/DOfS.2018.8587276.IOVWST, 2017, coaps.fsu.edu/scatterometry/meeting/past.php.

Isaksen, L., and A. Stoffelen, 2000, "ERS-Scatterometer Wind Data Impact on ECMWF's Tropical Cyclone Forecasts", IEEE-Transactions on Geoscience and Remote Sensing (special issue on Emerging Scatterometer Applications) 38 (4), pp. 1885-1892.

Isaksen, L. & Janssen, P.A.E.M. (2004). Impact of ERS scatterometer winds in ECMWF's assimilation system. *Q. J. R. Meteorol. Soc.* **130**(600), 1793–1814, Part A. DOI: 10.1256/qj.03.110.

Kennett, R.G. & Li, F.K. (1989). Seasat over-land scatterometer data, I: Global overview of the Ku-band backscatter coefficients. *IEEE Trans. Geosci. Rem. Sens.* **27**(5), 592–605.

Kerr, Y.H. (2007). Soil moisture from space: Where are we? *Hydrogeol. J.* **15**(1), 117–120.

King, Gregory P., Marcos Portabella, Wenming Lin, Ad Stoffelen (2017), Correlating extremes in wind and stress divergence with extremes in rain over the Tropical Atlantic, EUMETSAT Ocean and Sea Ice SAF Scientific Report OSI_AVS_15_02, V1.0, www.osi-saf.org/?q=content/correlating-extremes-wind-and-stress-divergence-extremes-rain-over-tropical-atlantic.

King, G., J. Vogelzang and A. Stoffelen, 2014, *Second-order structure function analysis of scatterometer winds over the Tropical Pacific,* J. Geophys. Res., **120**, doi:10.1002/2014JC009992.

Künzer, C., Zhao, D., Scipal, K., Sabel, D., Naeimi, V., Bartalis, Z., Hasenauer, S., Mehl, H., Dech, S. & Wagner, W. (2009). El Niño Southern Oscillation influences represented in ERS scatterometer-derived soil moisture data. *Appl. Geog.* **29**, 463–477.

Le Meur, D., Isaksen, L. Hansen, B., Saunders, R. & Janssen, P. (1998). *Global Validation of ERS Wind and Wave Products.* Final report to the European Space Agency, ESA contract No. 8488/95/NL/CN, ECMWF, Shinfield Park, Reading, Berkshire, UK.

Lin, C.C., M. Betto, M. Belmonte-Rivas, A. Stoffelen en J. de Kloe (2012), EPS-SG Windscatterometer Concept Tradeoffs and Wind Retrieval Performance Assessment IEEE Transactions on Geoscience and Remote Sensing, 50, 7, 2458-2472, doi:10.1109/TGRS.2011.2180393.

Lin, W., M. Portabella, A. Stoffelen, J. Vogelzang, and A. Verhoef (2016), On mesoscale analysis and ASCAT ambiguity removal, Quart. J. Roy. Meteorol. Soc., QJ-15-0247.R2 , in press.

Lin, W., M. Portabella, A. Stoffelen, A. Verhoef, and A. Turiel, "ASCAT wind quality control near rain," IEEE Trans. on Geoscience and Rem. Sens., 53(8), pp.4165-4177, 2015

Lin, W., Portabella, M., Stoffelen, A., Turiel, A., and Verhoef, A., "Rain identification in ASCAT winds using singularity analysis," *IEEE Geosci. Rem. Sens. Lett.*, **11** (9), pp. 1519-1523, doi: 10.1109/LGRS.2014.2298095, 2014.

Lin, W., Portabella, M., Stoffelen, A., and Verhoef, A., "On the characteristics of ASCAT wind direction ambiguities," *Atmos. Meas. Tech.*, **6**, pp. 1053-1060, doi:10.5194/amt-6-1053-2013, 2013.

Lindsley, Richard D. (2015), Enhanced-Resolution Processing and Applications of the ASCAT Scatterometer, PhD dissertation, Department of Electrical and Computer Engineering, Brigham Young University, December 2015

Lindsley, Richard D. (2016), A Parameterized ASCAT Measurement Spatial Response Function. IEEE Transactions on Geoscience and Remote Sensing 54 (8), 4570–4579, DOI: 10.1109/TGRS.2016.2544835

Liu, W.T. & Xie, X. (2006), Measuring ocean surface wind from space. In J. Gower (Ed), *Remote Sensing of the Marine Environment, Manual of remote Sensing*. 3rd edn, vol. 6, American Society for Photogrammetry and Remote Sensing, pp.149–178.

Liu, Y.Y., Parinussa, R.M., Dorigo, W.A., de Jeu, R.A.M., Wagner, W., van Dijk, A., McCabe, F.M. & Evans, J.P. (2011a). Developing an improved soil moisture dataset by blending passive and active microwave satellite-based retrievals. *Hydrol. Earth Syst. Sci.* **15** (2), 425-436.

Liu, Y.Y., R. A. de Jeu, M. F. McCabe, J. P. Evans, and A. I. van Dijk (2011b), "Global long-term passive microwave satellite-based retrievals of vegetation optical depth," *Geophys. Res. Lett.*, vol. 38, no. 18.

Long, D.G., Polar applications of space-borne scatterometers (2017), JSTARS May issue.

Long, D.G., and M.R. Drinkwater. 1999. Cryosphere applications of NSCAT data. *IEEE Transactions on Geoscience and Remote Sensing* 37(3): 1671-1684.

Long, D.G., M.R. Drinkwater, B. Holt, S. Saatchi, and C. Bertoia. 2001. Global ice and land climate studies using scatterometer image data. *EOS, Transaction of the American Geophysical Union* 82(43): 503. Also available online at http://www.agu.org/eos_elec/010126e.html. Paper and electronic versions are available in a PDF file (4 MB).

Long, D.G., and M.R. Drinkwater. 2000. Azimuth variation in microwave scatterometer and radiometer data over Antarctica. *IEEE Transactions on Geoscience and Remote Sensing* 38(4): 1857-1870.

Long, D.G., P. Hardin, and P. Whiting. 1993. Resolution enhancement of spaceborne scatterometer data. *IEEE Transactions on Geoscience and Remote Sensing* 31(3): 700-715.

Long, A.E. (1986). Towards a C-band radar echo model for the ERS-1 scatterometer. *3rd Int. Coll. Spectral Signatures in Remote Sensing*, Les Arc, France. ESA SP-247, European Space Agency, Noordwijk, the Netherlands, pp.29–34.

Magagi, R.D. & Kerr, Y.H. (1997). Retrieval of soil moisture and vegetation characteristics by use of ERS-1 wind scatterometer over arid and semi-arid areas. *J. Hydrol.* **188–189**, 361–384.

Makynen M, Hallikainen M 1998 C-band backscattering signatures of Baltic sea ice. Geosci. Remote Sens. Symposium Proceedings, 1998. IGARSS '98. 983–985.

McColl K. A., D. Entekhabi, and M. Piles, “Uncertainty analysis of soil moisture and vegetation indices using Aquarius scatterometer observations,” *Geosci. Remote Sens. IEEE Trans. On*, vol. 52, no. 7, pp. 4259–4272, 2014.

Moore, G.W. & Renfrew, I.A. (2005). Tip jets and barrier winds: a QuikSCAT climatology of high wind speed events around Greenland, *J. Climate* **18**, 3713–3725.

Moore, R.J. & Pierson, W.J. (1967). Microwave determination of winds at sea. *Proc. IEEE* **67**, 1504–1521.

Mougin, E., Lopes, A., Frison, P.L. & Proisy, C. (1995). Preliminary analysis of ERS-1 wind scatterometer data over land surfaces. *Int. J. Rem. Sens.* **16**(2), 391–398.

MRD, 2010, EUM/PEPS/REQ/06/0043, v3C, 25 June 2010, www.eumetsat.int/groups/pps/documents/document/pdf_peps_mrd.pdf

Naeimi, V., Scipal, K., Bartalis, Z., Hasenauer, S., Wagner, W., 2009. An Improved Soil Moisture Retrieval Algorithm for ERS and METOP Scatterometer Observations. IEEE Transactions on Geoscience and Remote Sensing 47, 1999–2013. doi:10.1109/TGRS.2008.2011617

Naeimi, Vahid, Christoph Paulik, Annett Bartsch, Wolfgang Wagner, Richard Kidd, Sang-Eun Park, Kirsten Elger, and Julia Boike. “ASCAT Surface State Flag (SSF): Extracting Information on Surface Freeze/Thaw Conditions From Backscatter Data Using an Empirical Threshold-Analysis Algorithm.” IEEE Transactions on Geoscience and Remote Sensing 50, no. 7 (July 2012): 2566–82. doi:10.1109/TGRS.2011.2177667.

NASA Jet Propulsion Laboratory. "Missions - NSCAT." Winds: measuring ocean winds from space. 2004.

http://winds.jpl.nasa.gov/missions/nscat/index.cfm.
Accessed December 2004.

NASA Jet Propulsion Laboratory. "Missions - SeaWinds on QuikSCAT." Winds: measuring ocean winds from space. 2004. http://winds.jpl.nasa.gov/missions/quikscat/index.cfm.
Accessed December 2004.

NASA Jet Propulsion Laboratory. "Missions - SeaWinds on ADEOS II." Winds: measuring ocean winds from space. 2004. http://winds.jpl.nasa.gov/missions/seawinds/index.cfm.
Accessed December 2004.

Naderi, F., M.H. Freilich, and D.G. Long. 1991. Spaceborne radar measurement of wind velocity over the ocean -- an overview of the NSCAT scatterometer system. *Proceedings of the IEEE* 79(6): 850-866. Invited paper.

Offiler, D. (1987). *ERS-1 Wind Retrieval Algorithms*. UK Met Office, MET O 19, Branch Memorandum, No. 86.

Otosaka, I., M. Belmonte Rivas and A. Stoffelen, "Bayesian Sea Ice Detection With the ERS Scatterometer and Sea Ice Backscatter Model at C-Band", *IEEE Trans. on Geosc. and Rem. Sens.*, vol. PP, no. 99, pp. 1-7, doi: 10.1109/TGRS.2017.2777670.

NWP SAF, 2017, scatterometer pages, nwpsaf.eu/deliverables/scatterometer/

OSCAR, 2017, Observing Systems Capability Analysis and Review tool (OSCAR), www.wmo-sat.info/oscar/ ; surface wind: www.wmo-sat.info/oscar/variables/view/183.

Parajka, J., Naeimi, V., Blöschl, G., Wagner, W., Merz, R. & Scipal, K. (2006). Assimilating scatterometer soil moisture data into conceptual hydrologic models at the regional scale. *Hydrol. Earth Syst. Sci.* **10**, 353–368.

Pellarin, T., Calvet, J.-C. & Wagner, W. (2006). Evaluation of ERS scatterometer soil moisture products over a half-degree region in southwestern France. *Geophys. Res. Lett*. **33**(17), L17401.

Peteherych, S., Wurtele, M.G., Woiceshyn, P.M., Boggs, D.H. & Atlas, R. (1984). First global analysis of SEASAT scatterometer winds and potential for meteorological research. *NASA Conf. Publ. CP2303*, pp.575–585.

Portabella, M., Stoffelen, A., Verhoef, A., and Verspeek, J., “A new method for improving scatterometer wind quality control,” *IEEE Geosci. Rem. Sens. Lett.,* **9** (4), pp. 579-583, doi:10.1109/LGRS.2011.2175435, 2012a.

Portabella, M., Stoffelen, A., Verhoef, A. & Lin, W. (2012b). Rain effects on ASCAT retrieved winds: towards an improved quality control, *IEEE Trans. Geosci. Rem. Sens.* **50**(7), 2495–2506.

Portabella, M., and Stoffelen, A., “On scatterometer ocean stress,” *J. Atm. and Ocean Techn.*, **26** (2), pp. 368–382, doi:10.1175/2008JTECHO578.1, 2009.

Portabella, M. & Stoffelen, A. (2006). Scatterometer backscatter uncertainty due to wind variability. *IEEE Trans. Geosci. Rem. Sens.* **44**(11), 3356–3362. doi:10.1109/TGRS.2006.877952

Portabella, M., and Stoffelen, A., "A probabilistic approach for SeaWinds data assimilation," *Quart. J. R. Met. Soc.,* **130** (596), pp. 127-152, doi:10.1256/qj.02.205, 2004.

Portabella, M., Stoffelen, A. & Johannessen, J.A (2002). Toward an optimal inversion method for SAR wind retrieval. *J. Geophys. Res.* **107**(C8), 1–13.

Portabella, M. & Stoffelen, A. (2002). A comparison of KNMI quality control and JPL rain flag for seawinds. *Can. J. Rem. Sens.* **28**(3), 424–430.

Portabella, M. & Stoffelen, A. (2001). Rain detection and quality control of sea winds. *J. Atm. Ocean Techn*. **18**(7), 1171–1183.

Pulliainen, J.T., Manninen, T. & Hallikainen, M.T. (1998). Application of ERS-1 wind scatterometer data to soil frost and soil moisture monitoring in boreal forest zone. *IEEE Trans. Geosci. Rem. Sens.* **36**(3), 849–863.

Pierson, W.J., 1989, Probabilities and statistics for backscatter estimates obtained by a scatterometer, *J. Geophys. Res.* **94**, 9743-9759; correction in *J. Geophys. Res.* **95**, 809, 1990.

Remund, Q, and D. Long, 1999, Sea ice extent mapping using Ku band scatterometer data, J.Geophys. Res., Vol. 104 No. C5, pp. 11515- 11527, May 1999.

Ricciardulli, L. and F. Wentz (2013), Towards a climate data record of ocean vector winds: The new RSS ASCAT, Proc. Int. Ocean Vector Wind Sci. Team Meet., Kona, HI, USA, May 2013, available here.

Sandu, I., A. Beljaars, P. Bechtold, T. Mauritsen, and G. Balsamo, 2011, Why is it so difficult to represent stably stratified conditions in numerical weather prediction (NWP) models?, J. Adv. Model. Earth Syst., 5, 117–133, doi:10.1002/jame.20013.

Sherwood, Steven C., Sandrine Bony & Jean-Louis Dufresne, 2014, Spread in model climate sensitivity traced to atmospheric convective mixing, Nature **505**, 37–42 (02 January 2014), doi:10.1038/nature12829

Schmullius, C.C. (1997). Monitoring Siberian forests and agriculture with the ERS-1 wind scatterometer. *IEEE Trans. Geosci. Rem. Sens.* **35**(5), 1363–1366.

Scipal, K., Drusch, M., Hasenauer, S., Wagner, W. & Jann, A. (2007). Towards the assimilation of scatterometer derived soil moisture in the ECMWF numerical weather prediction system. *Joint 2007 Eumetsat Meteorological Satellite Conf. and 15th Satellite Meteorology & Oceanography Conf. of the American Meteorological Society*, Amsterdam, the Netherlands.

Scipal, K., Scheffler, C. & Wagner, W. (2005). Soil moisture–runoff relation at the catchment scale as observed with coarse resolution microwave remote sensing. *Hydrol. Earth Syst. Sci.* **9**(3), 173–183.

Scipal, K., Wagner, W., Trommler, M. & Naumann, K. (2002). The Global Soil Moisture Archive 1992–2000 from ERS scatterometer data: First results. *Proc. IGARSS 2002*.

Sienkiewicz, J., Brennan, M.J., Knabb, R., Chang, P.S., Cobb, H., Jelenak, Z.J., Ahmad, K.A., Soisuvarn, S., Kosier, D. & Bancroft, G. (2010). Impact of the loss of QuikSCAT on NOAA MWS marine warning and forecast operations. *1st Int. Ocean Vector Winds Science Team Meeting*, Barcelona, Spain.

Spencer, M.W., C. Wu, and D.G. Long. 2000. Improved resolution backscatter measurements with the SeaWinds pencil-beam scatterometer. *IEEE Transactions on Geoscience and Remote Sensing* 38(1): 89-104.

SSMIS (2011). *www.ncdc.noaa.gov/oa/rsad/ssmi/swath/index.html*

Steele-Dunne, S. C., J. Friesen, and N. Van De Giesen. 2012. Using diurnal variation in backscatter to detect vegetation water stress. *IEEE Transactions on Geoscience and Remote Sensing* **50**(7): 2618-2629.

Stoffelen, Ad, Jur Vogelzang, Gert-Jan Marseille (2018a), High resolution data assimilation guide, EUMETSAT NWPSAF-KN-UD-008, V1.2, 10-09-2018, projects.knmi.nl/scatterometer/publications/pdf/high_resolution_data_assimilation_guide_1.2_def.pdf

Stoffelen, Ad, Marcos Portabella, Alexis Mouche, Federica Polverari, G.-J. van Zadelhoff et al. (2018b). C-band High and Extreme-force Speeds, CHEFS WP2: state of the art and user requirements, Report for EUMETSAT ITT 16/166, KNMI, DOI: 10.13140/RG.2.2.10541.13281.

Stoffelen, Ad, and Jur Vogelzang (2018), Wind Bias Correction Guide, EUMETSAT NWPSAF-KN-UD-007 v1.3, projects.knmi.nl/scatterometer/publications/pdf/wind_bias_correction_guide_v1.3_def.

Stoffelen, A., S. Aaboe, J.-C. Calvet, J. Cotton, G. De Chiara, J. Figa Salda˜na, A.A. Mouche, M. Portabella, K. Scipal, and W. Wagner (2017), "Scientific Developments and the EPS-SG Scatterometer", IEEE Journal of Selected Topics in Applied Earth Observations and Remote Sensing 10 (5), 2086-2097, doi: 10.1109/JSTARS.2017.2696424.

Stoffelen, Ad, Jur Vogelzang and Wenming Lin (2015), On buoys, scatterometers and reanalyses for globally representative winds, EUMETSAT NWP SAF Document NWPSAF-KN-TR-024, V1.1, www.nwpsaf.eu/publications/tech_reports/nwpsaf-kn-tr-024.pdf.

Stoffelen, A., A. Verhoef, J. Verspeek, J. Vogelzang, T. Driesenaar, Y. Risheng, C. Payan, G. De Chiara, J. Cotton, A. Bentamy, M. Portabella and G.J. Marseille (2013), Research and Development in Europe on Global Application of the OceanSat-2 Scatterometer Winds, Document extern project: 2013, NWP SAF report number: NWPSAF-KN-TR-022 OSI SAF report number: SAF/OSI/CDOP2/KNMI/TEC/RP/196, KNMI, www.knmi.nl/publications/fulltexts/oceansat_cal_val_report_final_copy1.pdf

Stoffelen, A., & Portabella, M. (2006). On Bayesian scatterometer wind inversion, *IEEE Trans. Geosci. Rem. Sens.* **44**(6), 1523–1533. doi:10.1109/TGRS.2005.862502

Stoffelen, Ad, Siebren de Haan, Yves Quilfen, and Harald Schyberg, 2000, ERS Scatterometer Ambiguity Removal Comparison, OSI SAF report, DOI: 10.13140/2.1.3958.4648.

Stoffelen, Ad, 1998, Toward the true near-surface wind speed: Error modeling and calibration using triple collocation JOURNAL OF GEOPHYSICAL RESEARCH **103** (C4), 7755-7766, April 15, 1998.

Stoffelen, Ad, 1998, Scatterometry, PhD thesis UU, dspace.library.uu.nl/handle/1874/636.

Stoffelen, A. & Anderson, D. (1997). Scatterometer data interpretation: measurement space and inversion. *J. Atm. Ocean Techn*. **14**(6), 1298–1313.

Stoffelen, A. & Anderson, D. (1997). Ambiguity removal and assimilation of scatterometer data. *Q. J. R. Meteorol. Soc*. **123**, 491–518.

Stoffelen, A. & van Beukering, P. (1997). *Implementation of Improved ERS Scatterometer Data Processing and its Impact on HIRLAM Short Range Weather Forecasts.* HIRLAM Technical Report No. 31, KNMI, the Netherlands.

Stoffelen, A. & Anderson, D. (1993). Wind retrieval and ERS-1 scatterometer radar backscatter measurements. *Adv. Space Res.* **13**(5), (5)53–(5)60.

Stoffelen, A. & Cats, G. (1991). The impact of SeaSat-A scatterometer data on high-resolution analyses and forecasts: The development of the QEII storm. *Mon. Wea. Rev.* **119**, 2794–2802.

Tokmakian, R. (2005). An ocean model's response to scatterometer winds. *Ocean Modeling* **9**, 89–103.

TPOS, 2014, ioc-unesco.org/index.php?option=com_oe&task=viewEventRecord&eventID=1383

UCM, 2008, EPS-SG User Consultation Workshop 3, Scatterometry mission, www.eumetsat.int/groups/pps/documents/document/pdf_peps_ucw3_15.pdf

Vachon, P. & Wolfe, J. (2011). C-band cross-polarization wind speed retrieval. *IEEE Trans. Geosci. Rem. Sens. Lett.* **8**(3), 456–459. doi: 10.1109/LGRS.2010.2085417.

Valenzuela, G. R. , 1978, Theories for the interaction of electromagnetic and ocean waves - a review, *Bound. Layer Meteor.*, 13, 612-685.

Verhoef, A., J. Vogelzang, J. Verspeek and A. Stoffelen, "Long-Term Scatterometer Wind Climate Data Records", IEEE Journal of Selected Topics in Applied Earth Observations and Remote Sensing, vol. 10, no. 5, pp. 2186-2194, May 2017, doi: 10.1109/JSTARS.2016.2615873.

Verhoef, Anton, Jur Vogelzang and Ad Stoffelen, 2015, SeaWinds wind Climate Data Record validation report; 25 and 50 km wind products (OSI-151), EUMETSAT Ocean and Sea Ice SAF Technical Note, SAF/OSI/CDOP2/KNMI/TEC/RP/221, KNMI, Version 1.3, March 2015, www.knmi.nl/scatterometer/publications/pdf/seawinds_cdr_validation.pdf.

Verhoef, A., M. Portabella and A. Stoffelen (2012), "High-Resolution ASCAT Scatterometer Winds Near the Coast," in IEEE Transactions on Geoscience and Remote Sensing, vol. 50, no. 7, pp. 2481-2487,. doi: 10.1109/TGRS.2011.2175001.

Verhoef, A., Portabella, M., Stoffelen, A., and Hersbach, H., "CMOD5.n – the CMOD5 GMF for neutral winds," *Report for the EUMETSAT OSI SAF*, SAF/OSI/CDOP/KNMI/TEC/TN/165, available at www.knmi.nl/scatterometer/publications/, 2008.

Verspeek, J., and Stoffelen, A., 2015, anomalies.

Verspeek, J., Stoffelen, A. Verhoef, A. & Portabella, M. (2012). Improved ASCAT wind retrieval using NWP ocean calibration. *IEEE Trans. Geosci. Rem. Sens.* **50**(7), 2488–2494.

Vogelzang, J., and Stoffelen, A. (2017), The ASCAT 6.25-km wind product, JSTARS May issue.

Vogelzang, Jur, and Ad Stoffelen (2017), ASCAT ultra-high resolution wind products on optimized grids, JSTARS May issue.

Vogelzang, J. & Stoffelen, A. (2012). Scatterometer wind vector products for application in meteorology and oceanography. *J. Sea Res.,* special issue Physics of Sea and Ocean, **74**, 16–25.

Vogelzang, J., A. Stoffelen, A. Verhoef and J. Figa-Saldana (2011), *On the quality of high-resolution scatterometer winds,* J. Geophys. Res. **116**, C10033, doi:10.1029/2010JC006640.

Vogelzang, J., 2007, *Two dimensional variational ambiguity removal (2DVAR)* , Technical report NWPSAF-KN-TR-004, EUMETSAT, Digital copy

Vreugdenhil, M., W. A. Dorigo, R. De Jeu, W. Wagner, S. Hahn and M. van Marle. "Analysing the Vegetation Parameterisation in the TU-Wien ASCAT Soil Moisture Retrieval." IEEE Transactions on Geoscience and Remote Sensing, in Press.

Vries, de, J., Stoffelen, A and Beysens, J, Ambiguity Removal and Product Monitoring for SeaWinds, NWP SAF report NWPSAF_KN_TR_001.

Wagner, W., Hahn, S., Kidd, R., Melzer, T., Bartalis, Z., Hasenauer, S., Figa, J., de Rosnay, P., Jann, A., Schneider, S., Komma, J., Kubu, G., Brugger, K., Aubrecht, C., Zuger, J., Gangkofner, U., Kienberger, S., Brocca, L., Wang, Y., Bloeschl, G., Eitzinger, J., Steinnocher, K., Zeil, P., Rubel, F. (2013). The ASCAT soil moisture product: Specifications, validation results, and emerging applications. Meteorologische Zeitschrift, 22(1), 5-33.

Wagner, W., Bartalis, Z., Naeimi, V., Park, S.-E., Figa-Saldana, J. & Bonekamp, H. (2010). Status of the METOP ASCAT soil moisture product. *Proc. IEEE Geoscience and Remote Sensing Symp., IGARSS 2010*, Honolulu, USA, pp.276–279.

Wagner, W., de Jeu, R. & van Oevelen, P. (2009). Towards multi-source global soil moisture datasets for unravelling climate change impacts on water resources. *Proc. 33rd Int. Symp. on Remote Sensing of Environment (ISRSE).* Joint Research Centre of the European Commission, Stresa, Italy, p.3.

Wagner, W., Blöschl, G., Pampaloni, P., Calvet, J.-C., Bizzarri, B., Wigneron, J.-P. & Kerr, Y. (2007). Operational readiness of microwave remote sensing of soil moisture for hydrologic applications. *Nordic Hydrol.* **38**(1), 1–20.

Wagner, W., Scipal, K., Pathe, C., Gerten, D., Lucht, W. & Rudolf, B. (2003). Evaluation of the agreement between the first global remotely sensed soil moisture data with model and precipitation data. *J. Geophys. Res. D: Atmospheres* **108**(D19), Art. No. 4611.

Wagner, W., Lemoine, G., Borgeaud, M. & Rott, H. (1999a). A study of vegetation cover effects on ERS scatterometer data. *IEEE Trans. Geosci. Rem. Sens.* **37**(2), 938–948.

Wagner, W., Noll, J., Borgeaud, M. & Rott, H. (1999b). Monitoring soil moisture over the Canadian Prairies with the ERS scatterometer. *IEEE Trans. Geosci. Rem. Sens.* **37**(1), 206–216.

Wagner, W., Lemoine, G., and Rott, H. "A Method for Estimating Soil Moisture from ERS Scatterometer and Soil Data. (1999c)." Remote Sensing of Environment 70, no. 2: 191–207. doi:10.1016/S0034-4257(99)00036-X.

Wang, Zhixiong, Ad Stoffelen, Biao Zhang, Yijun He, Wenming Lin and Xiuzhong Li (2019), Inconsistencies in scatterometer wind products based on ASCAT and OSCAT-2 collocations, Rem. Sensing Environm., accepted.

Wang, Z.; A. Stoffelen; F. Fois; A. Verhoef; C. Zhao; M. Lin; G. Chen, "SST Dependence of Ku- and C-Band Backscatter Measurements", IEEE Journal of Selected Topics in Applied Earth Observations and Remote Sensing , vol.PP, no.99, pp.1-12, doi: 10.1109/JSTARS.2016.2600749.

Wen, J. & Su, Z.B. (2003). A time series based method for estimating relative soil moisture with ERS wind scatterometer data. *Geophys. Res. Lett.* **30**(7), 1397.

Wentz, F. J., *et al.*, "Evaluating and Extending the Ocean Wind Climate Data Record", *IEEE Journal of Selected Topics in Applied Earth Observations and Remote Sensing*, vol. 10, no. 5, pp. 2165-2185, May 2017, doi: 10.1109/JSTARS.2016.2643641.

WindSat (2011). *www.nrl.navy.mil/WindSat/*

Wismann, V. (2000). Monitoring of seasonal thawing in Siberia with ERS scatterometer data. *IEEE Trans. Geosci. Rem. Sens.* **38**(4 II), 1804–1809.

Woodhouse, I.H. & Hoekman, D.H. (2000). Determining land-surface parameters from the ERS wind scatterometer. *IEEE Trans. Geosci. Rem. Sens.* **38**(1), 126–140.

Zadelhoff, van, G.J. A. Stoffelen, P.W. Vachon, J. Wolfe, J. Horstmann and M. Belmonte-Rivas, 2014, *Retrieving hurricane wind speeds using cross-polarization C-band measurements*, Atmospheric Measurement Techniques, 2014, **7**, 473-449, doi:10.5194/amt-7-437-2014.

Zhang, Biao, Alexis Mouche, Yiru Lu, William Perrie, Guosheng Zhang, He Wang (2019), A Geophysical Model Function for Wind Speed Retrieval from C-band HH-Polarized Synthetic Aperture Radar, Geoscience and Remote Sensing Letters, accepted, ID GRSL-01248-2018.R1.

Zhao, D., Su, B. & Zhao, M. (2006). Soil moisture retrieval from satellite images and its application to heavy rainfall simulation in eastern China. *Adv. Atmos. Sci.* **23**(2), 299–316.

Zribi, M., André, C. & Decharme, B. (2008). A method for soil moisture estimation in Western Africa based on the ERS scatterometer. *IEEE Trans. Geosci. Rem. Sens.* **46**(2), 438–448.

Zwieback, S., C. Paulik, and W. Wagner (2015). Frozen soil detection based on advanced scatterometer observations and air temperature data as part of soil moisture retrieval. *Remote Sens.*, **7**, 3206-3231; doi:10.3390/rs70303206.

10.2 Acronym List

ADEOS	Advanced Earth Observing Satellite
AEG	Application Expert Group
AMI	Active Microwave Instrument
AR	Ambiguity Removal
ASCAT	Advanced SCAtterometer
BUFR	Binary Universal Format Representation
CF	Climate Format (NetCDF)
CDR	Climate Data Record
SCA	EPS/MetOp-SG C-band SCATterometer
DAAC	Distributed Active Archive Center
EARS	EUMETSAT Advanced Retransmission Service
EPS	EUMETSAT Polar System
ERS	European Remote-sensing Satellite
ESA	European Space Agency
ESCAT	AMI ERS-1/2 satellites in scatterometer mode
EUMETCast	EUMETSAT's Digital Video Broadcast Data Distribution System
EUMETSAT	European Organisation for the Exploitation of Meteorological Satellites
HDF	Hierarchical Data Format
JAXA	Japanese Aerospace Exploration Agency
JPL	Jet Propulsion Laboratory (NASA)
KNMI	Royal Netherlands Meteorological Institute
MetOp	Meteorological Operational Platform
MLE	Maximum Likelihood Estimator
NASA	National (US) Aeronautics and Space Administration
NOAA	National (US) Oceanic and Atmospheric Administration
NSCAT	NASA Scatterometer
NRT	Near-real time
NWP	Numerical Weather Prediction
OSI SAF	Ocean and Sea Ice SAF (EUMETSAT)
PDF	Probability Density Function
PMET	EPS-SG Program Mission Experts Team

QA	Quality Assurance
QC	Quality Control
QuikScat	Quick scatterometer mission(NASA)
RMDCN	Regional Meteorological Data Communication Network
SAF	Satellite Applications Facility
SAG	Science Advisory Group
SAR	Synthetic Aperture Radar
SASS	Seasat-A Scatterometer System
SCA	Scatterometer on EPS/Metop-SG
SCAT	Scatterometer on ERS
SeaWinds	scatterometer on-board the QuikSCAT, ADEOS-II and RapidScat platforms
-SG	Second Generation (as in EPS-SG or MetOp-SG)
SST	Sea Surface Temperature
u	West-to-east wind component
U10S	Stress-equivalent 10-m-height wind speed
v	South-to-north wind component
WVC	Wind Vector Cell